Vol. I No. 2 (77-134)
June 2012

ISSN 2223-8905
CODEN JPMTBI
UDC 655

2-2012

Journal of Print and Media Technology Research

Scientific contents

Published by iarigai
www.iarigai.org

The International Association of Research Organizations for the Information, Media and Graphic Arts Industries

JPMTR 1(2012)2, 77-134
June 2012

No. 2-2012

ISSN 2223-8905
CODEN: JPMTBI

Journal of Print and Media Technology Research

A peer-reviewed quarterly

PUBLISHED BY

The International Association of Research Organizations for the Information, Media and Graphic Arts Industries

Washingtonplatz 1, D-64287 Darmstadt, Germany
http://www.iarigai.org E-mail: journal@iarigai.org

A mission statement

To meet the need for a high quality scientific publishing platform in its field, the International Association of Research Organizations for the Information, Media and Graphic Arts Industries, iarigai, publishes this quarterly peer-reviewed research journal.

The journal will foster multidisciplinary research and scholarly discussion on scientific and technical issues in the field of graphic arts and media communication, thereby advancing scientific research, knowledge creation, and industry development. Its aim is to be the leading international scientific journal in the field, offering publishing opportunities and serving as a forum for knowledge exchange between all those interested in contributing to or learning from research in this field.

By regularly publishing peer-reviewed, high quality research articles, position papers, surveys, and case studies as well as, in a special section, review articles, topical communications, opinions, and reflections, the journal promotes original research, international collaboration, and the exchange of ideas and know-how. It also provides a multidisciplinary discussion on research issues within the field and on the effects of new scientific and technical developments on society, industry, and the individual. Thus, it serves the entire research community, as well as the global graphic arts and media industry.

The journal covers fundamental and applied aspects of at least, but not limited to, the following topics:

Printing technology and related processes

Conventional and special printing
Packaging
Printed functionality (including polymer electronics, sensors, and biomaterials)
Printed decorations
Printing materials
Process control

Premedia technology and processes

Color reproduction and color management
Image and reproduction quality
Image carriers (physical and virtual)
Workflow and management
Content management

Emerging media and future trends

Media industry developments
Developing media communications value systems
Online and mobile media development
Cross-media publishing

Social impact

Media in a sustainable society
Consumer perception and media use

The Journal of Print and Media Technology Research is published both in print and electronically.

Further details and guidelines for authors can be found on the inside back cover, as well as downloaded from http:// www.iarigai.org/publications/journal

Subscriptions

http:// www.iarigai.org/publications/journal/order or send a request to office@iarigai.org

✉ Contact e-mail: journal@iarigai.org

Journal of Print and Media Technology Research

2-2012

June 2012

JPMTR 1(2012)2, 77-134

Printed in Croatia by Narodne Novine d.d. Zagreb

Contents

Peer reviewed papers

Topicalities

Edited by Raša Urbas

JPMTR 005 | 1105
UDC 676.226.017:655.344

Research paper
Received: 2011-06-28
Accepted: 2012-04-16

Isolating contributions to gloss from surface mechanical and optical roughness, thin layer refractive index and wavelength filtering as a function of illumination and geometry of incidence

Patrick Gane[1, 2], Pertti Silfsten[3], Carl-Mikael Tåg[4], Pertti Pääkkönen[3], Jouni Hiltunen[3], Kalle Kuivalainen[3], Antti Oksman[3], Kai-Erik Peiponen[3]

[1] Aalto University, Helsinki, Finland — E-mail: patrick.gane@omya.com
[2] Omya Development, Oftringen, Switzerland — E-mail: patrick.gane@omya.com
[3] University of Eastern Finland, Joensuu, Finland — E-mails: pertti.paakkonen@uef.fi; kalle.kuivalainen@uef.fi
[4] (Former) Forest Pilot Center Oy, Raisio, Finland

Abstract

Gloss is a commonly used parameter to express the surface optical and aesthetic quality of materials. In many cases of finished products, the dependence of gloss values derived from commonly used and emerging instrumentation is poorly understood. Examples of such products are surface lacquered furnishings or dye/pigmented laminates as well as printed matter, including printed paper. Paper is a porous medium and exhibits surface roughness related to the fibrous and fillercomponents and the void structure interface with the surface. This roughness is manifest in both its structural profile evaluated by stylus profilometry, and convoluted with the stylus pressure and dimension, as well as in the form of an optical boundary by using laser profilometric techniques. Relating these two different methods of surface roughness characterisation to the gloss, as determined by broad spectrum illumination at two angles of incidence (60° and 75°), it is possible to show that the data fall into two families depending on whether the paper is printed with offset formulated ink or remains either unprinted or treated with ink diluent oil only. This separation of the data illustrates the impact of both refractive index and roughness on the gloss value obtained. The ratio between specular and diffuse reflectance is probed as a function of incidence angle and angle of acceptance, and further reveals the action of transmittance through the applied optically thin layer (ink). By using a diffractive optical element at well-defined wavelength in a method adopting normal incidence (μDOG), it could be shown that the colour filter effect of the thin printed ink film acting in partial transmittance impacted additionally on the represented gloss by partial absorbance of incident intensity in addition to the inclusion of the rougher underlying substrate boundary reflection. The offset ink colour set yellow (Y), magenta (M) and cyan (C), with the corresponding black (K), in that order, progressively reduced the apparent gloss due to the filtering of the incident red laser light, thus forming a series of separate correlations with structural roughness depending on print colour and optical print density. Similarly, when using laser profilometry to determine roughness, the geometry and wavelength used defines the apparent roughness observed. The role of the scale of roughness amplitude was illustrated by exploring the correlations between printed and unprinted surfaces according to whether the roughness was determined by stylus or optical methods. Using combinations of these techniques it is therefore possible to identify independently the impacts of (i) surface structural and optical roughness, (ii) refractive index, and (iii) thin layer optical filtering on measured gloss.

Keywords: gloss, coated paper, offset printing, composite surface quality, surface roughness and optics, thin layer optics, geometry of gloss measurement

1. Introduction

Perception of gloss from microrough surfaces is known to be dependent on the geometry of illumination and observation (Gate and Leaity, 1991; Elton, 2009; Oksman et al., 2008). In the case of thin layer pigmented, lacquered or coloured laminates, for example as used for hard finish furnishings and decorative surfaces, as well as in printed products, such as paper and board, the perceived gloss is not only dependent on geometry in respect to surface roughness but is dependent on refractive index differential and colour filtration occurring between the constructive layers (Gate and Leaity, 1991; Elton, 2009; Preston and Gate, 2005).

Typical gloss measuring devices apply either monochromatic, broad band or white light sources, and in the latter case frequently pre-filtered to a defined narrow optical wavelength region. Much work is invested in forming gloss measurement standards, often particular to specific industries, for example the Tappi test method (T480 om-09), ISO 8254-1:2009 or DIN 67530 standard gloss in the paper and printing industry. In these standards, attention is paid primarily to the geometry of incidence and observation, and in each case the confinement of collection angles considered most appropriate to the perception of the end-user. In the case of printed surfaces, the target end-users can vary. For example if the target is to enhance information transfer through the printed word or image, then the optical density and contrast in gloss between the print and the background surface becomes an important aesthetic and image recognition exercise. Many observers select a preference for a glossy image, but readers on the other hand prefer high optical density and an overall matt surface (MacGregor et al., 1994). In view of these demanding requirements to meet aesthetic qualities it is necessary to understand more deeply the relationship between the optical properties of thin layer, transparent and frequently coloured structures in respect to the perceived gloss they generate when placed on the top of intrinsically rough substrates, such as constructional and natural materials, including paper.

In the case of coated paper, the fibre structure is covered by a layer of white pigment. Gloss and its relationship to factors such as coating formulation, particle packing, coating amount, pore structure, and especially refractive index and surface roughness, has been widely studied (Lepoutre, 1989; Elton and Preston, 2006a, 2006b; Gate et al., 1973; Béland, 2001). It has been demonstrated that the relation between pores and pigments cause scattering in the pigmented coating structure, and not the pigment particles alone (Lepoutre, 1989).

To investigate the effects of topographical roughness, typical instrumentation adopts either mechanical stylus contact, for example Gane and Hooper (1989), or non-contact laser optical confocal, interferometric or simple reflective profilometry (Wennerberg et al., 1996). However, structural roughness alone does not describe the gloss as measured by reflectance, as was shown, for example, by Xu et al. (2005), who showed that incidence angle altered the correlation of gloss between stylus and atomic force microscopy, but rather the optical properties of the interface between the surface and air, including refractive index, and, depending on angle of incidence, together with the thin layer bulk properties of refractive index and spectral absorbance in the case of surface printed materials. Little attention is paid in the literature to these effects, and without their fuller understanding erroneous conclusions can be drawn, such as the measured gloss of a print being lower than the gloss of the surrounding paper, contrary to human perception (Oksman et al., 2011; Silvennoinen et al., 2008).

2. Materials

Unprinted and printed paper were used to illustrate the effects of porous surfaces in contrast to thin layered structures in which a high refractive index ink layer is printed onto the porous paper surface, rendering a smoother, non-porous high gloss surface, having a bandwidth filter effect to generate its colour. The prints were made using an offset ink colour set. The paper coating was first applied to the fibre substrate by a blade metering application[1]. The printing substrates used in the test printings were coated with either a fine broad particle size distribution ground calcium carbonate[2] (bfGCC), having 90 wt-% of the particles finer than 2 μm, or a coating made from a fine narrow particle size distribution ground calcium carbonate[3], having 75 wt-% of particles finer than 1 μm (nfGCC). Both were used as sole coating pigment dispersions applied on a woodfree fine basepaper. The applied coat weight was 12.5 gm^{-2} per side single coat. Eleven (11) parts of a styrene acrylic latex[4], based on 100 parts pigment by weight, was used as binder, chosen because if its known lack of interaction with ink and water components (Rousu et al., 2005). The solids content for the applied coating dispersion was 66.2 %. The nfGCC coated papers were additionally calendered to different levels of smoothness using different linear loads in the calender[1]. The temperature in the calender nips was kept constant at 80 °C, and the paper passed 4 + 4 nips consisting of steel and polymer rolls.

The individual nature of the coating structures *per se* is not of fundamental importance to this study, other than to realise that it is a microporous layer of ill-defined optical surface, which retains some of the larger scale roughness of the underlying fibrous paper.

[1] OptiConcept, Opticoat Jet, Valmet (currently Metso), Fabianinkatu 9 A, PO Box 1220, FIN-00101 Helsinki, Finland

[2] HC90 (Hydrocarb 90, Omya AG, Baslerstrasse 42, CH-4665 Oftringen, Switzerland

[3] CC75 (Covercarb 75), Omya AG, Baslerstrasse 42, CH-4665 Oftringen, Switzerland

[4] Acronal 504 D is a product name of BASF, Ludwigshafen, Germany

Table 1: Test papers

Sample	Coating dispersion	Calendering linear load [kNm^{-1}]
kp4	nfGCC	-
kp14	bfGCC	-
kp401	nfGCC	500
kp404	nfGCC	200
kp406	nfGCC	50

The application of inks to form the printed surfaces was performed with a Prüfbau[5] printability tester according to the ISO 2834 standard. No fountain solution was applied in the printing of the test strips, so changes in the structure of the underlying fibrous mat or of the moisture in the coating were avoided. The ink film was applied with one revolution of the applicator roller on the paper over a 20 mm wide strip by a rubber printing blanket. The circumferential speed of the application cylinder was 1 ms^{-1} and the application pressure was 20 Nmm^{-1}. The inks were applied on the papers keeping the transferred amount of ink constant at 1.4 gm^2. The resulting ink densities on the test papers are shown in Table 2.

Table 2: Print density values after application of constant ink load 1.4 gm^{-2} (without raster) using a Prüfbau printing wheel at 100 % targeted surface coverage

	Density			
	Cyan %	Magenta %	Yellow %	Black %
Trial point (kp)	C100	M100	Y100	K100
4	1.69	1.74	1.44	2.06
14	1.71	1.67	1.45	2.11
401	1.63	1.45	1.37	2.04
404	1.62	1.47	1.41	2.12
406	1.76	1.63	1.44	2.16

Ink oils were separately applied to demonstrate whether non-drying or drying oils, as found in offset inks, affected the measured gloss. This was done with a brush, resulting in an amount applied that was somewhat uncontrolled. The target, however, to get an even application on the papers appeared to be achieved.

3. Methods I

The methods applied were identified from a range of specific techniques to analyse structural roughness and optical interface roughness as well as gloss by a variety of geometrically different, illumination controlled glossmeters.

3.1 Profilometry

The stylus profilometer method is perhaps the longest established technique, consisting of recording the vertical displacement of a stylus tracking across the sample surface. Parameters of importance in this technique are:

(a) the statistical length and direction of scanning in respect to the subsequent gloss measuring geometries, and in detail the step length between data collection defining the lateral data point frequency (Figure 1),
(b) the dimensions of the stylus tip in relation to the lateral depth profile of the surface, as the roughness is a convolution of tip radius and surface feature width (Figure 2), and
(c) the pressure applied by the tip in respect to the compressibility of the surface and/or its susceptibility to damage (Figure 3)

In the same way as the stylus profilometer adopts a tracking protocol, so too does the optical profilometer, which in this case operates on the principle of planar interference under normal incidence.

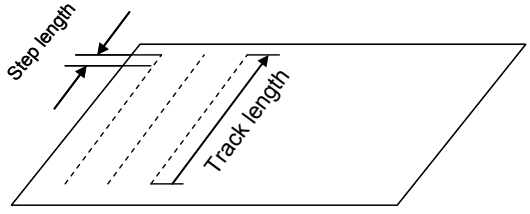

Figure 1: Profilometer sampling protocol showing track length and step length

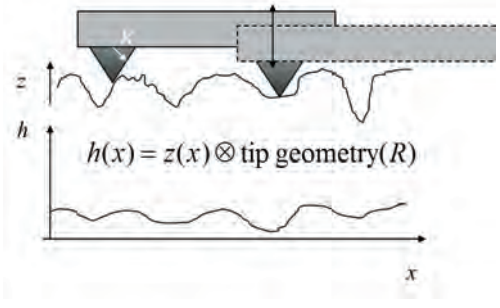

Figure 2: Convolution of profile and stylus tip leads to smoothing in the case where the tip is larger than the surface profile depth and lateral features

[5] Prüfbau Dr.-Ing. H. Dürner GmbH, Dr.-Herbert-Dürner-Platz, Peissenberg, Germany

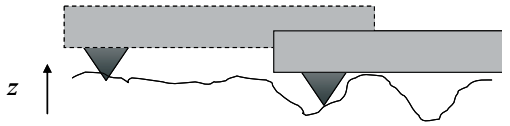

Figure 3: Effect of excessive pressure in relation to surface compressibility and susceptibility to damage

In the same way as the stylus profilometer adopts a tracking protocol, so too does the optical profilometer, which in this case operates on the principle of planar interference under normal incidence.

When light incidence is along the normal, then translucent layers act as partial reflectors and the profile measured is a convolution of the two surface reflected beams, that from the outer surface and that from the interface. Thin layer effects may lead to secondary interference between the two beams in combination with capture of some diffuse scattering (Figure 4).

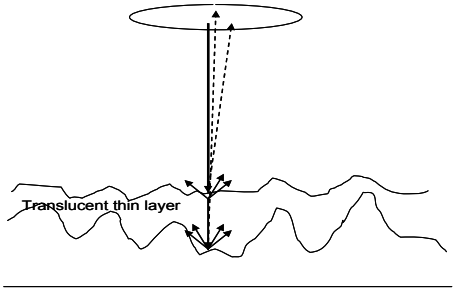

Figure 4: Normal incidence and interference potential between reflectance from the thin translucent layer boundaries

The principle of the optical interference profilometer is shown schematically in Figure 5. Alternatively, confocal methods could be used to eliminate such effects to some extent (Pawley, 2006).

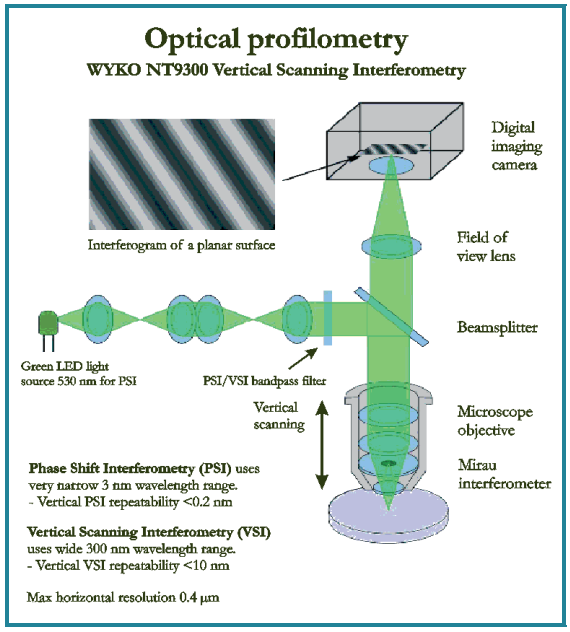

Figure 5: Schematic (taken from Veeco Terminal Drive, Plainview, NY 11803) of the monochromatic optical profilometer showing the constructional sensitivity to disturbance of the critical interferometric analysis

The details of the profilometers, including their respective sampling protocols and resolution, are given in Table 3.

Table 3. Parameters and specification of the stylus and optical profilometers

	Stylus	Optical interference
Stylus profiler:	Dektak 150+ from Veeco[6] (currently owned by Bruker-AXS)	WYKO NT9300 from Veeco (currently owned by Bruker-AXS)
Method:	Vertical displacement of tracking stylus tip: Radius, R = 2.5 µm	Illumination: peak wavelength 532.17 nm, FWHM 9.17 nm (VSI filter)
	Stylus cone angle: 42°	Vertical scanning interferometry (VSI) with vertically moving optics head
	Stylus force (weight): 5 mg	Optics used: 50x Mirau objective, numerical aperture (NA) 0.55 with 0.55x field of view extender
Resolution:	Offset resolution between data points = 0.01 % of value	Pixel resolution: 0.36 µm, diffraction limited resolution 0.49 µm
Calibration standard used:	4 255 nm +/- 59 nm (95% confidence limit) NIST traceable step height standard	8 471 nm +/- 69 nm (95 % confidence limit) NIST traceable step height standard
Measured offset:		0.5 % (<1 % guaranteed by the manufacturer)
Measured repeatability:	0.62 nm standard deviation (STD)	7.4 nm (STD)
Sampling:	5 samples covering 2 000 µm x 2 000 µm area	25 samples in a square grid covering 2 000 µm x 2 000 µm area
Sample length/area:	2 000 µm	230 µm x 170 µm (640 x 480 pixels)

(Table 3 continued on the following page)

[6] Dektak 150 and WYKO NT9300 are products of Bruker AXS GmbH, Östliche Rheinbrückenstrasse 49, Karlsruhe, Germany

(Table 3 continued from previous page)

	Stylus	Optical interference
Results reported:	*Ra* and *Rq* with corresponding standard deviations (*N*=5)	*Ra* and *Rq* with corresponding standard deviations (*N*=25)
***Ra* description:**	arithmetic average deviation from the mean line within the assessment length	arithmetic average deviation from the mean plane within the assessment area
***Rq* description:**	root-mean-square deviation from the mean line within the assessment length	root-mean-square deviation from the mean plane within the assessment area
Filtering used:	High pass filtering at 5 mm^{-1} to remove sample tilt and waviness and to retain roughness only	none, only plane fit to remove tilt

4. Results and discussion I

4.1 Comparing stylus and interference optical profilometry

A typical surface profile, obtained by optical profilemetry, of the sample types under study, is shown in Figure 6.

As can be seen from this topological representation, the roughness can be readily discerned as consisting of two major components, both microscopic and larger magnitude regions depending on the lateral scale of view. As we shall see later, this observation plays an important role in terms of the gloss observed as a function of incidence angle.

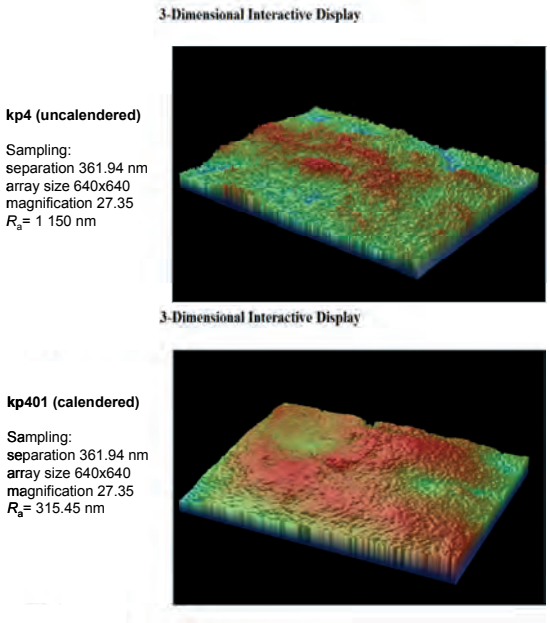

Figure 6: Laser interferometry profiles of paper sample kp4 before calendering (above) and kp401 (below) after calendering

By studying the correlation between stylus profile data and optical profile data, differences between structural and optically layered surfaces can be established.

Figure 7 shows a direct plot of stylus against optical roughness, R_a (see Table 3). The stylus data have been filtered using a high pass filter to remove the larger scale waviness of the sample. The filter was applied at 5mm^{-1}.

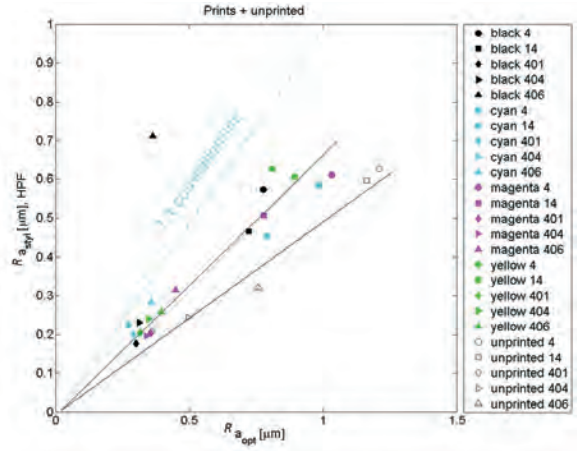

Figure 7: Correlations between stylus and optical interference profilometry - exemplifying the problem of defining the true "surface" of a micro porous material. HPF denotes high pass filtering which was used to filter the local waviness of the sample

Apart from the outlier (black 406), we see that the correlation data fall into two identifiable families, that of unprinted and that of printed surfaces. In the case of unprinted paper, the surface is a single interface, whereas in the case of printed paper the surface contains a thin translucent layer of high refractive index. In neither case does one obtain a direct absolute equivalence (dotted line), but what is important is that the correlations are essentially linear (R^2>0.9 across all sets). This means that the convolution problem of stylus size and surface roughness amplitude can be largely eliminated as a source of the separation between the unprinted and printed data sets, as if this were the case it would bias strongly toward rougher surfaces and create a curved relation increasingly biased toward the optical device, with the stylus progressively underestimating the roughness as the amplitude increased. Additionally, this should in principle apply to all surfaces irrespective of whether printed or unprinted. The relative difference between each line data set must, therefore, be predominantly related to another cause, and may arise from the action

of the higher refractive index of the ink layer acting in respect to its non-porous continuity to define a more consistent boundary in respect to the optical data than that of an unprinted surface. The unprinted sample presents a porous structure with an ill-defined "surface", such that the light can scatter randomly and/or penetrate in some cases deeply into the void structure. Basically, it is difficult to define a relevant optical "surface" for a porous structure. Thus, if we assume that the higher refractive index printed boundary provides the basic calibration curve between the two devices, we see that the optical device "overestimates" the printed structural roughness in relation to the mechanical stylus device, i.e. by considering the line representing the higher refractive index printed surfaces compared with that of the unprinted papers, as shown in Figure 7, we see a trend which shows a slow approach to the 1:1 correspondence the higher the refractive index of the surface. This may relate to the spatial filtering applied to the stylus data to eliminate the effect of sample tilt/corrugation, whereas the optical device includes this roughness element acting about the overall mean plane (see Table 3). The concept of how a paper surface becomes modified by printing is shown in the optical micrographs in Figure 8. The distribution of the coating layer and the inks is shown in the microscopic cross sections in Figure 9.

We now go on to establish the relationships between roughness and gloss, and, in turn, the geometry of gloss measurement and wavelength relationships with surface optical filtering in respect to the coloured ink layers.

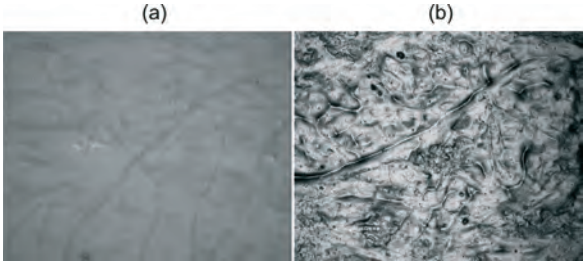

Figure 8: Optical micrographs of the nfgcc coated paper kp401 (a) unprinted and (b) black printed paper. The dimensions of sample represented in the micrographs were 0.7 mm for vertical direction and 0.9 mm for horizontal direction

Figure 9: Optical micrographs of printed paper in cross section kp401 (a) magenta, (b) black. The coating can be clearly seen beneath the ink layer

5. Methods II

5.1 Glossmeters

Measuring gloss and deriving a value for perceived quality is a complex undertaking. Issues, such as angle of observation and illuminating light characteristics, as well as collecting geometry to mimic the action of the human eye, make demands on device design. The result is that no single device can be considered the total solution, though day-to-day quality control standards are established. Thus, to develop new surfaces or to improve the perception quality of products it is becoming increasingly necessary to understand in more detail the links between the various optical factors and their impact on gloss. In all cases, the geometry is that of specular reflection, with angle of incidence equalling the angle of reflection, α, (Figure 10).

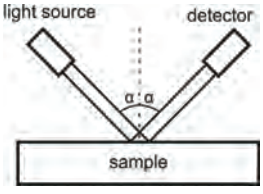

Figure 10: Specular reflection geometry as adopted by a standard glossmeter

The standard type of glossmeter used in the paper and printing industry adopts a range of angles to the normal, spanning usually α = 30°-75°, depending on the application, a white light illumination and a wide collecting angle. An example of such a meter is the Zehnter ZGM 1050[7]. The instrument adopts a halogen lamp illuminant A (ISO/CIE), representing a typical household tungsten

[7] Zehnter GmbH Testing Instruments, Gewerbestrasse 4, CH-4450 Sissach, Switzerland

filament, with a measuring accurancy of ± 1% over the gloss measuring range of 0-199.9 gloss units (GU). The Specim (Oulu, Finland) product, ImSpector V10E[8] imaging spectrograph, was used in gloss detection to complement the practical but otherwise less well defined standard glossmeter. The slit width is 30 μm and the spectral resolution 2.3 nm. This device works either in the visible (VIS) 380-800 nm, or in the very near infrared (VNIR) 400-1 000 nm spectral range, adopting a halogen lamp and diffuser to develop uniform illumination over the sample, developing a root mean square (rms) spot size of < 9 μm. The device thus detects specular reflection from a narrow line. Due to the prism-grating-prism element of the device it is possible to capture the image of the thin line, and from each pixel of the line a spectrum. The device detects more than 1 000 spectra instantaneously along the line. As a reflectance reference we used the gloss standard of the Zehntner glossmeter. The gloss was calculated from the averaged reflectance spectrum using 200 spectrum channels of the detector, applying to the standard illuminant C light source and human eye sensitivity curve V(λ).

Spectrophotometry is also exemplified in this work, adopting an integrating sphere. In this arrangement it is possible to measure complete integrated reflection intensity, i.e. diffuse reflection with specular reflection included. Subtracting the diffuse component by studying the variable intensity components as a function of wavelength, one obtains the specular reflection. The spectrophotometer used in this case was a Perkin Elmer Lambda 18[9] covering the spectral range 380-780 nm. The angle of incidence in this instrument is 8° to the normal, and so allows a comparison to be made between the standard glossmeter, the imaging spectrograph, both at higher incidence angle, and the case of close to normal incidence.

For normal incidence, an on-line diffractive optical element glossmeter, μDOG 1D (Oksman et al., 2008; Oksman et al., 2011) is used. The μDOG is a compact solid state device that is possible to use in an industrial environment, as can be seen in Figure 11.

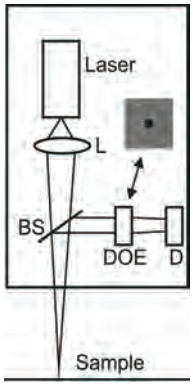

Figure 11: Principle of the diffractive optical element glossmeter (μDOG 1D), operating at 635 nm (Oksman et al., 2008; Oksman et al., 2011)

The light source of the μDOG 1D is a semiconductor laser, operating at 635 nm, and the reflected light is detected using a single-cell photodetector. The comparison of the μDOG 1D and a conventional glossmeter was already made by Oksman et al. (2011), however, the impact of printed layers acting as filtering medium was not considered in detail.

The gloss reading, G, is defined in the case of the μDOG 1D as:

$$G = \frac{I_{\text{sample}}}{I_{\text{reference}}} \times 100, \qquad [1]$$

where I_{sample} and $I_{\text{reference}}$ are light irradiances of the 4 × 4 light spot matrices recorded by the single-cell photodiode and measured from the sample and the gloss standard, respectively.

The mean gloss G_{mean} is defined as:

$$G_{\text{mean}} = \frac{1}{L}\int_{L} G(x)\mathrm{d}x, \qquad [2]$$

where $G(x)$ is a measured gloss profile and L is measurement length.

6. Results and discussion II

Correlation of the results from the standard glossmeter and the imaging spectrograph at 750 is shown in Fig. 12. Here we see a similar effect as was observed between the two profilometers, i.e. in this case again, the spectrograph forms a separate data set for the unprinted paper compared with the printed papers viewed at 75° angle of gloss detection. This was assumed in the case of the mechanical versus optical profilometers to illustrate the problem of defining an effective surface of a porous medium when viewed optically. However, now that we are comparing two optical methods, the assumption made previously in this case may not be the sole reason for the current data set separation, in that the measurement differences in this comparison are one of illuminant and angle of acceptance only - the spectrograph having a broad spectral illuminant C with reflected light captured only in a narrow aperture slit versus the also broad spectrum illuminant A in the standard and a wider ac-

[8] ImSpector is a product name of Spectral Imaging Ltd., Teknologiantie 18A, 90571 Oulu, Finland

[9] Perkin Elmer, 940 Winter Street, Waltham, Massachusetts 02451, USA

ceptance angle. The common factor between the spectrograph and the interferometric profilometer are, on the other hand, the narrow acceptance angle only. Thus, it remains to consider the angle of incidence and the potential impact of monochromatic illuminance in respect to their interactions with high refractive index layers, such as a colour filter ink layer. Inhomogeneities in refractive index and filter path length may also play a role in respect to variation of the results. The subsequent analysis methods are designed to answer these questions.

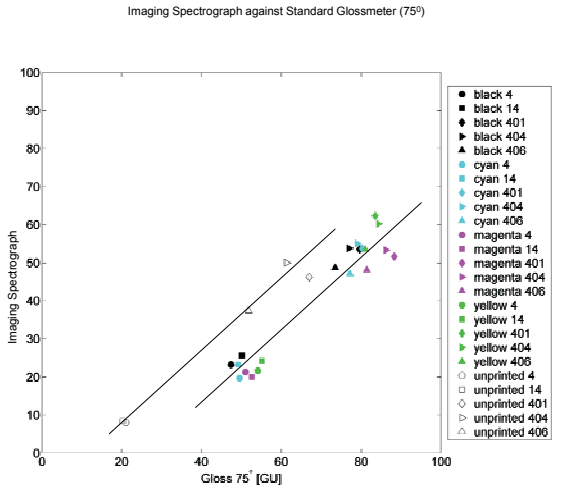

Figure 12: Correlation of the imaging spectrograph (narrow acceptance angle) against a standard glossmeter (wide acceptance angle)

To take this correlation study further, a comparison between the roughness and observed gloss was made for each of these gloss measuring devices - the imaging spectrograph and the standard glossmeter. It is, therefore, revealing to plot the gloss values against the measured roughness. This is done for both the standard glossmeter and the imaging spectrograph in Figures 13, 14, 15 and 16, in which the roughness is expressed as both the optical interference roughness and the structural stylus roughness, respectively.

Contrasting Figures 13 and 14, it is clear that the standard glossmeter maintains the separate data set behaveour in relation to the optical profilometer, but that the narrow acceptance angle imaging spectrograph does not. Therefore, viewing either roughness or gloss at large oblique incidence angle and small acceptance angle links the gloss property with that of roughness, but wider acceptance angle and broader wavelength range leads to a different response depending on the surface refractive index change (increased refractive index with the print as opposed to the unprinted paper surface) and thin layer optical behaviour.

To identify which of these two parameters (or both) defines the controlling link between roughness on this scale and standard gloss, the behaveour in relation to mechanically measured roughness is considered.

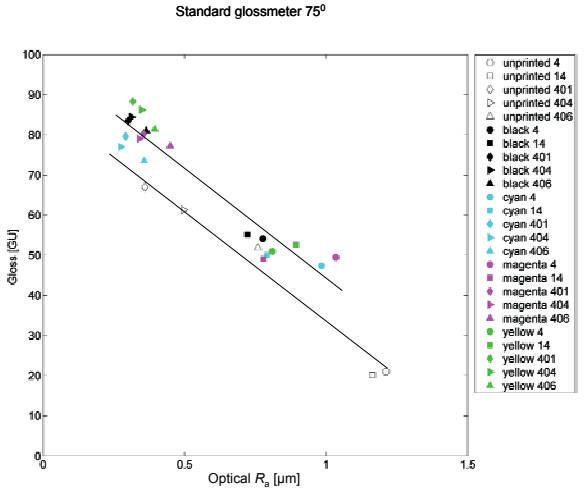

Figure 13: Standard gloss (75°) plotted against optical roughness profilometry

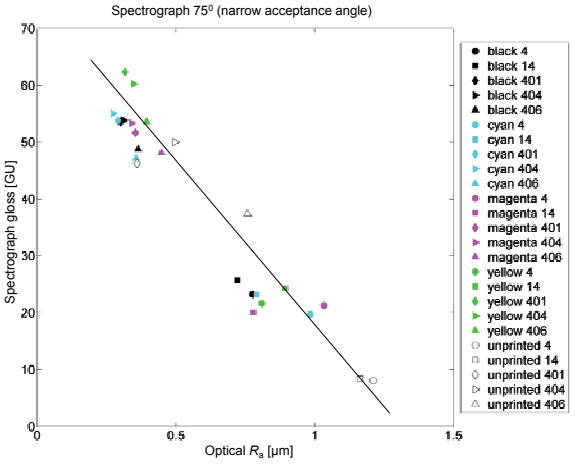

Figure 14: Imaging spectrograph (75°) gloss (narrow acceptance angle) plotted against optical roughness profilometry

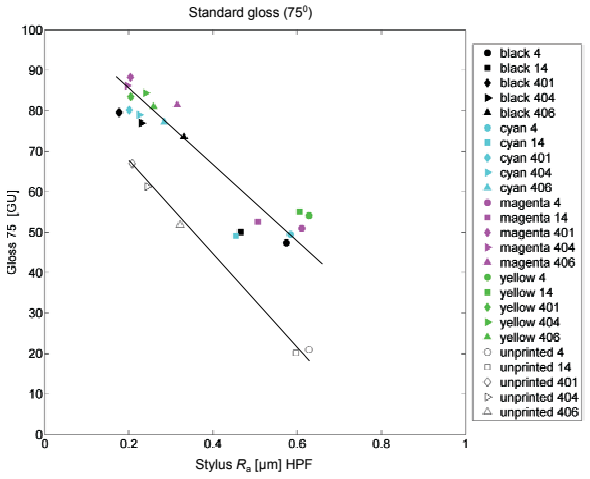

Figure 15: Standard gloss as a function of structural roughness determined using the stylus profilometer - separation of printed and unprinted is maintained

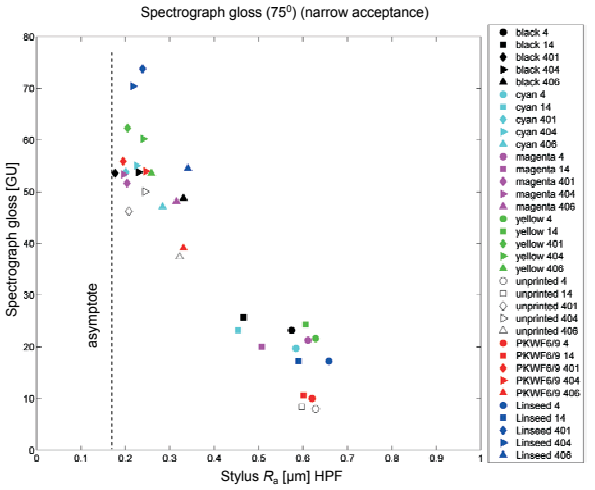

Figure 16: Reduced differentiation between printed and unprinted surfaces using the narrow acceptance angle, when displayed as a function of mechanically measured surface roughness. Newly, oil only has been included

As was seen previously in the case of optical profilometry (Figures 13 and 14), the oblique angle broad spectrum and wide acceptance geometry of the standard glossmeter retains a differentiation between the gloss and roughness parameters for printed and unprinted papers (Figure 13), whereas the oblique, narrow acceptance geometry of the spectrograph shows much reduced differentiation (Figure 14). In the case of the stylus measurement (Figure 15) we must recognise the potential for the convolution between stylus tip (machine function) and the surface profile (Figures 2 and 3) to introduce a smoothing function on the rougher surface, which might account for the slight remaining tendency to differentiate between the surfaces in the case of the spectrograph, though as can be seen in Figure 16 this differentiation is tending toward becoming statistically insignificant.

Interestingly, in Figure 16, it can be seen that the roughness values reach an asymptote in respect to high gloss values, and this illustrates the limitation of the stylus in respect to identifying the resolution of the finest scale roughness and is a clear indication of the limitation of the mechanical method when comparing with the scale of optically relevant surface roughness factors. However, whether the roughness is determined by optical interference or by mechanical means, there remains a difference between the gloss-roughness relations depending on acceptance geometry when a broad spectrum illuminant is used (Figures 13 and 15).

Newly amongst the data in Figure 16 are additional points relating to the application of typical ink oils, i.e. mineral oil (PKWF6/9) and linseed oil. Optical profilemetry was considered unreliable when measuring such inhomogeneous transparent materials as oil-treated uncoated paper, and so the data are confined to the mechanically measured surface profiles. Mineral oil is a non-oxidising diluent, whereas linseed oil, used to solubilise lower molecular weight resins, becomes oxidised and forms a coherent polymerised layer. Clear to see is that the dried applied linseed oil tends toward higher gloss values than the mineral oil, which data in turn lie close to those of the unprinted values.

6.1 Impact of incidence angle

The discussion above has concentrated on the factors affecting the measured gloss as a function of the acceptance geometry at oblique angle of incidence (75°). First of all a check was made to see if this relationship was retained at the less oblique angle (60°). The plot in Figure 17 shows the relationship between the less oblique observation angle and the mechanically determined roughness. The curvature of the data trends allows us to conclude that the reduced angle of incidence accentuates the sensitivity to the finer scale surface roughness and retains the differentiation of the printed versus unprinted surfaces. This observation now generates a firmer link with the wider acceptance angle in the oblique geometry as a convoluting factor between Fresnel planar reflection, associated with the larger scale roughness, and diffuse reflection arising from the finer scale microroughness, as discussed in relation to papers by Gate and Leaity (1991) and Elton (2009), i.e., the measurement becomes more sensitive to the finer scale roughness as the angle of incidence decreases. The use of the stylus, which limits sensitivity to the finest scale roughness, serves to confirm this as the asymptote becomes more prominent, illustrated by the more curved relationship in Figure 17.

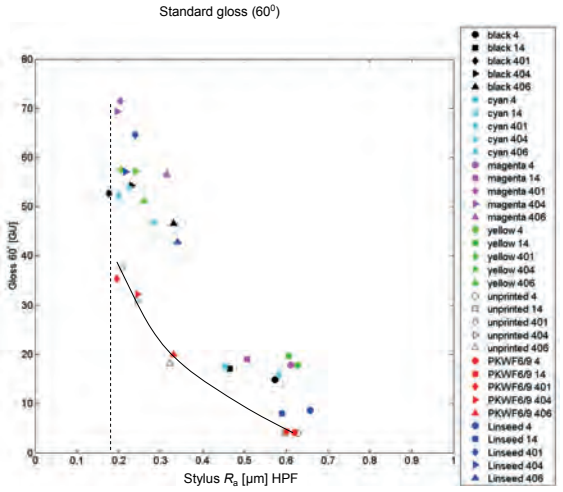

Figure 17:
Less oblique incidence and wide acceptance angle begins to display more clearly the convolution of different scales of roughness in respect to gloss measurement accentuated due to the fine scale roughness limit of the stylus profilometer

Furthermore, in Figure 17, it can be seen that the two oils once again fall each into one of the two classes of data, i.e. the mineral oil effectively follows the class of unprinted surface, whereas the linseed oil with its varnishing effect follows the class of printed surfaces. This confirms the impact of the nature of the surface and the change from a high component of diffuse reflectance for the unprinted surfaces to that of planar Fresnel reflectance associated with the higher refractive index and finer scale smoothness of the printed surfaces. The spectrophotometer with integrating sphere is used to provide broad spectrum specular gloss values at an incidence angle closer to the normal, namely 8°. We can see in Figures 18 and 19 that, independent of roughness measure, the differentiation between the gloss of unprinted and printed surfaces becomes even greater, supporting the roughness convolution principle for the finescale microroughness and the larger scale roughness of the sheet, seen already emerging above in Figure 17. Interestingly, the cyan surface now starts to separate from all the other printed surfaces. Since this spectrophotometer uses also a broad spectrum illumination (average value from the spectrophotometer wavelength scan), we must conclude that either cyan has more microroughness than the other prints or it is more transmitting/transparent to the light, such that it samples to some extent the underlying microroughness of the ill-defined substrate surface.

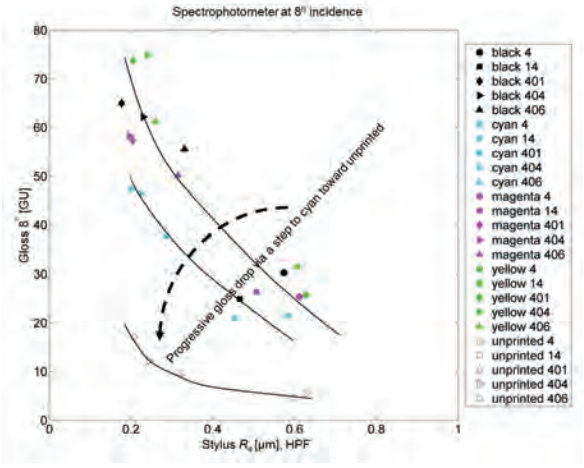

Figure 18: Approaching normal incidence (8°) the differentiation between unprinted and printed gloss becomes exaggerated, and there is indication that cyan acts as a transition optical structure

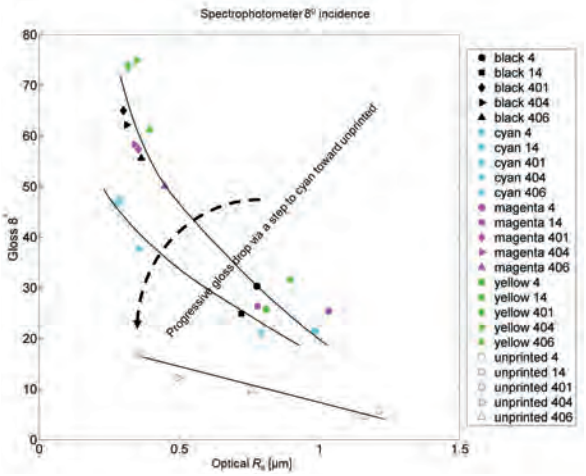

Figure 19: As for the correlations in Figure 18, the thin layer cyan print forms a transition between the remaining printed samples and the unprinted result

From Figure 20 it is clear that the wider angle of acceptance is effectively measuring a higher gloss and so must also be accepting more diffuse scatter. Conversely, since the ratio of specular to diffuse scattering at low angles of incidence decreases (Beckmann and Spizzichino, 1963), the specular component is also relatively decreasing as the normal is approached.

Figure 21 supports this latter assumption as the near normal purely specular data of the spectrophotometer

are compared with narrow acceptance angle on the imaging spectrograph at 75°. The linear relationships show the exclusion of the diffuse component, but the progressive separation of the cyan toward the correlation

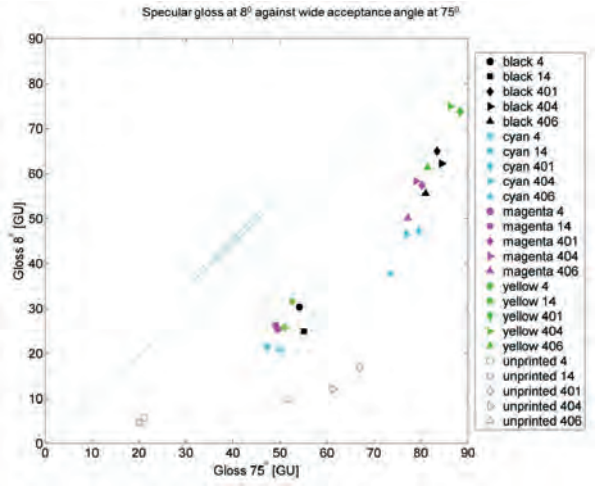

Figure 20: Comparing the broad spectrum illumination approaching normal incidence (8°) with the wide acceptance angle broad spectrum illuminant A standard glossmeter we see the clear separation for the unprinted sheets, i.e. the near normal incidence, at the specular only definition of the spectrophotometer, falls below that of the higher angle of incidence wide angle acceptor

The term transmittance, T, in this case of gloss measurement, is considered to be the complement of the specular reflectance, $R_{specular}$, i.e. $T = 1\text{-}R_{specular}$, which, in turn, is defined as a function of incidence angle and the surface refractive index contrast, given by the well-known Fresnel equations. Thus, for an optically thin layer, such as ink, if the refractive index contrast of one colour is lower than the rest, then the transmittance increases. The corollary of this is, that cyan likely has a lower refractive index than the other inks. This is confirmed when we study Figure 22, which shows the real component of the refractive index, n, plotted against wavelength for offset cyan and magenta ink as dried ink layers - the data being taken from the work of Niskanen et al. (2007) and Peiponen et al. (2008). By integrating under the respective refractive index curves as a function of wavelength we can achieve the following ratio,

$$\frac{\int_{400}^{800} n_{\text{cyan}}(\lambda)\mathrm{d}\lambda}{\int_{400}^{800} n_{\text{magenta}}(\lambda)\mathrm{d}\lambda} \approx 87\% \qquad [3]$$

which provides a rough impact factor of the refractive index in respect to specular contribution versus transmittance.

Given that transmittance through an applied optically thin layer at near normal incidence can be a reason for apparent loss of gloss at a given layer surface smooth-

of the ill-defined surface of the unprinted sheet leads the observer to consider the role of transmittance of the cyan. In both cases the illuminance spectral range is relatively broad.

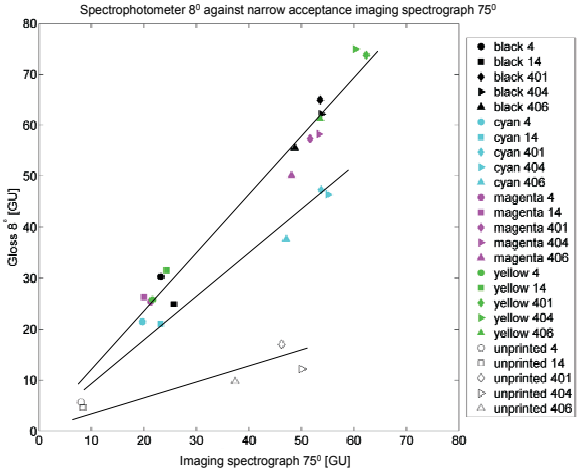

Figure 21: Excellent linear relationships between the near normal (8°) specular reflectance and narrow acceptance angle at 75°. The linearity confirms the exclusion of the extra diffuse reflectance, seen with the wide acceptance angle previously, from these gloss measurements, but the separation of cyan and the unprinted surfaces from the rest accentuates the probable role of transmittance

ness, due to the combination of surface and interface roughness with the underlying substrate, the effect of colour filtering as an additional factor when viewing at normal incidence needs to be included.

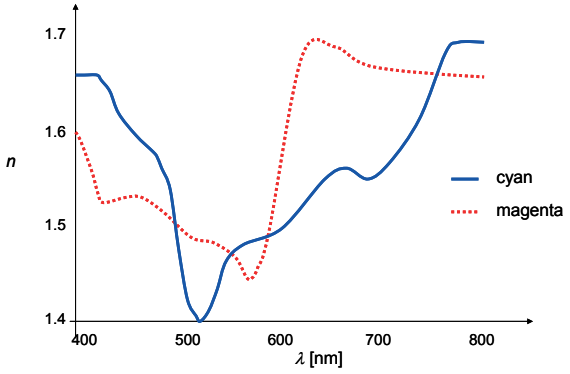

Figure 22: Refractive index, n, of dried layers of cyan and magenta offset inks - taken from (Niskanen et al., 2007; Peiponen et al., 2008)

Normal incidence using monochromatic illumination and narrow acceptance angle is provided by the diffractive optical element glossmeter, μDOG. In this apparatus, confinement to normal incidence is a geometrical necessity for compactness and the maintenance of alignment for the diffractive condition.

Correlation between average surface roughness obtained with low coherence optical tomography and average gloss obtained by the diffractive element meter for

matt and glossy black print was studied in Silvennoinen et al. (2008) and Juuti et al. (2007) for slow and fast setting ink. Here we focus on the impact of the thin layer colour filtration when transmittance occurs.

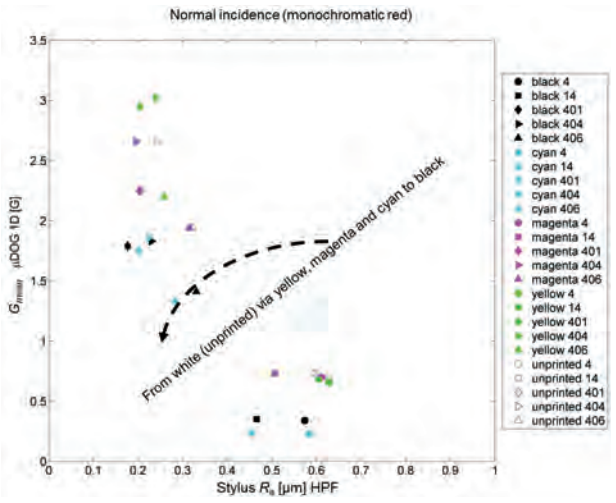

Figure 23: Normal incidence with monochromatic light introduces a colour filter effect. Due to the drift across the print colours, relating to the filter effect, a single line cannot be applied as the data no longer cluster into subgroup families

Tracing the gloss values in Figure 23 as a function of ink colour, it can be seen that the gloss relationship to roughness drops as a function of the colour filter. The unprinted white paper has the highest gloss set, whereas moving progressively form white through yellow, magenta and cyan progressively filters the returned intensity of the monochromatic red illuminance, with the farthest spectral filter blue returning gloss values similar to the effective high/total absorbance black. The effects of transmittance and resulting absorbance (filtering) explain the at first surprising result that printed papers can have a lower apparent gloss than unprinted papers when using this device (Oksman et al., 2008; Oksman et al., 2011), which contradicts both standard glossmeter values and the human perception.

Thus, the colour filter effect of thin layer, optically refractive surfaces, must be considered when viewing with instruments limited in spectral range at normal or close to normal incidence. Once again the works of Niskanen et al. (2007) and Peiponen et al. (2008) provide us with the absorbance comparison between cyan and magenta. The broad band absorbance of cyan (Figure 24) clearly shows the impact on red light as used by the µDOG.

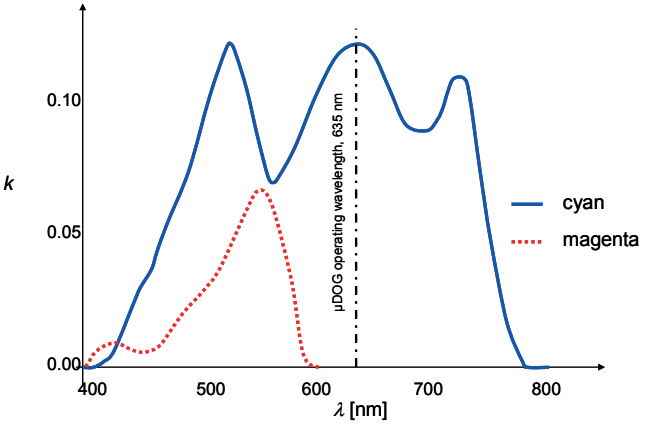

Figure 24: Absorbance, k, affects the extinction of light during transmittance, with cyan having a broad VIS spectrum absorbance - taken from (Niskanen et al., 2007; Peiponen et al., 2008). The operating wavelength of the µDOG 1D at 635 nm is shown (Oksman et al., 2008; Oksman et al., 2011)

6.2 Nature of the roughness being considered

In the case of Gaussian height distribution, the specular reflectance obeys also a Gaussian function depending on the angle of light incidence, surface roughness and the wavelength of the light according to the formula of Beckmann and Spizzichino (1963).

The straight line relationships between the square root of the logarithm of gloss and the mean roughness deviation, as shown in Figure 25, suggests that the surface can be realistically described as having a Gaussian distribution of roughness amplitude about the local mean

plane either defined by optical interferometry or by stylus profilometry. This was also proposed by Gate and Leaity (1991) and by Elton and Preston (2006a) for unprinted paper. We note that in the work of Elton and Preston (2006b) it is assumed that the light is monochromatic, whereas in the case of the standardised glossmeter white light is used. Nevertheless, the signal of the standard gloss-meter seems to fit well with the theoretical model of Beckmann and Spizzichino (1963).

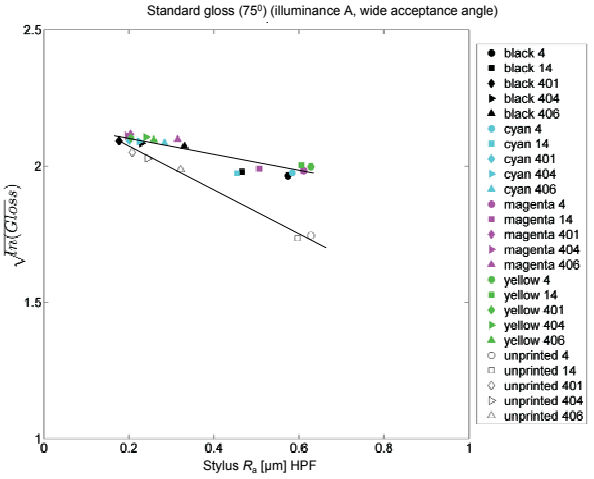

Figure 25: Evidence for the Gaussian distribution of surface roughness amplitude due to the linearity of the square root logarithmic relationship of gloss with roughness

7. Conclusions

1. The definition of a practically realistic surface in respect to a porous medium takes different forms depending on the method used to define the surface profile. Impact of the convolution of the machine function with the surface profile is potentially more likely when using a mechanical contact device, such as a stylus, compared to an optical method, though the nature of the surface can affect the result of optical devices.
2. Surface roughness scale, both in terms of amplitude and lateral distribution, affects the observed gloss depending on the system used to determine that gloss. Comparing less oblique incidence, together with a broad spectral range of illuminance and narrow acceptance, versus more oblique incidence and wide acceptance angle (Figure 26) sensitises the measurement toward the inclusion of diffuse reflectance associated with small scale roughness (approximating Rayleigh scattering). A mechanical profile filtering, such as that generated as a function of stylus size, can be used to highlight this dependence. Narrowing of acceptance angle and resort to monochromatic illumination would reduce the influence of the small scale microroughness at oblique angle (Gate and Leaity, 1991).
3. At acute or normal incidence (Figure 27), the thin layer structure of a high refractive index filter, such as an ink layer, influences the amplitude of return signal of monochromatic illuminance depending on the wavelength in relation to the colour of the filtering thin layer. Additionally, at higher transmittance, some inclusion of the underlying substrate roughness component occurs.

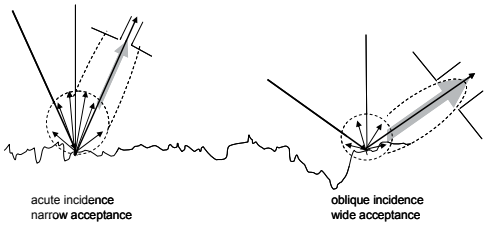

Figure 26: Dependence of gloss on contribution of diffuse reflectance

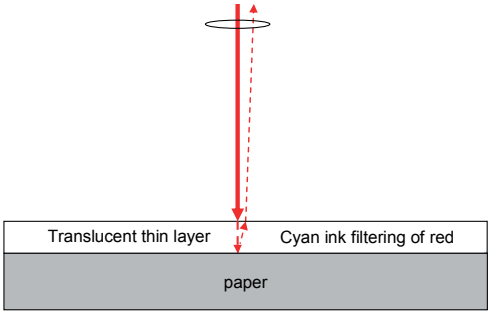

Figure 27: Filter effect of thin translucent layer at normal incidence

In conclusion, there are recognisable implications arising in terms of describing what is perceived by the human eye as gloss in relation to what is measured by various devices. By applying combinations of different illuminations and geometries, it is possible to deconvolute specular and diffuse reflectance. This is of particular importance when considering the quality of thin layer high refractive index translucent structures, such as decorative finishes, lacquers or, as exemplified in detail here, printed media. The impact of these findings extends to other areas of research, such as the use of NIR methods to determine moisture content, in that the substrate will return a value reduced by the optically thin layer applied according to the colour (filtering wavelength) of the material within that layer. Thus, surface layer applications can behave as bandwidth filters when observed under normal or close to normal incidence.

Acknowledgements

The financial support of TEKES, the Finnish funding agency for technology and innovation, is gratefully acknowledged. This work was carried out as part of the project THEOS, "Thermal Effects and Online Sensing".

References

Beckmann, P. and Spizzichino, A., 1963. *The Scattering of Electromagnetic Waves from Rough Surfaces.* Oxford: Pergamon.

Béland, M.-C., 2001. *Gloss variation of printed paper: relationship between topography and light scattering.* Doctoral thesis, KTH Royal Institute of Technology, Stockholm.

Elton, N. J., 2009. Optical measurement of microroughness of pigment coatings on rough substrates. *Measurement Science and Technology*, *20(025303), doi: 10.1088/0957-0233/20/2/025303*.

Elton N. J. and Preston J. S., 2006a. Polarized light reflectometry for studies of paper coating structure Part I. Method and Instrumentation, *TAPPI Journal*, 5(7), pp. 8-16.

Elton, N. J. and Preston, J. S., 2006b. Polarized light reflectometry for studies of paper coating structure Part II. Application to coating structure, gloss and porosity, *TAPPI Journal*, 5(8), pp. 10-16.

Gane, P. A. C. and Hooper, J. J., 1989. Coating profilometry: an analysis of coating colour-basepaper interactions. *Fundamentals of Papermaking, Trans. of the Ninth Fund. Res. Symp., vol II*, London: Mech. Eng. Publ. Ltd., pp. 871-893.

Gate, L., Windle, W., and Hine, M., 1973. The relationship between gloss and surface microstructure of coatings. *TAPPI Journal*, 56(3), pp. 61-65.

Gate, L. F. and Leaity, K., 1991. New Aspects on the Gloss of Coated Paper, *TAPPI 1991 Coating Conference Proc.*, pp. 473-478.

International Standards Office and International Commission on Illumination, 1999/1998. *ISO 10526:1999/CIE S005/E-1998,* CIE *Standard Illuminants for Colorimetry.* Joint ISO/CIE Standard.

Juuti, M., Prykäri, T., Alarousu, E., Koivula, H., Myllys, M., Lähteelä, A., Toivakka, M., Timonen, J., Myllylä, R. and Peiponen, K.-E., 2007. Detection of local specular gloss and surface roughness from black prints. *Colloids and Surfaces A: Physicochem. Eng. Aspects*, 299, pp .101-108.

Lepoutre. P., 1989. The structure of paper coatings: an update. *Progress in Organic Coatings*, 17, pp. 89-106.

MacGregor, M. A., Johansson, P.-Å. and Béland, M.-C., 1994. Measurement of small-scale gloss variation in printed paper: topography explains much of the variation for one paper. *Proc. TAPPI 1994 International Printing and Graphic Arts Conference*, pp. 33-43.

Niskanen, I., Räty, J., Peiponen, K.-E., Koivula, H. and Toivakka, M., 2007. Assessment of the complex refractive index of an optically very dense solid layer: Case study offset magenta ink. *Chemical Physics Letters*, 442, pp. 515-517.

Oksman, A., Juuti, M., and Peiponen, K.-E., 2008. Sensor for the detection of local contrast gloss of products. *Optics Letters*, 33(7), pp. 654-656 .

Oksman, A., Kuivalainen, K., Tåg, C.-M., Juuti, M., Matila, R., Gane, P.A.C. and Peiponen. K.-E., 2011. Diffractive optical element based glossmeter for the on-line measurement of normal reflectance on a printed porous coated paper. *Journal of Optical Engineering (USA): Optical Engineering*, 50(4), 043606, 9 pp.

Pawley, J.B. (ed.), 2006. *Handbook of Biological Confocal Microscopy* (3rd ed.). Berlin: Springer. ISBN 038725921X.

Peiponen, K.-E., Kontturi, V., Niskanen, I., Juuti, M., Räty, J., Koivula, H. and Toivakka, M., 2008. On estimation of complex refractive index and colour of dry black and cyan offset inks by a multi-function spectrophotometer. *Measurement Science and Technology*, 19, pp. 115601-7.

Preston, J. S. and Gate, L. F., 2005. The influence of colour and surface topography on the measurement of effective refractive index of offset printed coated papers. *Colloids and Surfaces A: Physicochemical and Engineering Aspects*, 252(2-3), pp. 99-104. DOI: 10.1016/j.colsurfa.2004.10.002.

Rousu, S., Gane, P. and Eklund, D., 2005. Print quality and the distribution of offset ink constituents in paper coatings. *TAPPI Journal*, 4(7), pp. 9-15.

Silvennoinen, R., Juuti, M., Koivula, H., Toivakka, M. and Peiponen, K.-E., 2008. Diffractive glossmeter for measurement of dynamic gloss of prints. *TAGA Journal*, 4(2), pp. 59-71.

Wennerberg, A., Ohlsson, R., Rosén, B.-G. and Andersson, B., 1996. Characterizing three-dimensional topography of engineering and biomaterial surfaces by confocal laser scanning and stylus techniques. *Medical Engineering and Physics*, 18(7), pp. 548-556.

Xu, R., Fleming, P.D. III, Pekarovicova, A. and Bliznyuk, V., 2005. The effect of ink jet paper roughness on print gloss. *Journal of Imaging Science and Technology*, (49)6, pp. 660-666.

JPMTR 006 | 1109
UDC 327.2:655.332

Technical paper
Received: 2011-07-27
Accepted: 2012-04-16

Bidirectional flexible mouldable electroluminescent lamps fabricated by screen printing

Karin Weigelt[1], *Eifion H. Jewell*[2], *Chris O. Phillips*[3], *Timothy C. Claypole*[3], *Arved C. Hübler*[1]

[1] TU Chemnitz, Chemnitz, Germany
[2] Baglan Innovation Centre, Swansea, UK
[3] WCPC, Swansea, UK

E-mails: name.surname@mb.tu-chemnitz.de
E-mail: e.jewell@swansea.ac.uk
E-mails: c.o.phillips@swansea.ac.uk; t.c.claypole@swansea.ac.uk

Abstract

Flexible thick film electroluminescent devices illuminating into both directions were fabricated using screen printing. The lamps are based on commercially available materials of electroluminescent phosphors and transparent conducting and dielectric inks. The bidirectional illuminating lamps compare favourably to unidirectional illuminating lamps regarding the emission spectra and the luminance. The emission is uniform in both directions and the luminance is in the range of unidirectional lamps. The printed bidirectional lamps offer a means of producing thin flexible illumination which may be advantageous to the lighting designer.

Keywords: flexible lighting, electroluminescence, bidirectional illumination

1. Introduction

The term electroluminescence (EL) refers to the emitting of electromagnetic radiations (visible or near visible) due to the application of an electric field (AC or DC) (Vij, 2004). There are two different physical principles, which cause the light emission. Light emitting diodes (LEDs) or organic light emitting diodes (OLEDs) relies on the emission of light due to injection of electrons and holes near the p-n-junction. In contrast, thin and thick film EL is based on the acceleration of electrons by strong electric fields causing the excitation by impact (Mauch, 1996).

OLED devices potentially offer large area flexible lighting, but the commercial realisation of such devices is 10 years away due to challenges in the manufacturing stages and barrier requirements of the technology (Hecker, 2009).

In contrast, thick film printed EL is a mature technology and is used in LCD backlighting, promotional advertising and mood lighting (Hecker, 2009; Zovko, 1999). In comparison to OLED, the luminance of EL is lower (limited to approximately 250 cd m^{-2}), the lamps operate at high voltage (100-200 V), the luminance half life is typically 3 000 hrs and colour range is limited at higher luminance levels. EL-lamps are usually fabricated by screen printing (Ono, 1995). The typical build-up consists of four layers: the transparent electrode, the phosphor layer, the dielectric and the rear electrode, Figure 1(a).

A typical phosphor material is zinc sulphide doped with transition metals or rare-earth ions defining the emission spectrum of the material. The colour of the lamps can be changed by blending two or more phosphors (Zovko, 1999; Yang, 2003) or by combining one phosphor with various coloured dielectrics (Philips, 2009). The dielectric material is usually a suspension of high dielectric constant particles (such as barium titanate) in a high voltage breakdown binder. Phosphor and dielectric materials are commercially available as material systems from various suppliers. Silver inks are typically used as the rear electrode. These are chosen for their widespread availability, conductivity, low impedance and stability.

The most common material used as transparent electrode is indium tin oxide (ITO) as this provides the highest transparency and conductivity of any material (Kirckmeyer, 2005). There has been considerable interest in the development of transparent conductors across many photonic industries. The key drivers for removing the ITO in EL are cost, ease of patterning, improved flexibility and improved adhesion. Conductive polymers such

poly(3,4-ethylenedioxythiophene): poly (styrene sulphonate) (PEDOT:PSS) are becoming options for the transparent conductor. There has been rapid improvement in the transparency and conductivity over the last 5 years (Nardes, 2008). At present however, the conductivity of the PEDOT:PSS is significantly lower than ITO (between 5 and 100 less for the same transparency). Commercial printable formulations are becoming available and their use as transparent electrodes in a number of applications including OPV (Winther-Jensen, 2006) and OLED (Harkema, 2009) is being investigated. In addition to counter the lower conductivity there have been developments in printing a micro-scale conductive silver grid onto the PEDOT:PSS layer to increase conductivity, while retaining the transparency of the electrode (Deganello, 2010). This allows the fabrication of large-area EL-lamps without ITO. Furthermore, EL-lamps with Carbon Nanotubes (CNTs) as transparent conductor have been presented recently. (Schrage, 2009; Kim, 2009).

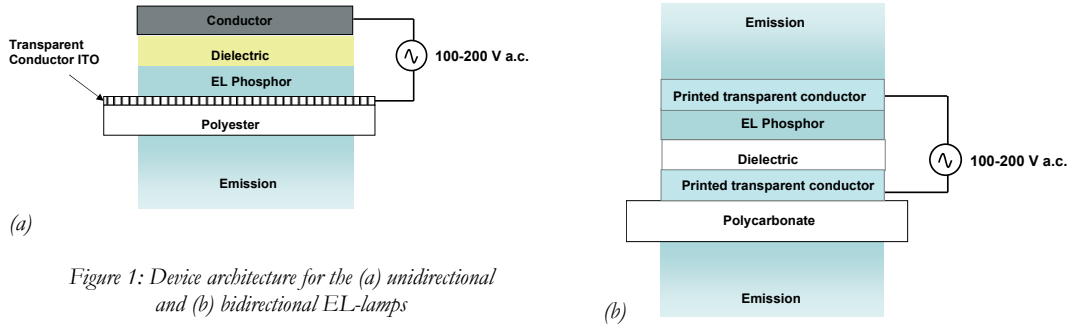

Figure 1: Device architecture for the (a) unidirectional and (b) bidirectional EL-lamps

The improvement in conductivity and transparency of printable electrodes is particularly interesting as it potentially allows the production of bidirectional lighting where light is emitted from both surfaces of a single film. Possible products based on this technology include illuminated signs, decorative room dividers or shelves. The development programme presented was developed with the subsequent fabrication steps in mind. Such a development is already being perceived with OLED lighting (Uchida, 2006; Jung, 2008) but this requires significant alteration of the ITO in order to meet the low work function requirements of the cathode which is typically made from calcium deposited under vacuum. This technology is at a much earlier stage in development.

A further possibility provided by the ductile nature of the PEDOT:PSS (Langa, 2009) compared to the brittle ITO is the integration of printed lamps into three dimensional designs or even plastic parts by film insert moulding, also known as in-mould decoration. In-mould unidirectional emission technology is being comercialised for applications such as in car lighting. Bidirectional mouldable lamps will enable the creation of various novel light-emitting 3 dimensional objects. Such a development would be difficult with OLED technology as there would also be significant challenges in maintainning the integrity of thin films (typically around 200 nm) under stress which are critical to correct function of the OLED lamp.

2. Experimental method

Screen printing was used for the fabrication of the EL-lamps. This is the process of choice for EL manufacture as it allows the large (up to 25 μm) phosphor particles to be deposit, it is able to lay a thick dielectric film which is able to withstand the high AC driving voltage and it allows cost-effective manufacture. Screen printing has the added benefit that it is a common process used in the film insert moulding industry. All the printing steps were done on a semiautomatic screen printer (DEK 248) using polyester screens with a mesh number of 61 filaments/cm, a mesh-opening of 64 μm and a mesh angle 45°. The printing speed was 70 mm s^{-1} and the snap-off 2.5 mm, i.e. the distance between the mesh and the substrate.

A test layout including square test lamps with a side length of 30 mm was used. Hence, the luminescent area is 9 cm^2. Figure 1 (b) shows the device architecture used for the bidirectional EL-lamps. As substrate a 200 μm polycarbonate film from Bayer MaterialScience (Makrofol DE 1-4 (one side glossy and one side very fine matt) was used. This material was chosen as it is most suitable for subsequent film insert moulding processes. The light transmission of 200 μm thick Makrofol DE14 is quoted as 91% at 490 nm and remains almost constant in the range of visible light.

The front electrode was printed on the glossy side with a water-based dispersion of poly(3,4-ethylenedioxythiophene) doped with poly (styrenesulfonate) (PEDOT : PSS) from Agfa (Orgacon EL-P3042). The printed layer was cured in a belt dryer for 3 minutes at 100 °C. As phosphor two commercially available blue-green high brightness phosphors were used: DuPont Luxprint 8152B and Gwent C2061027D13. Curing parameters were 5 minutes and 100 °C. To realise bidirectional EL lamps,

one challenge was to find an appropriate transparent dielectric. The encapsulant material DuPont 5036 (a clear ink with a break-down voltage greater than 20 V μm^{-1}) meets those requirements. Two layers of this material were printed one upon the other and each cured for 5 min at 100 °C. Finally, another layer of Agfa Orgacon EL-P3042 was deposited and cured as rear electrode. For the evaluation of the EL lamps illuminating in both directions (hereinafter referred to as bidirectional lamps), reference lamps (hereinafter referred to as unidirectional lamps) were fabricated using the same phosphor as for the bidirectional lamps in combination with compatible dielectrics and silver inks for the rear electrode. The fabrication procedure was the same as for the bidirectional lamps. Separate lamps were produced using both DuPont and Gwent inks. For the DuPont unidirectional lamp the white barium titanate filled dielectric Du Pont Luxprint 8153 and the silver ink DuPont 5029 were used. The materials used for the unidirectional Gwent lamp are the pink dielectric Gwent D2090130D5 and the Gwent flexible silver ink G2090210D12. The material combinations for all samples are summarised in Table 1.

The EL devices were driven by a sinusoidal voltage produced by a power supply for EL lamps LM30 from Light & Motion. The luminance and the EL spectra of the lamps were measured by a Gretag Macbeth Spectrolino spectrophotometer measuring in emission mode with a measurement spot size of 4 mm. When measuring the bidirectional lamps, a matt black (L*<4) sub surface material was placed under the lamp. The capacitance was measured using an Agilent E 4980 A Precision LCR Meter. Printed film thicknesses and topography were measured using white light interferrometry.

Table 1: Materials used for bidirectional and unidirectional lamps

Layer	Gwent bidirectional	DuPont bidirectional	Gwent unidirectional	DuPont unidirectional
Rear electrode	Agfa Orgacon EL-P3042	Agfa Orgacon EL-P3042	Gwent C2090210D12	Dupont 5029
Dielectric	DuPont 5036	DuPont 5036	Gwent D2090130D5	DuPont Luxprint 8153
Phosphor	Gwent C2061027D13	DuPont Luxprint 8152B	Gwent C2061027D13	DuPont Luxprint 8152B
Front electrode	Agfa Orgacon EL-P3042	Agfa Orgacon EL-P3042	Agfa Orgacon EL-P3042	Agfa Orgacon EL-P3042

3. Results and discussion

EL spectra of the unidirectional and bidirectional lamps at the applied voltage of 140 V and the frequency 830 Hz are shown in Figure 2.

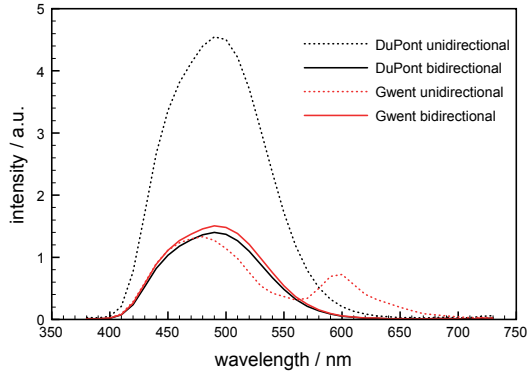

Figure 2: Spectral output of the lamps for each build and material manufacturer

The emission peaks of the DuPont unidirectional lamp and both bidirectional lamps are in the blue-green part of the visible spectrum at 490 nm. The peak intensity of the DuPont unidirectional lamp is significantly higher than those of the other lamps. In comparison to the Dupont lamp, the unidirectional lamp based on the Gwent products shows one major peak at 480 nm and another one at 600 nm. This is due to the re-emission from the pink dielectric used which produces a broader spectrum lower luminance output in contrast to the white Dupont dielectric. This effect has already been mentioned by Chadha (1993).

Another reason for the relative higher intensity of the DuPont unidirectional lamp is the higher capacitance of its dielectric layer since large dielectric capacitance leads to increased luminance (Hitt, 2001). The combination of the thinner ink film produced by the DuPont (23 μm compared to 30 μm) dielectric and its higher dielectric constant (13.2 compared to 8.9) results in a higher capacitance lamp, Table 2 and Figure 3. The capacitance of the lamp constructed from the DuPont material (5.2 nF) is around twice that of the Gwent lamp (2.6 nF).

Table 2: Properties of dielectric layers

	DuPont unidirectional (DuPont 8153)	GEM unidirectional (D2090130D5)	Bidirectional (DuPont 5036)
Printed thickness (μm)	23	30	17
Ra (μm)	1.7	4.3	1.0
Capacitance (nF)	5.2	2.6	2.1
Dielectric constant	13.2	8.9	4.0

Both bidirectional lamps show similar capacitance as the dielectric is the same in each case. Increasing the capacitance (and hence brightness) of the bidirectional lamps by additional dielectric particle content may sacrifice the transparency of the lamps. Reducing the film

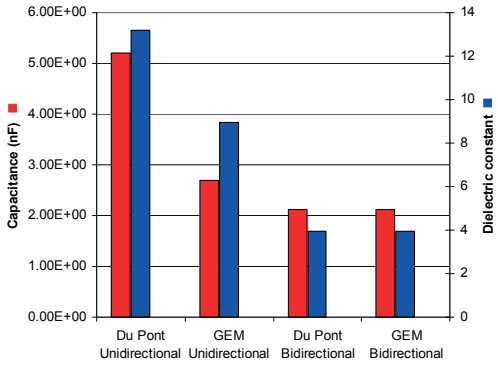

Figure 3: Capacitance and relative dielectric constant for each material and build at 830 Hz

thickness to increase capacitance, would improve transparency but would risk breakdown of the dielectric layer and lamp shorting between the electrodes. There is room for some optimization of the transparent dielectric layer to increase brightness. For the bidirectional lamps, there is no significant difference in the spectra for the two illumination directions, although there is a small difference between the phosphor materials, Fig. 4.

For both phosphor materials, the spectral distributions measured through the printed transparent electrode (front) and substrate film (rear) are almost identical. The negligible difference between the luminance between the two faces of the lamp may also be attributed in part to the measurement method. When the lamp operates in a bidirectional mode, a small portion of light emitted from the sub surface may be reflected from the matt black measurement surface may also be re transmitted through the film to the measurement surface.

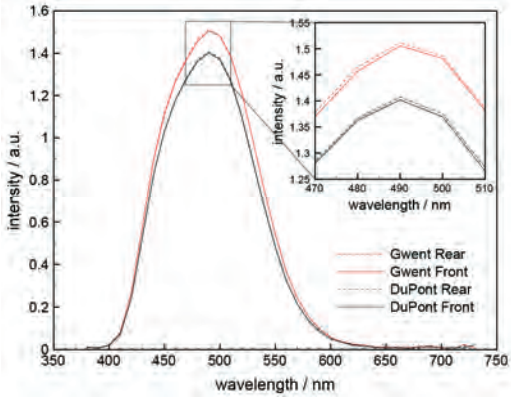

Figure 4: Spectral output for the bidirectional lamps measured through the front and rear emission surfaces

The results of the luminance measurements are in agreement with the emission spectra, Figure 5. The luminance of the bidirectional lamps is slightly lower than of the Gwent unidirectional lamps and significantly lower compared to the DuPont unidirectional lamp. With the Dupont material, this is associated with the lower capacitance of the translucent dielectric material and light emission from both surfaces compared to the single surface emission of the unidirectional lamps.

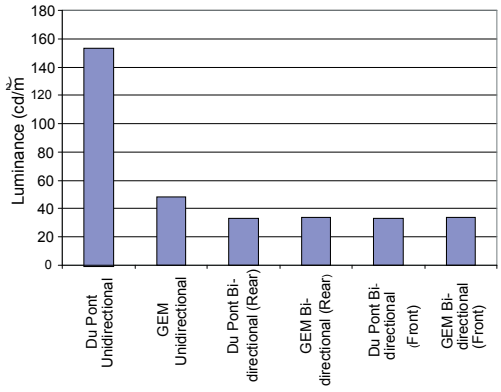

Figure 5: Lamp luminance for each build and material manufacturer

The build for each of the phosphor materials, therefore provides a flexible bidirectional lamp. Figure 6 shows the flexible, bidirectional EL-lamp in front of a mirror. The emission is uniform into both directions and over the entire surface. The size of this lamp can readily be enlarged utilising the conductive micro grids mentioned previously as these would facilitate improved conductivity into the lamp centres. It may also be possible to utilise PET as a substrate for such lamps as all processing temperatures are within the operating window for PET. PET has superior optical performance to polycarbonate and is the commonest substrate for EL lamps. PET is however less amenable to in-mould applications.

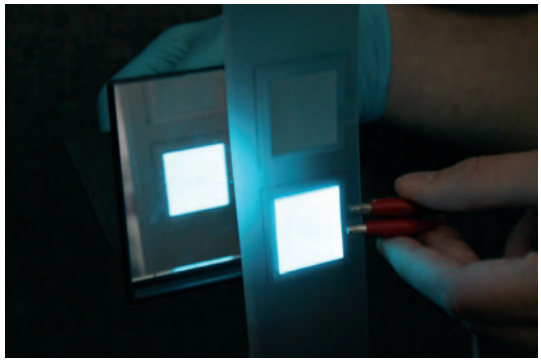

Figure 6: Image of bidirectional lamp operating in front of a mirror for illustrative purposes

In order to examine the applicability of the bidirectional lamps to produce 3D structure the lamps were uniaxially strained to 50% using a Hounsfield tensile testing system at room temperature. This is beyond the elastic limit for the Makofoil substrate which is approximately 10% (Philips, 2008). The emission spectra for the Gwent lamps are shown in Figure 7 and shows that there is only a small change in light output when the lamps are subjected to plastic deformation.

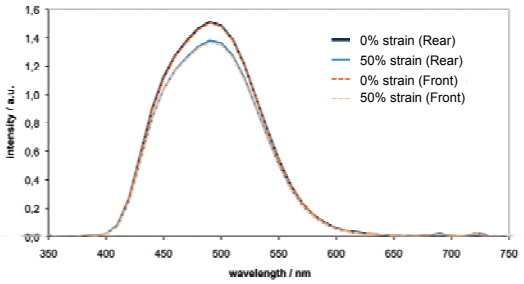

Figure 7: Spectral distributions for the Gwent lamp measured before and 50% plastic strain

The bidirectional Dupont lamps failed just beyond the elastic material of the polycarbonate material as a result of cracking of the phosphor layer which led to failure of the dielectric. This is most likely a result of a more brittle binder in the Dupont material. The Gwent bi-directional lamps could also undergo uni-axial strain while illuminating in both directions with the ultimate strain being dictated by the failure of the substrate.

When manufacturing 3 dimensional objects, any strain is likely to be biaxial with localised regions of high strain at locations such as corners and bends, (Phillips, 2008). Further development is required to examine the key relationships between the mechanical strain inducedin the lamps, the deformation temperature and their subsequent effect of the luminance variation of the lamps.

4. Conclusions

A new type of fully printed thick film EL lamps illuminating in both directions has been demonstrated.

There is no need for ITO and silver ink to fabricate these lamps as both electrodes are based on the transparent conducting polymer PEDOT:PSS and a clear dielectric paste has been utilised successfully. The emission of the fabricated lamps is uniform in both directions and the luminance is in the range of unidirectional lamps. One of the successful bidirec-tional lamps could be subjected to 50% plastic deformation with minimal reduction in lamp output. The mechanical properties and formability of the lamps under two dimensional strain of commercial forming process at higher temperatures is of importance and appropriate examinations are currently ongoing.

Acknowledgements

The authors thank S. Hamblyn, D. Deganello, T. Korochkina, and W. Foerster for valuable discussions and technical support. In addition, K. Weigelt thanks the Stiftung Industrieforschung, Cologne (Germany) for funding.

References

Chadha, S. S., 1993. Powder electroluminescence. In Kitai, A., ed. 1993. *Solid State Luminescence. Theory, materials and devices*, London: Chapman & Hall.

Deganello, D., Cherry, J., Gethin, D., Claypole, T., 2010. Patterning of microscale conductive networks using reel-to-reel flexographic printing. *Thin Solid Films.*

Harkema, S., Rooms, H., Wilson, J., Van Mol, T., Mennema, S., Barink, M. and Bollen, D., 2009. Large area ITO-free flexible white OLEDs with Orgacon PEDOT:PSS and printed metal shunting lines. *Proc. SPIE 7415*, 74150T. doi:10.1117/12.825246.

Hecker, K. (ed.), 2009. *OEA Roadmap*, 3rd edition. VDMA.

Hitt, J. C., Wager, J. F., 2001. Insulator issues in alternating-current thin film electroluminescent devices. *Journal of Applied Physics*, 90, pp. 2711-2717.

Kim, M. J., Shin, D. W., Kim, J.-Y., Park, S. H., Han, I. T, Yoo, J. B., 2009. The production of a exible electroluminescent device on polyethylene terephthalate films using transparent conducting carbon nanotube electrode. *Carbon*, 47, pp. 3461-3465.

Kirchmeyer, S., Reuter, K., 2005. Scientific importance, properties and growing applications of poly (3,4-ethylenedioxythiophene). *Journal of Materials Chemistry*, 15, pp. 2077-2088.

Jung, C.H., Tai, P.H., Kang, Y.K., Jang, D.S., Yoon, D.H., 2008. $12CaO{\cdot}7Al_2O_3$ doped indium-tin-oxide thin film for transparent cathode in organic light-emitting devices. *Surface & Coatings Technology*, 202, pp. 5421–5424.

Langa, U., Naujoks, N., Duala, J., 2009. Mechanical characterization of PEDOT:PSS thin films, *Synthetic Metals*, 159, pp. 473-479.

Mauch, R. H., 1996. Electroluminescence in thin films. *Applied Surface Science*, 92, pp. 589- 597.

Nardes, A.M., Kemerink, M., de Kok, M.M., Vinken, E., Maturova, K., Janssen, R.A.J., 2008. Conductivity, work function, and environmental stability of PEDOT:PSS thin films treated with sorbitol. *Journal of Organic Electronics*, 9, pp. 727–734

Ono, Y. A., 1995. *Electroluminescent Displays*, Series on Information Display. Singapore: World Scientific Publishing Co. Pte. Ltd.

Phillips, C. O., Claypole, T. C. and Gethin, D. T, 2008. Mechanical properties of polymer films used in in-mould decoration. *J. Mater. Process. Technology*.

Phillips, C., Sulem, N., Job, D., 2009. Colour combinations in printed EL. WCPC Annual Technical Conference 2009, Swansea.

Schrage, C., Kaskel, S., 2009. Flexible and transparent SWCNT electrodes for alternating current electroluminescence devices. *ACS Applied Materials & Interfaces*, 1, pp. 1640-1644.

Takayuki, U., Toshifumi, M., Masao, O., Toshio, O., Mieko, I., Azusa, S. and Yutaka, S., 2006. Cesium-incorporated indium-tin-oxide films for use as a cathode with low work function for a transparent organic light-emitting device, *Thin Solid Films*, 496, pp. 75-80.

Vij, D. R. (ed.), 2004. *Handbook of Electroluminescent Materials*, London: Institute of Physics Publishing.

Winther-Jensen, B., Krebs, F. C., 2006. High-conductivity large-area semi-transparent electrodes for polymer photovoltaics by silk screen printing and vapour-phase deposition. *Solar Energy Materials & Solar Cells*, 90, pp.123-132.

Yang, H., Holloway, P. H. and Ratna B. B., 2003. Photoluminescent and electroluminescent properties of Mn-doped ZnS nanocrystals. *Journal of Applied Physics*, 93, pp. 586-592.

Zovko, C., Nerz T., 1999. White polymer thick film electroluminescent lamps and their applications for backlighting liquid crystal displays in portable electronic devices. *Displays*, 20, pp. 155-159.

JPMTR 006 | 1111
UDC 667.52.033.22:655.353

Research paper
Received: 2011-07-27
Accepted: 2012-04-16

Formulation of water based silver inks adapted for rotogravure printing on ceramic green tapes

Rita Faddoul, Anne Blayo and Nadège Reverdy-Bruas

Laboratory of Pulp and Paper Science and Graphic Arts, Saint-Martin-d'Hères, France
E-mails: rita.faddoul@pagora.grenoble.fr; anne.blayo@pagora.grenoble-inp.fr; nadege.reverdy@pagora.grenoble.fr

Abstract

The aim of this work is to study the printability of silver inks on LTCC (Low Temperature Co-fired Ceramics) flexible tapes by rotogravure printing. Commercial and newly developed LTCC tapes with different surface energies and pore sizes were investigated. Silver inks were prepared and formulated by adding 35 to 55% silver particles (D50 ~ 2-3 μm) to a mixture of water/ethylene glycol/glycerol. Ink surface tension and viscosity were determined in order to establish their effects on the ink transfer from the cylinder to the substrate. Substrates were printed by rotogravure printing process with the formulated inks. The printing cylinder was engraved in intaglio, with a 45 μm cell depth to allow deposition of high ink thickness. Printed line properties such as thickness, width and roughness, were determined in order to establish the relationship between substrates characteristics, ink properties and printability. High silver contents (50-55%) and viscosities allowed deposition of thick lines (5.6 μm). Thus, 55% silver ink was printed on different substrates. An optimum 45% silver weight allowed printing of narrower (160 μm) and smoother (1.4 μm) lines.

Keywords: water-based ink formulation, surface tension, viscosity, ceramic, surface energy, rotogravure printing, topography

1. Introduction and background

This work is part of a European project, MULTILAYER (FP7-NMP4-2007-214122), aiming to develop mass production techniques for manufacturing microelectronic devices on ceramic substrates. Rotogravure printing is an appropriate method for mass production because of its high throughput. It is a roll-to-roll process allowing printing on flexible substrates. Many studies were performed about gravure printing onto plastic or paper flexible tapes.

For example, Noh et al. (2010) studied silver ink gravure printing and scalability on polyethylene terephthalate (PET) foils. They deposited lines with 317 μm width and 0.44 μm thickness.

Mäkela et al. (2003) printed polyaniline conductive polymer ink on paper substrates by rotogravure process. They achieved a minimum 60 μm line width.

Pudas et al. (2005) succeeded to deposit a silver line with 4 to 7 μm thickness on plastic foils. They used a gravure cylinder with cell depth of 20 to 60 μm.

Schmidt et al. (2010) developed a new printing method combining flexography and gravure printing processes. The experiments were carried out by paying a special attention on the substrates wettability by the ink. They performed gravure printing of PEDOT:PSS (Poly-EthyleneDiOxy-Thiophene doped with Poly-Styrene-Sulfonate) dispersion on PET foil corona treated and structured by flexography with a low surface tension polymer ink. Tracks with 10 μm length and 30-150 nm thickness were printed for the realization of source/drain electrodes.

Pudas et al. (2004) worked on the gravure offset printing technique. This roll-to-plate method allows printing on both flexible and rigid substrates. They managed to deposit an ink loaded with 85% silver onto ceramic tapes. Lines with 300 μm width, 17 μm thickness and 5 mOhm/square sheet resistance were successsfully printed. The gravure cylinder cells depth was equal to 30 μm.

Inks for ceramic substrates, usually contain large particles (1-10 μm) compared to particles classically used for rotogravure printing (≤ 1 μm). Larger particles allow deposition of thick films before sintering.

The sintering process occurs in three main stages (Liu and Chung, 2004; Xu et al., 2009):

i. The early sintering stage characterized by plastic deformation of the material. At this stage, neither material densification nor shrinkage takes place. Only organic materials are burnt out.

ii. The intermediate or middle sintering stage characterized by material densification, inorganic particles softening, melting, growth and adhesion to each other and to the substrate.

iii. The final sintering stage which is the end of the densification process characterized by pore size decrease. A continuous conductive network is created after sintering. In some cases, no more pores are observed.

Glass powders are usually added in order to enhance conductive particles adhesion to substrates. Figure 1 shows Scanning Electron Microscopy (SEM) micrographs of LTCC tapes before (a-1) and after (a-2) sintering and of flexography printed silver ink before (b-1) and after (b-2) sintering. After sintering, pore size decreased and a compact network is formed.

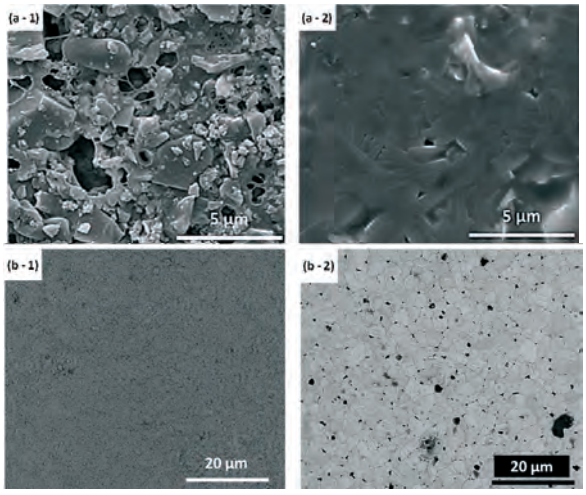

Figure 1: SEM micrographs of LTCC tape before (a-1) and after (a-2) sintering and flexography printed ink before (b-1) and after (b-2) sintering (micrographs realised at Grenoble INP - LGP2)

Faddoul et al. (2012) have demonstrated that after sintering at 850 °C for 10 minutes of conductive silver tracks printed by flexography on ceramic substrates resistivity values as low as 2.8 to 12.0x10^{-8} Ohm.m close to that of bulk silver resistivities (1.6x10^{-8} Ohm.m) were reached. This was attributed to a continuous silver network formation when sintering was performed.

After co-firing at 800-900 °C, organic vehicle burns out and silver particles melt leading to line thickness decrease (Buzby and Dobie, 2011). Glass frits - a mixture of silicone, barium, magnesium and other oxides - are added in order to insure adhesion to the substrate after sintering (Bless et al., 1990). Industrial glass powders are large with a 3 µm mean diameter. A classical gravure printing cylinder with cell depths smaller than 20 µm cannot ensure printing of inks with large particle size: gravure cells could be blocked by the large particles of ink.

One of the few studies about rotogravure printing onto ceramic substrates was performed by Kittilä et al. (2004). They used a thin silicone polymer gravure material patterning and covering the metal base of the printing cylinder. When silicone polymer with 35 µm gravure grooves depth was used, lines with 160 µm width and 17 µm thickness were obtained. A 25 µm gravure depth was also used; lines with 20 to 320 µm width and 8 to 10 µm thickness were achieved. Commercial silver co-fired paste from DuPont was used. This paste had a viscosity of 120-200 Pa.s at 25 °C when agitated at 10 rotations per minute (rpm) (Materials Data Sheet - Heraeus). This viscosity range is very high for a typical gravure printing process for which viscosities vary from 40 to 100 mPa.s (Blayo and Pineaux, 2005).

In the present work, properties of LTCC tapes such as surface energy, porosity and roughness were studied. Then, new inks with different silver contents were formulated. Inks and substrates properties effects on printed line characteristics (width and thickness) were investigated. A ceramic gravure printing cylinder with 46 µm depth channels was mechanically engraved in intaglio, in order to allow printing of inks containing particles with a mean diameter ranging from 2 to 3 µm. Cylinder channels widths were measured from 136 to 605 µm. Only lines printed with 136 µm engraved channels were studied.

2. Materials and methods

2.1 Substrate properties

Two commercial LTCC tapes, DP951 and CT700, were provided by Micro System Engineering (MSE) - Germany. These tapes are commercialized by DuPont - USA and Heraeus - Germany, respectively. A new LTCC tape, developed by Swerea IVF - Sweden (SIVF) was also studied. In order to determine the appropriate ink formulation - particle size, solvent - substrate properties such as pore sizes, roughness and surface energies were determined.

A Quanta 200 FEI ESEM (Environmental Scanning Electron Microscope) was used to perform substrate surface micrographs and then determine the particle and pore size distribution. 100 to 200 measurements per tape were carried out. Area of studied samples was equal to 1.5 µm^2.

An Alicona infinite focus 3D profilometer was used to determine the substrates roughness (Ra). The minimum length investigated to measure roughness was 4 mm according to ISO standards 4287 and 4288. Topographies

were performed with 100 magnification allowing ±10 nm vertical resolution.

A contact angle system OCA (Dataphysics) was used in sessile drop mode in order to determine the surface energy of the substrates. Contact angles between the studied substrates and five solvents (water, ethylene glycol, diiodomethane, α-bromonaphtalene and aminoethanol) were measured. The Owens-Wendt-Rabel-Kaelble (OWRK) method was applied to calculate, both dispersive and polar components of the surface energy (Owens and Wendt, 1969).

2.2 Inks

Ink vehicle was prepared by adding dispersing, antifoaming and wetting agents to a mixture of water/ethylene glycol/glycerol (3/6/1). This mixture decreased solvent evaporation rate during printing and avoided impression cylinder channels blocking. Surfactant decreased ink surface tension. Dispersing and antifoamming agents enhanced suspension stability. Dispersive agent (Hydropalat 216), antifoaming agent (Foamaster 8034) and wetting agent (Hydropalat 140) were provided by Cognis - France.

Spherical silver particles - Ag300-02-Heraeus - with 2-3 μm diameter were added to the vehicle (35 to 55% weight).

Organic acrylic polymers were added to bind particles before sintering. BASF provided Joncryl 8055 and 2136 acrylic polymers. Finally, a rheological agent - XP53 (Coatex) - was added in order to increase viscosity.

Mechanical dispersion of solid particles in liquid solvents was performed with a Dispermat apparatus at 2 000 rotations per minute for 20 minutes.

The rheological behavior of the inks was determined with a cone-plate rheometer Aanton Paar at shear rate varying from 1 to 10 000 s^{-1}. The gap was equal to 0.5 mm and measurements were performed 25 °C. The cone angle was equal to 1° and its diameter to 5 cm.

OCA Data Physics system in pendant drop mode allowed measuring the ink surface tension ($mN.m^{-1}$).

2.3 Printing

In the gravure printing process ink is doctored into the gravure cells. Ink is directly transferred onto the substrate. The excess of ink is removed using a doctor blade. Ink pick-up is dependent on ink doctoring and cylinder properties such as aspect ratio (the ratio of cell depth to cell width), printing parameters (speed, force), substrates (surface energy, pore size) and ink (viscosity, surface tension) (Kipphan, 2001; Leach and Pierce, 1993).

Channels were engraved on an intaglio printing ceramic cylinder with different aspect ratios. An IGT Global Standard Tester (GST) 3H gravure printing laboratory press was used to print at 0.5 $mm.s^{-1}$ speed and 1 000 N force. Figure 2(a) is a schematic representation of the rotogravure printing process. Figure 2(b) is a picture of the IGT GST 3H laboratory tester.

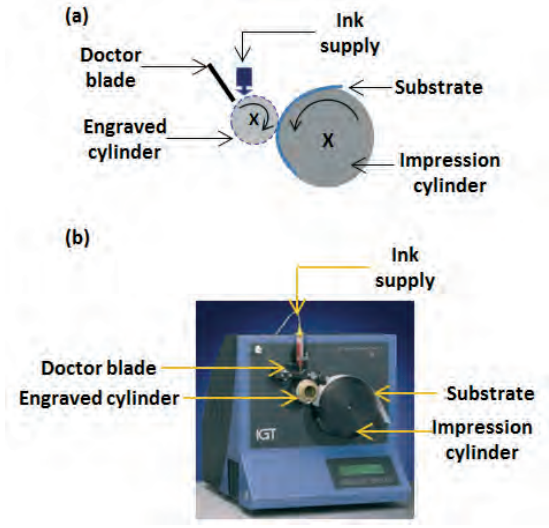

Figure 2: Schematic representation of the rotogravure process (a), IGT GST 3H laboratory tester (b)

The IGT tester was designed to study the printability of a wide range of substrates such as paper, cardboard and foils. Fields of application are primarily for quality control and research. Simulation of the ink transfer is also possible with small ink quantities. It allows 0.2 to 4.0 $m.s^{-1}$ printing speed and 50 to 1 000 N printing force. Typical printing speed for flooring, for example, is 0.5 $m.s^{-1}$. The laboratory tester may therefore simulate industrial conditions, in some cases, expected the tension. Indeed, in an industrial process, the web is submitted to a tension which is not the case with the IGT GST 3H.

All the inks were printed onto DP951 LTCC substrate displaying the lowest surface energy. Ink containing 55% silver was also printed on substrates with higher surface energies, CT700 and SIVF. Printed line thickness, width and roughness were measured with the Alicona 3D profilometer.

2.4 Sintering

Sintering was performed under normal atmosphere in a StaTop Nagat traditional furnace at 800 °C for 15 minutes.

A thermogravimetric analyze was performed with a Perkin Elmer TG-DTA (Thermo Gravimetric Analyzer coupled to Differential Thermal Analyzer) on the dried ink. Sample was heated from 105 °C to 800 °C and kept for 15 minutes at peak temperature.

2.5 Electrical properties

The main challenge of this work was to deposit an ink quantity sufficient to withstand sintering temperature as high as 800 °C. It was therefore necessary to print continuous and thick enough silver lines. The pattern resistivity can be calculated according to Equation 1.

$$\rho = R \cdot \frac{w \cdot th}{L} \quad [1]$$

where:
- ρ (Ohm.m) is the electrical resistivity,
- R (Ohm) is the resistance,
- w (m) is the line width,
- th (m) is the line thickness,
- and L (m) is the line length.

The resistance, R, is calculated according to equation by a 2 probes device (the current is fixed and the voltage is measured).

$$R = \frac{U}{I} \quad [2]$$

where:
- R (Ohm) is the resistance,
- U (V) is the voltage,
- and I (A) is the current.

That is why it is crucial to obtain continuous lines and to determine carefully their geometrical characteristics such as thickness and width.

3. Results

3.1 Substrates characterization

3.1.1 Scanning electron microscopy

Fig. 3 shows SEM micrographs of green LTCC surfaces. Particles had, mainly, diameters varying from 1 to 2 µm.

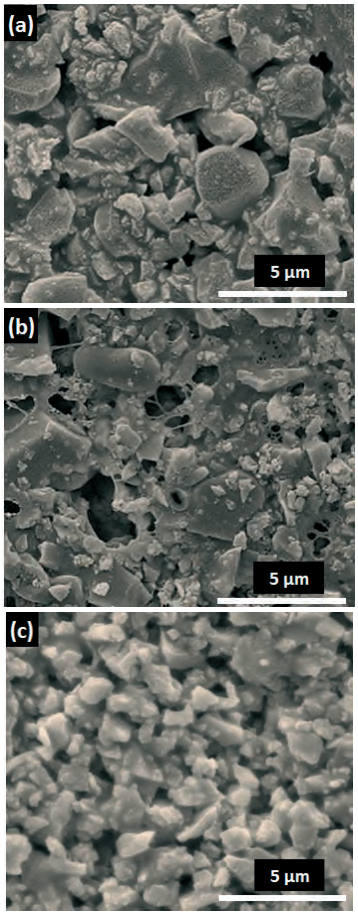

Figure 3 (a,b,c): Green LTCC surface SEM micrographs: (a) DP951, (b) CT700 and (c) SIVF

3.1.2 Substrates pore sizes and roughness

Figure 4 shows the pore size distribution of LTCC tapes.

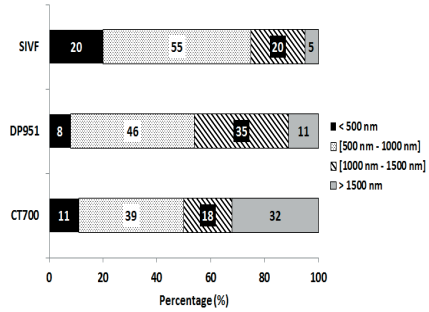

Figure 4: LTCC pore size distribution

More than 50% of measured pores ranged from 0.5 to 1.5 µm. Regarding the standard deviation, roughness can be considered as the same for these tapes (Table 1).

Table 1: LTCC tapes surface roughness

	DP951	CT700	SIVF
Ra (µm)	0.23 ± 0.01	0.26 ±	0.23 ±

Substrates roughness is dependent on ceramics powder and aggregates size. For examples, Hu et al. (2004) showed that 0.05-0.10 µm barium strontium titanate (BST) particles formed zirconia tapes with 0.15 µm roughness after casting. And 0.60 to 1.50 µm BST powders formed 0.20 µm roughness tapes. In addition, Vozdecky and Roosen (2010) prepared alumina tapes with nano-sized powders (≤ 0.06 µm) to get smooth tape surface (Ra ~ 0.17 µm) compared to commercial tapes (Ra ~ 0.60 µm). To print these tapes, inks with particle diameter larger than 1 µm are preferred in order to block the tapes surface pores by only depositing one layer.

Sood et al. (2010) explained that with low roughness, less coat weight is needed to cover the surface pores of a paper substrate.

3.1.3 Substrates surface energy

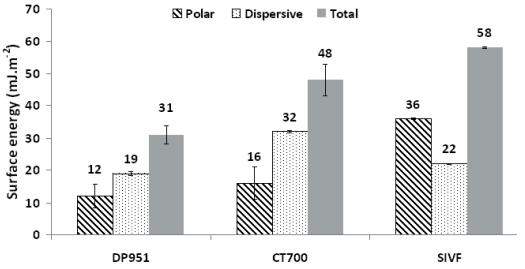

Figure 5: Surface energies (polar, dispersive and total) of different LTCC substrates

Figure 5 depicts surface energies of tested LTCC tapes. Table 2 summarizes dispersive component to total surface energy ratio.

Table 2: Dispersive component to total surface energy ratios

	DP951	CT700	SIVF
γ_s^d/γ_s	0.61	0.67	0.38

Substrates surface energy is related to the organic vehicle used to prepare the suspension before casting. Theoretically, a liquid is able to wet a substrate when the substrate surface energy is higher than the ink surface tension. SIVF tape was cast from a water-based suspension. For this reason, it had the highest surface energy (58 mJ.m^{-2}) and the lowest dispersive component. This tape is more compatible with polar water based inks with surface tension close to 50 mN.m^{-1}. DP951 and CT700 were cast from solvent based suspensions. DP951 tape exhibited the lowest surface energy, 31 mJ.m^{-2}. To print this substrate ink with a surface tension lower than 30 mN.m^{-1} could be used. Mixture of solvent with surface tension lower than that of water (72.8 mN.m^{-1}) could therefore be formulated. Surfactant or wetting agent could be added in order to enhance substrate wettability by the ink. CT700 displayed higher surface energy (48 mJ.m^{-2}) than the DP951 tape; in particular, the polar part of its surface energy was half the value of the disperse part (16 versus 32 mJ.m^{-2}).

3.2 Inks

According to substrates properties, water based inks, with a mean particle diameter larger than 1 µm and a surface tension lower than 30 mN.m^{-1} were prepared.

3.2.1 Ink rheological behavior and viscosity

All inks exhibited a shear thinning behavior. Ink viscosity and transfer from engraved cylinder to the substrate under the doctor blade were dependent on printing speed. Figure 6 shows viscosity results as a function of silver percentage at 1 and 10 000 s^{-1} shear rates.

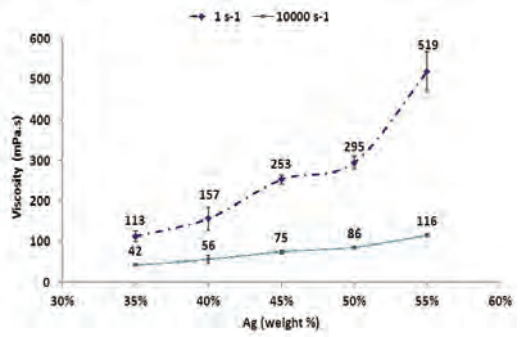

Figure 6: Viscosity versus silver content at 1 and 10 000 s^{-1} shear rates - 25 °C

Viscosity increased when silver content increased because of particle interactions (Van der Waals) enhancement when more silver powders are added. The inks had higher viscosities than the classical gravure printing inks. Viscosity increased from 113 mPa.s with 35% silver to 519 mPa.s with 55% silver at 1 s^{-1} shear rate.

3.2.2 Ink surface tension

Figure 7 shows surface tension values of different inks as a function of silver content.

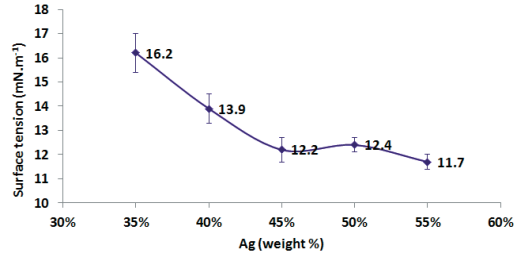

Figure 7: Surface tension of different silver inks as a function of silver content

The surface tension was lower than 17 mN.m^{-1} for all the inks. These values were very low and were attributed to the wetting agent, modified silicone oil. Inks could then wet all the LTCC substrates. When silver content increased from 35 to 55% ink surface tension decreased from 16 to 12 mN.m^{-1}.

This was attributed to the decrease of water content with the increase of silver content. At higher silver contents (45-55%) surface tension was considered as constant.

3.3 Printing

3.3.1 Gravure cylinder description

In order to print the pattern shown on Figure 8, channels with different widths were engraved (Table 3).

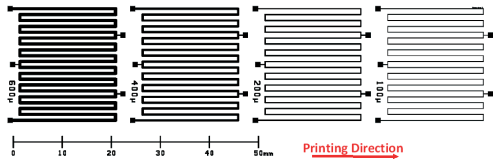

Figure 8: Rotogravure printed pattern

The cell depth was equal to 46 µm in order to allow printing of a minimum 5 µm line thickness and use ink containing particles with a 2 - 3 µm diameter.

Figure 9 illustrates topographies of cylinder channels (G1 to G4). Figure 10 depicts cylinder channels profiles.

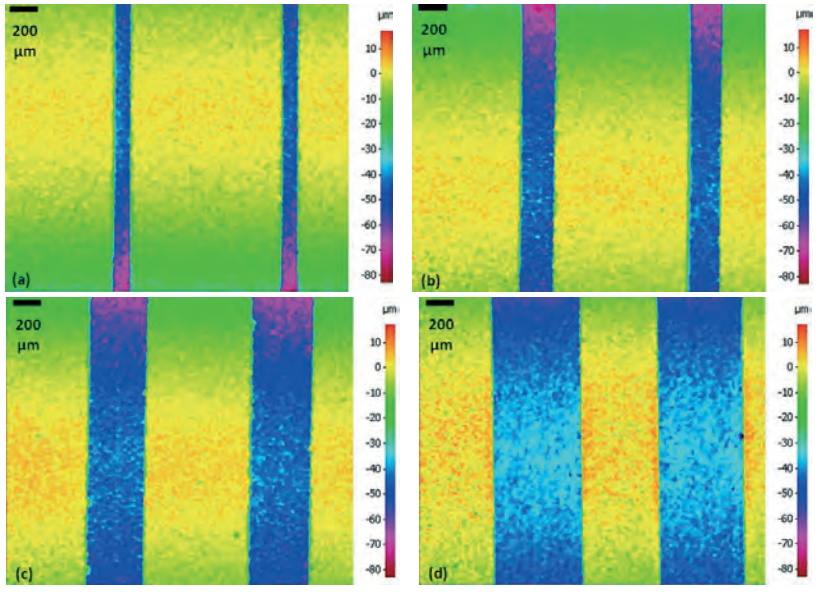

Figure 9: Channels topographies of G1 (a); G2 (b); G3 (c) and G4 µm (d) engraved cylinder - Printing direction from bottom to top (Alicona 3D profilometer)

Table 3: Properties of the engraved cylinder pattern

	G1	G2	G3	G4
Depth (µm)	47 ± 1	46 ± 0	46 ± 0	47 ± 1
Theoretical width (µm)	100	200	400	600
Engraved cylinder width (µm)	136 ± 5	222 ± 13	414 ± 21	605 ± 18

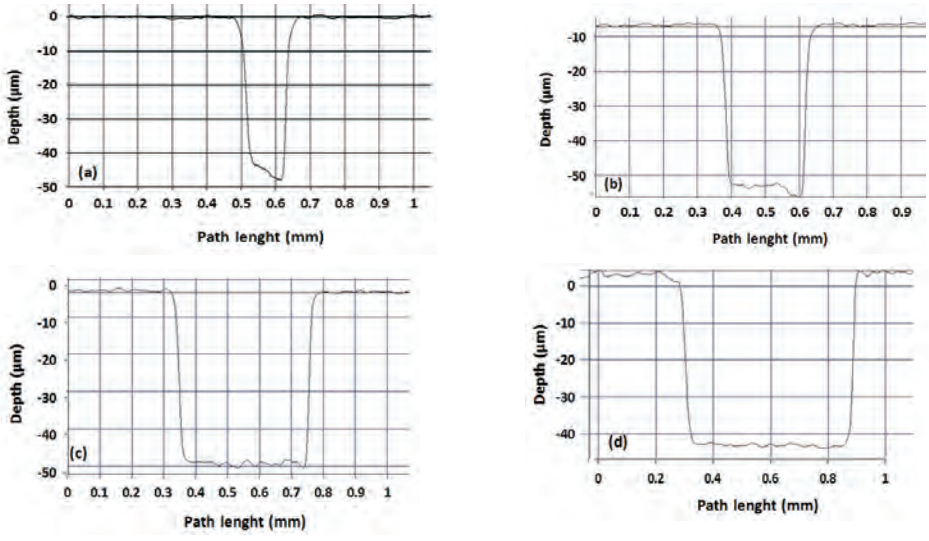

Figure 10: Channels profiles of G1 (a); G2 (b); G3 (c) and G4 µm (d) engraved cylinder (Alicona 3D profilometer)

3.3.2 Printed lines aspect

Lines printed with channels larger than 136 µm were not very well defined. The line centre was not printed. Ink was deposited on the line edges. Figure 11 shows optical microscope images of lines printed with different channel widths.

When channel width increased a gap was formed at line center. The gap width decreased when channel width decreased. And, only lines printed with G1 channel had a continuous aspect.

Sung et al. (2010) explained that when using intaglio cylinder engraved the printing direction (perpendicular to cylinder axis), the ink is only partially transferred to the substrate. This is called the pick-out effect. It is due to the large channel width compared to the channel depth. In the same way, identical results were observed in the present study. Regarding the printed lines, only those printed with G1 channels were investigated.

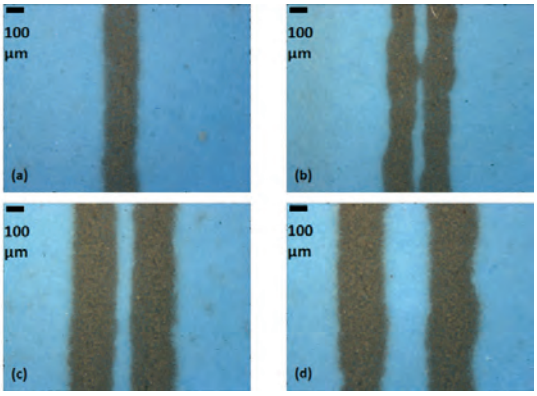

Figure 11: Silver line printed with a 136 µm (a), 222 µm (b), 414 µm (c) and 605 µm (d) gravure cylinder channels widths (Optical microscopy - Alicona)

3.3.3 Roughness and geometrical properties of deposited lines

Figure 12 shows the topography of a 100 µm line printed with a 50% silver content ink. Figure 13 illustrates the obtained profile on this line.

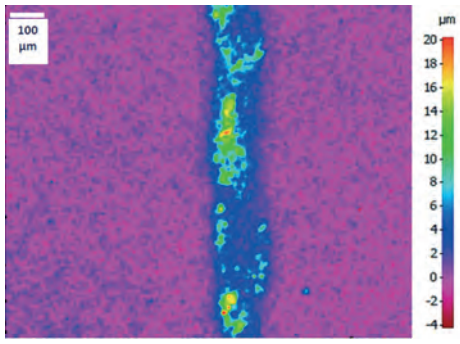

Figure 12: Topography of a 136 µm line width printed by rotogravure process with a 50% silver ink (Alicona 3D profilometer)

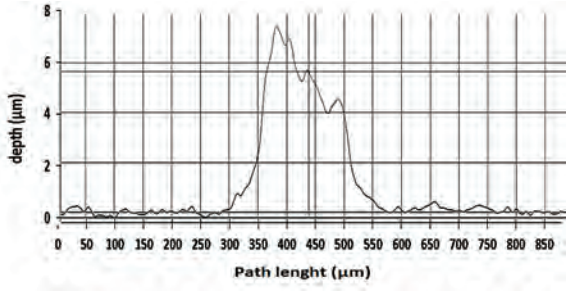

Figure 13: Profile of a 136 µm line width printed by rotogravure process with a 50% silver ink (Alicona 3D profilometer)

Thickness peak was lower than 8 µm. Mean line thickness, width and roughness were measured with the Alicona 3D profilometer. Figure 14 shows thickness, width and roughness of lines printed on DP951 tape.

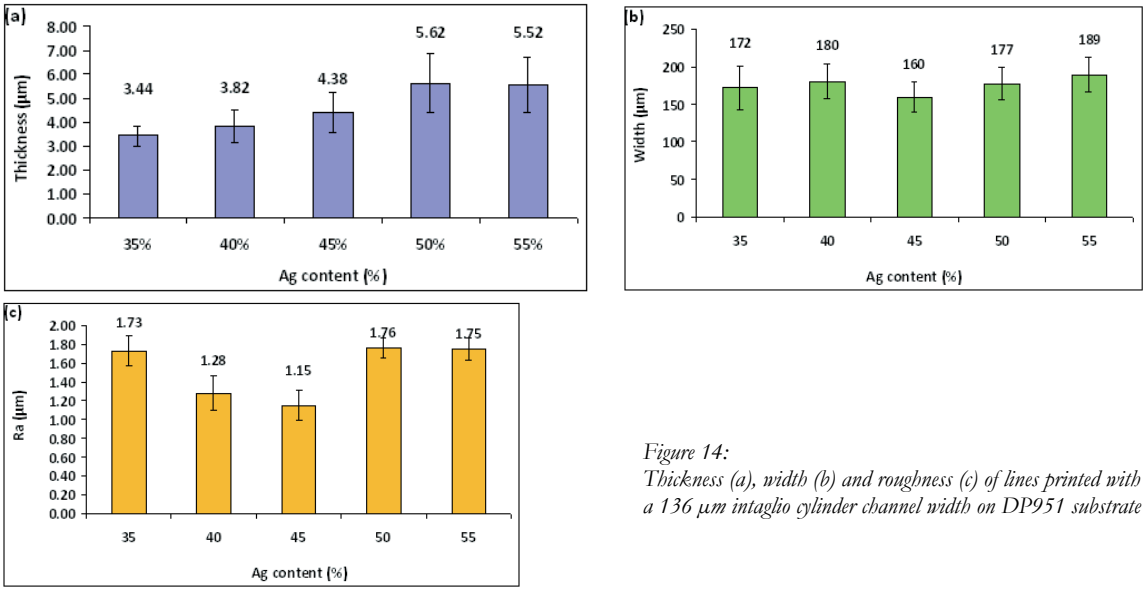

Figure 14: Thickness (a), width (b) and roughness (c) of lines printed with a 136 µm intaglio cylinder channel width on DP951 substrate

Line thickness is dependent on silver content. When silver content and viscosity increased, line thickness increased from 3.4 to 5.6 µm. However, above 50% silver, thickness remained constant. With 55% silver, viscosity was too high and the ink transfer to the substrate was not completed.

Regarding line widths and standard deviations, width was almost the same whatever the silver content was. A minimum 160 µm width was obtained with a 45% silver ink. Furthermore, a line width larger than the theoretical cylinder channel width was also expected because of spreading after printing. Sung et al. (2010) showed that printed lines width was generally 2 to 3 times larger than nominal width.

Regarding roughness results, the smoother line (Ra = 1.15 µm) was obtained with a 45% silver ink. And, when line width increased, line roughness increased, too. The rougher lines - 1.75 µm roughness - contained 50 and 55% silver. This poor smoothness was expected because of the large particle size (2-3 µm) and the thickness higher than 3 µm. Sung et al. (2010) explained that if viscosity was too high, printed ink would not flow smoothly. When viscosity is too low, thin lines are printed. Thus, they defined an optimum viscosity allowing printing of smooth, narrow and uniform lines. This viscosity was obtained for 45% silver in the present work. Ink containing 55% silver was printed on different substrates because it allowed high thickness deposition (5.5 µm - Figure 14). Figure 15 shows the obtained results.

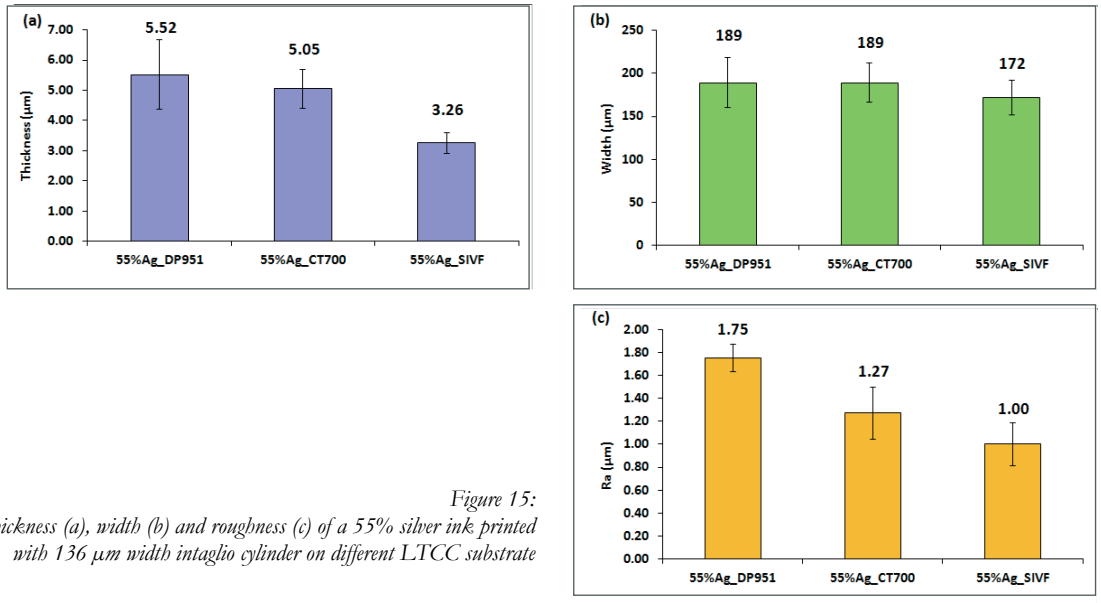

Figure 15: Thickness (a), width (b) and roughness (c) of a 55% silver ink printed with 136 µm width intaglio cylinder on different LTCC substrate

When tape surface energy increased, thinner, narrower and smoother lines were printed.

This can be related to a poor affinity between the ink with a low surface tension (~ 12 $mN.m^{-1}$) and the substrates with large surface energies. For this reason, the thickest line (5.5 µm) was obtained on the DP951 substrate with the lowest surface energy (31 $mJ.m^{-1}$). Ink transfer is reduced when surface energy increased.

To print the Swerea IVF LTCC substrate, formulation of water-based inks without wetting agent is preferable. Besides, slighlty narrower and smoother lines were printed on high surface energy tapes. The same phenomenon was observed by Tay and Edirisinghe (2001). They studied inkjet printing of zirconia ink with a surface tension equal to 24 $mN.m^{-1}$. Tapes surface energies varied from 20 to 74 $mJ.m^{-2}$. They observed that when surface tension was higher than substrate surface energy (20 $mJ.m^{-2}$), ink was not able to wet the substrate. Furthermore, they showed that when tapes had high surface energies (74 $mJ.m^{-2}$) spreading was limited compared to tapes with lower surface energies (42-50 $mJ.m^{2}$). They attributed this to high γ_s^d/γ_s (> 0.91) of low surface energy tapes compared to high surface energy substrates (γ_s^d/γ_s < 0.55).

Similar result was obtained in the present study: narrower and smoother lines were printed on high surface energies LTCC with low γ_s^d/γ_s - 0.38 (see Table 2).

4. Sintering

Sintering of 100 µm lines was performed at 800 °C for 15 minutes. Sintering led to poor line definition, pores and discontinuities formation (Figure 16). Thus, lines were not conductive and it was not possible to determine the resistivity. During sintering organic materials burnt out and silver softened and melted. Thus, thick-

ness decreased and pores are formed. Buzby and Dobie (2011) explained that line thickness decreases by 50% after sintering. In order to establish a possible link between thickness variation and silver particles behavior at 800 °C, a thermogravimetric analysis coupled to dynamic thermal analysis (TG - DTA) was performed on dried ink (Figure 17). Bounded water evaporated at temperature close to 150 °C. Ethylene glycol (EG) evaporated at temperature lower than 200 °C and glycerol at temperature close to 280-290 °C. These transformations are highlighted by endothermic peaks on heat flow curve and weight loss on TG curve. An exothermic peak (Figure 17) was observed between 230 and 280 °C. This peak is linked to organic polymer de-composition.

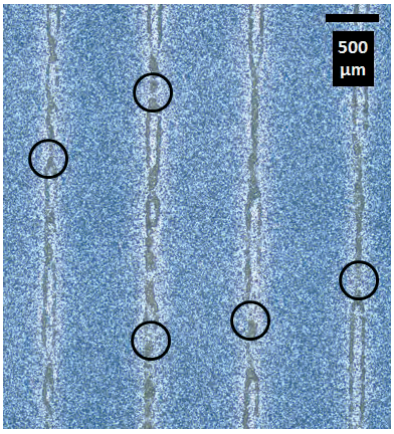

Figure 16: 100 µm line after sintering - Discontinuities are encircled (50% Ag) (Optical microscopy - Alicona)

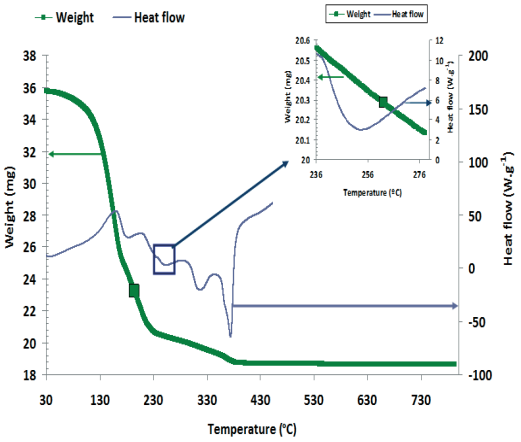

Figure 17: TG-DTA results of 50% Ag ink

An endothermic peak was also observed at 330 °C. It is attributed to silver particles softening and melting. Silver oxidation is not obvious, but an exothermic peak going with 0.79 mg weight loss may be due to silver oxide decomposition (Songping, 2007). Patnaik (2002) explained that silver absorbs oxygen at temperatures close to its melting point and then it rejects oxygen at higher temperatures before solidification. Silver melting and oxidation are coupled to a slight weight loss (0.79 mg). The continuous increase in heat flow at temperatures higher than 800 °C was due to furnace temperature and it was not possible to detect any physical transfor-mation above these temperatures. However, no weight changes were observed.

5. Conclusions and perspectives

This work aimed to study the printability of LTCC substrates by rotogravure printing process and the possibility to deposit lines of 5-10 µm thickness with laboratory formulated inks.

The used engraved cylinder ensured better definition of narrower lines due to pick up effect occurring on larger lines. This is due to high channel width to depth ratio.

Ink properties, such as surface tension and viscosity, had a great influence on ink transfer from the engraved cylinder to the substrate. Line thickness increased when silver content and viscosity increased. An optimum 45% silver weight allowed deposition of smooth and narrow lines.

Narrower and smoother lines were also deposited on high surface energy tape (SIVF) because of large difference between ink surface tension and tape surface energy and a low γ_s^d/γ_s. However, printed line thickness was low (3.3 µm). Finally, sintering showed that deposited silver quantity was too small to allow connections establishment after silver melting.

In order to achieve conductive and continuous lines after sintering, thickness should be increased. Thus, new cylinder with deeper cells could be tested. It is also possible to formulate inks with higher surface tension in order to perform printing of thicker lines on high surface energies tapes.

Acknowledgments

The authors would like to thank the European Union for financial support through the MULTILAYER project (FP7-NMP4-2007-214122), T. Haas and C. Zielmann from Micro System Engineering and J. Stiernstedt from Swerea IVF for providing us by LTCC tapes.

References

Blayo, A. and Pineaux, B., 2005. Printing processes and their potential for RFID printing. *ACM international conference proceeding series,* 121, pp. 27-30.

Bless, P.W., Wahlers, R.L. and Stein, S.J.J., 1990. Application of glasses in thick film technology. *The American ceramic society - Ceramic transactions*, 20, pp. 397-417.

Buzby, D. and Dobie, A., (2011). Fine line screen printing of thick film pastes on silicone solar cells. *Heraeus - White papers*.

Faddoul R., Reverdy-Bruas N., Blayo A., Haas T. and Zeilmann C., 2012. Optimisation of silver paste for flexography printing on LTCC substrate. *Microelectronics Reliability*, doi: 10.1016/j.microrel.2012.03.004.

Hu, T., Jantunen, H., Uusimäki and Leppävuori, S., 2004. BST powder with sol-gel process in tape casting and firing. *Journal of European Ceramic Society,* 24, pp. 1111-1116.

Kipphan, H., 2001. *Handbook of print media: technologies and production methods*. Berlin: Springer.

Kittilä, M., Hagberg, J., Jakku, E., and Leppävuori, S., 2004. Direct gravure printing (DGP) method for printing fine-Line electrical circuits on ceramics. *IEEE transactions on electronics packaging manufacturing*, 27(2), pp. 109-114.

Leach, R.H. and Pierce, R.J., 1993. *The ink print manual*. Kluwer Academic.

Liu, Z. and Chung, D.D.L., 2004. Comparative study of electrically conductive thick films with and without glasses. *Journal of Electronic Materials*, 33(3), pp. 194-202.

Mäkelä, T., Jussila, S., Vilkman, M., Kosonen, H. and Korhonen, R., 2003. Roll-to roll method for producing polyaniline patterns on paper. *Synthetic metals,* 135-136, pp. 41-42.

Material Data Sheet of 6145 Ag cofireable conductor, 2001. Dupont Microcircuit Material.

Noh, J., Yeom, D., Lim, C., Cha, H., Han, J., Kim, J., Park, Y. and Subramanian, V., 2010. Scalability of roll-to-roll gravure printed electrodes on plastic foils. *IEEE transactions on electronics packaging manufacturing,* 33(4), pp. 275-283.

Owens, D.K. and Wendt, R.C., 1969. Estimation of the surface free energy of polymers. *Journal of Applied Polymer Science***,** 13(8), pp. 1741-1747.

Patnaik, P., 2002. *Handbook of inorganic chemicals*. McGraw-Hill.

Pudas, M., Hagberg, J. and Leppävuori, S., 2004. Printing parameters and ink components affecting ultra-fine-line gravure-offset printing for electronics applications. *Journal of the European ceramic society,* 24, pp. 2943-2950.

Pudas, M., Halonen, N., Granat, P. and Vähäkangas, J., 2005. Gravure printing of conductive particulate polymer inks on flexible substrates. *Progress in organic coatings*, 54(4), pp. 310-316.

Schmidt, G.C., Bellman, M., Meier, B., Hambasch, M., Reuter, K., Kempa, H. and Hübler, A.C., 2010. Modified mass printing technique for the realization of source/drain electrodes with high resolution. *Organic electronics***,** 11, pp. 1683-1687.

Songping, W., 2007. Preparation of micron flake size powders for conductive thick films. *Journal of Materials Science: Materials in Electronics*, 18, pp. 447-442.

Sood, Y.V., Tyagi, S., Tyagi, R., Pande, P.C. and Tandon, R., 2010. Effect of base paper characteristics on coated paper quality. *Indian Journal of Chemical Technology*, 17, pp. 309-316.

Sung, D., de la Fuente Vornbrock, A. and Subramanian V., 2010. Scaling and optimization of gravure-printed silver nanoparticle lines for printed electronics. *IEEE transactions on components and packaging technologies*, 33(1), pp. 105-114.

Tay, B.Y. and Edirisinghe, M.J., 2001. Investigation of some phenomena occurring during continuous ink-jet printing of ceramics. *Journal of Materials Research*, 16(2), pp. 373-384.

Vozdecky, V. and Roosen, A., 2010. Direct tape casting of nanosized Al_2O_3 slurries derived from autogenous nanomilling. *Journal of American Ceramic Society*, 95(5), pp. 1313-1319.

Xu, F., Hu, X.-F., Niu, Y., Zhao, J.-H. and Yuan, Q.-X. 2009. In situ observation of grain evolution in ceramic sintering by SR-CT technique. *Transactions of nonferrous metals society of China*, 19, pp. 684-688.

JPMTR 008 | 1204
UDC 667:535.6

Original scientific paper
Received: 2012-03-02
Accepted: 2012-04-16

Colorimetric characterization of thermochromic composites with different molar ratios of components

Ondrej Panák[1], *Nina Hauptman*[2*], *Marta Klanjšek Gunde*[2], *Marie Kaplanová*[1]

[1] University of Pardubice, Czech Republic E-mails: ondrej.panak@upce.cz; marie.kaplanova@upce.cz
[2] National Institute of Chemistry, Ljubljana, Slovenia E-mails: nina.hauptman@mf.uni-lj.si; marta.k.gunde@ki.si
[*] Present address: UL, Medical Faculty, Ljubljana, Slovenia

Abstract

The thermochromic composites used for this study were prepared by applying crystal violet lactone as a leuco dye together with bisphenol A of different molar ratios as a developer and 1-octadecanol as a solvent. The colorimetric properties of all composites were measured during heating and cooling within a broad temperature range, which makes it possible to characterize entire colour hysteresis loops. It was demonstrated how these properties depend on the developer and solvent ratios. The investigations concentrated in particular on the total colour contrast between the coloured and the discoloured states, the temperature interval needed for the colour to change, and the width of the hysteresis loop. It was shown that composites with the same colorimetric properties could be prepared by applying a relatively broad range of dye/developer concentration ratios.

Keywords: crystal violet lactone, bisphenol A, colour hysteresis, total colour contrast, thermochromism

1. Introduction

Thermochromic (TC) inks have become increasingly important for various applications in smart packaging, security printing and marketing (Kerry and Butler; 2008; Phillips, 2000; White and LeBlanc, 1999). Leuco dye-based composites, encapsulated in a polymer envelope and embedded in a suitable binder system are almost exclusively used as pigments in TC inks. Such inks exhibit thermally-induced reversible colour change (Seenoth and Lötzsch, 2008). TC inks with activation temperature from 15 °C up to 65 °C are available in all major ink types such as water-based, solvent-borne and UV-curable ones, which are designed for application on paper, plastic, metal and textile substrates by different printing techniques. Ink manufacturers commonly provide a colour shade and the activation temperature of the product and recommend appropriate printing and drying conditions.

Most leuco dye-based TC composites have three components: a colour former (leuco dye), a developer and a solvent. Their colour changes as a result of two competing reactions, one between the dye and the developer, the other between the solvent and the developer. The first reaction prevails below the melting point of the solvent and forms coloured complexes. The second reaction occurs when the solvent melts; it destroys the dye-developer complexes and hence discolours the composite. The melting point of the applied solvent determines which of the two reactions will be effective, and hence the colour of the composite; it is referred to as switching temperature (Seeboth et al., 2007), discoloration temperature (MacLaren and White, 2003a; 2003b; 2005) or activation temperature (Johannson, 2006; Kulčar et al., 2009; 2010). Leuco dyes are electron donating compounds, e.g. spirolactones, fluoranes or spiropyranes (Burkinshaw, 1998). In most research works on leuco dye-based TC composites published so far crystal violet lactone (CVL) was applied. The developper is an electron donor compound such as Bisphenol A, gallates, phenols, hydroxybenzoates and hydroxy-coumarin. The solvents could be long-chain alkyl alcohols, esters, or acids (White and LeBlanc, 1999; Seeboth and Lötzsch, 2008; Seeboth et al., 2007; MacLaren and White, 2003a; 2003b; 2005; Burkinshaw et al., 1998; Seeboth et al., 2006; Zhu and Wu, 2005; Luthern and Peredes, 2000; 2003).

The microencapsulation process of TC composites produces spherical capsules, so-called TC pigments. The polymer envelopes are mostly made from epoxy or melamine resins (Small and Highberger, 1999). The size of the capsules could be up to 20 μm. Larger capsules are used for screen printing, smaller ones for offset printing, for the capsules must withstand greater shearing

forces during the offset printing. The rheological parameters of TC inks differ significantly from the rheological properties of conventional inks (Panák et al., 2010). In the offset printing machine the inks are also influenced by small droplets of the dampening solution (Panák et al., 2011).

Prints with leuco dye-based TC inks are coloured at temperatures well below the activation temperature and discoloured well above this temperature. Both processes exhibit sigmoidal-like temperature dependence of the parameters describing the colour. This dependence could be very asymmetric and in some cases it has a slightly different shape, especially below the activation temperature (Gunde et al., 2011). Discoloration occurs typically at higher temperatures than coloration. The colour of a sample thus depends on the temperature and on thermal history, which is represented by colour hysteresis (Kulčar et al., 2009; 2010). All colour states inside a hysteresis loop are temporarily stable for more than 10 hours (Kulčar et al., 2010). TC inks of the same basic colour and with the same activation temperature (i.e. with the same ink manufacturer's data) could have very different loops: narrow or wide, fairly symmetrical or highly asymmetrical. In very asymmetrical systems the two colour-changing processes are expressed by different sigmoidal-like curves (Gunde et al., 2011). Interesting properties were also found in mixtures of TC inks. The hysteresis loop of a TC ink mixture reveals a binary nature only if the individual TC inks have well separated hysteresis loops; this requires significantly different activation temperatures. In a mixture of inks with similar activation temperatures the individual loops fuse into a single loop. (Kulčar et al., 2011). In the previous study we have addressed several issues concerning the application of commercially available TC inks as are the total colour contrast and the corresponding width of the temperature interval in which the colour change is detected (temperature sensitivity interval) and the width of hysteresis loops. This research has brought useful results and has helped to understand the behaviour of these complicated systems in practical applications.

We have demonstrated that colour hysteresis is a characteristic property of all leuco dye-based TC inks; its nature, however, remains unclear. One of the basic questions is whether it appears only in encapsulated leuco dye-based TC pigments as a result of different thermal conductivity properties of the pigment envelope and the ink binder material, or whether it is an intrinsic property of the pigment core material (the TC composite).

Another thing which has not as yet been clarified is the mathematical description of the behaviour of colour hysteresis loops. In literature, these properties of TC composites were described very rarely or only superficially, without any deeper analysis and explanation (Seeboth et al., 2007; MacLaren and White, 2003a; 2003b; 2005; Johansson, 2006; Burkinshaw et al., 1998; Seeboth et al., 2006; Zhu and Wu, 2005; Luthern and Peredes, 2000; 2003). The effect of the concentration ratios of the three components of a TC composite has already been investigated (Luthern and Peredes, 2000; 2003), but the authors evaluated their results only by absorbance or reflectance parameters, and did so separately for variations of the dye, the developer and the solvent ratio. Our aim was to describe the colorimetric properties of TC composites. We have, therefore, taken into account the entire visual spectral response. We have studied CVL-based TC composites in a wide range of solvent/developer ratios. The present work employs the results of our research in an effort to answer the question how the concentration ratios of the three components of TC composites influence (a) the basic colorimetric parameters, (b) the temperature interval within the colour change is detected and (c) the parameters of colour hysteresis loops.

2. Materials and methods

2.1 Preparation of samples

The TC mixtures were prepared by applying crystal violet lactone (CVL, 6-(dimethylamino)-3,3-bis[p-(dimethylamino)phenyl]phthalide, > 95%), bisphenol A (BPA, 2,2-bis(4-hydroxyphenyl)propane, > 99%) and 1-octadecanol (OD, > 98%) from TCI Europe. All chemicals were used without further purification. OD acts as a sol-vent (its melting point indicated by the manufacturer is 59 °C), in which the colour former (CVL) and the developer (BPA) are dissolved.

Thirteen TC composites were prepared with varying molar ratios of the developer (x_{BPA} = moles of BPA/moles of CVL) and the solvent (x_{OD} = moles of OD/moles of CVL).

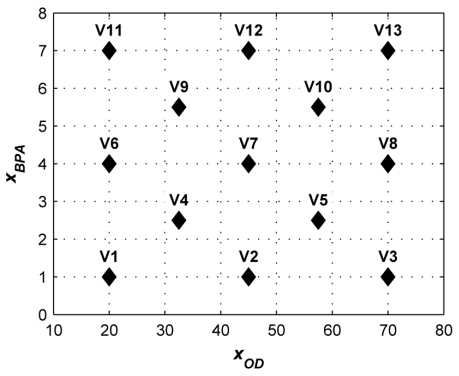

Figure 1: Concentration map of the TC composite mixtures studied (x_{OD} - molar ratio of the solvent, x_{BPA} - molar ratio of the developer)

Figure 1 shows the concentration map of all the TC compositions prepared for this study. The middle point with the molar ratio x_{BPA} = 4 (sample V7) was chosen according to the data published in literature (Luthern and Peredes, 2000).

The first step in the preparation of the TC composites was dissolving CVL in OD at 140 °C. Then a corresponding amount of BPA was added. When the dissolution was completed, the melted composite was poured into distilled water (approximately 20 °C) and then stirred at high speed. In this way the composite was quickly cooled and small irregular coloured particles were obtained. After filtration the coloured particles dried out under laboratory air conditions.

2.2 Colour measurement

For colour measuring of the thin layers of the composites, a special aluminium measuring cell was prepared. It has the shape of a 150 μm deep cup of the dimensions 6.5 × 9 mm² with a white-coated bottom. The particles of each sample were melted in the cup (at the temperature of about 8 °C), then covered by a 154 μm thick microglass plate and quenched to room temperature (~ 20 °C). Much attention was devoted to preventing the formation of any air bubbles in the cup. The microglass cover was used to avoid changes in the thickness of the measured sample during its subsequent heating and melting. The measuring cell was fixed on top of a temperated copper water block by a Teflon plate with a hole allowing to measure the optical parameters by the Eye-One Pro X-Rite spectrophotometer. The copper water block (EK Water Blocks) was connected to a thermostatic circulator which allows adjusting of the temperature. The measurements were taken in the temperature interval of 35-65 °C with a 1 °C step within the temperature range of the hysteresis loop and with a 2 °C step outside this range. The Eye-One Pro spectrometer operates at the geometry of 45/0. The colorimetric parameters were computed using the D50 standard illumination and the 2 °C standard observer. The temperature of the sample was measured by the Pt100 RTD fast response temperature sensor (Omega) attached to the surface of the micro-glass plate near to the colour measuring area.

2.3 Data evaluation

The colorimetric properties of the temperature-controlled samples were evaluated in terms of CIELAB lightness (L^*) and colour difference CIEDE2000 (dE_{00}). The calculation of colour difference dE_{00} at each temperature was carried out as a deviation from the CIELAB coordinates measured at T = 35 °C (the starting temperature) (Sharma et al., 2005).

The boundaries of a typical colour hysteresis loop (measured during the heating and subsequent cooling of the sample) are two sigmoidal-like curves (Figure 2a). They were characterized by a five-parametric logistic function $f(x)$ (Ricketts and Head, 1999), described by equations [1-3], in which x is an independent variable (in our case it was the temperature value), A describes the first plateau, B the second plateau of the $f(x)$ function, C and E are the curvature parameters and D describes the x value corresponding to the middle value of the interval B - A (see Figure 2a).

$$f(x) = A + \frac{B - A}{1 + f_x \cdot e^{C(D-x)} + (1 - f_x) \cdot e^{E(D-x)}} \qquad [1]$$

where:

$$f_x = \frac{1}{1 + e^{\overline{CU}_f (D-x)}} \qquad [2]$$

and

$$\overline{CU}_f = \frac{2 \cdot C \cdot E}{|C + E|} \qquad [3]$$

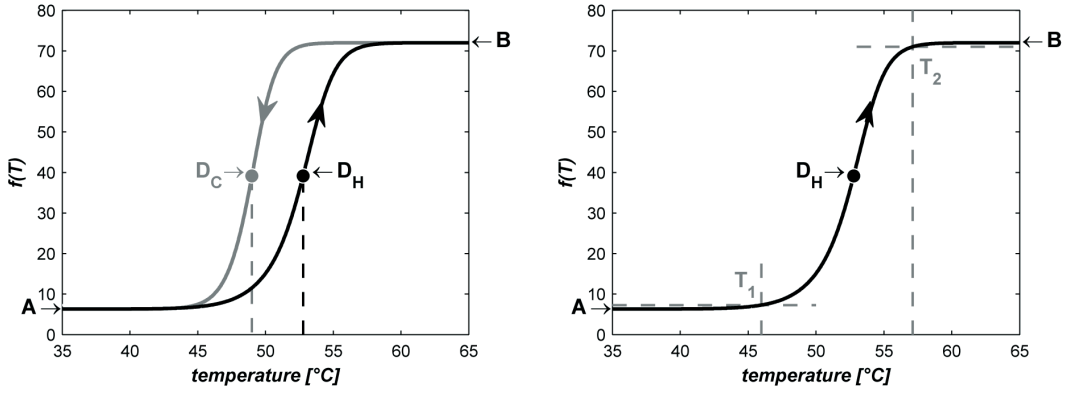

a) *b)*

Figure 2: Typical course of the heating and cooling sigmoidal curves f(T) and the parameters that characterize the hysteresis loop (a) and the temperature sensitivity interval of the heating curve (b)

The $f(x)$ function described was fitted in the L^* and dE_{00} values measured within the above-mentioned temperature range and the heating and cooling $L^*(T)$, and $dE_{00}(T)$ functions were determined. To fit the function in the data in Matlab, a non-linear method, LAR (least absolute residual), was used. In order to specify the colour changes and colour hysteresis of the TC composites, calculated parameters A, B, D were used to determine: the minimum and the maximum lightness (L^*_{min} and L^*_{max} , the A and B parameters of $L^*(T)$ function), the total colour contrast (B parameter of $dE_{00}(T)$ function), the lightness contrast dL^* (B - A of $L^*(T)$ function), the width of the colour hysteresis loop (D_H - D_C of $L^*(T)$ functions, see Figure 2a).

The temperature at which the colour change starts (T_1) was determined from the $L^*(T)$ function as the temperature, at which the colorimetric parameter increases by 1 unit from the first plateau A. The temperature at which the colour change stops (T_2) was determined as the temperature, at which the colorimetric parameter is 1 unit below the second plateau B (see Figure 2b). The temperature sensitivity interval was evaluated from the heating curve as the difference between the temperatures T_2 and T_1. In the following text, the maximum total colour contrast, narrow temperature sensitivity interval and narrow hysteresis loop of a TC system will be considered to be the optimum parameters of a thermally induced colour change.

3. Results and discussion

3.1 Temperature dependence of the colorimetric parameters

Figure 3a shows the L^* a^* b^* coordinates of all prepared composites as they changed during the heating and subsequent cooling of the samples in the whole temperature interval (35-65 °C). The uniform behaviour of all composites is demonstrated by formation of nearly the same colour path in the CIELAB space when temperature changes. This could be attributed to the fact that there is only one type of a colour complex and the changes have to do with its concentration only. For all 13 composites the parameters of $L^*(T)$ and $dE_{00}(T)$ sigmoidal functions (eq. 1-3) were found separately for heating and subsequent cooling. The goodness of the fit was relatively satisfactory (all correlation coefficients were above 0.99). However, the values of the curvature parameters C and E were not very good in some cases.

A typical example is shown in Figure 3b, where some uncertainties can be observed in the region, where the colour change starts.

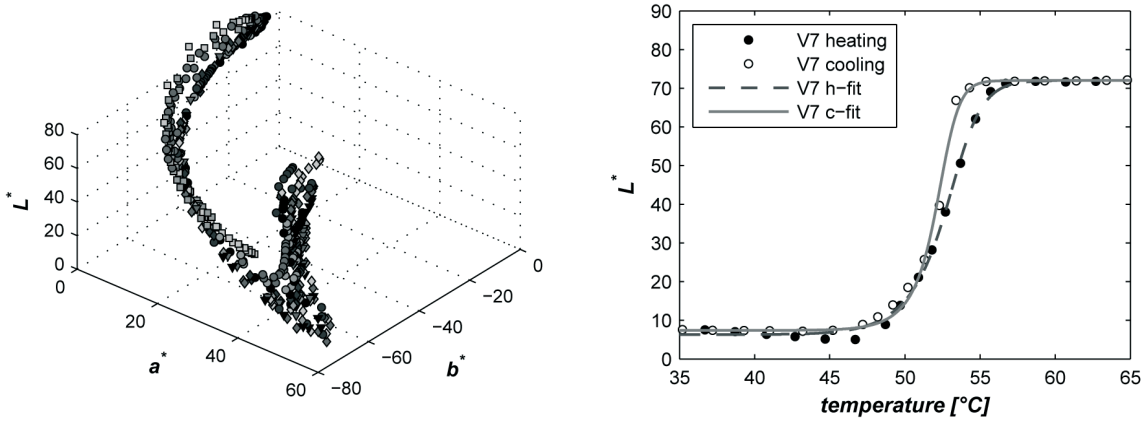

a) *b)*

Figure 3: The L a* b* parameters of all thirteen composites (full signs denote heating, open signs cooling) (a), and the fit of L*(T) functions of the sample V7 (x_{BPA} = 4, x_{OD} = 45) (b)*

3.2 Lightness and total colour contrast during heating

At low temperatures all composites with $x_{BPA} \geq 2.5$ showed deep blue colour corresponding to the low lightness values (the minimum lightness L^*_{min} in Figure 4a). This implies that mixtures with $x_{BPA} < 2.5$ do not contain enough of the developer to interact with all molecules of the dye in the system. The resulting smaller quantity of the dye-developer complexes gives less deep colour (i.e. higher L^*_{min} values) of the corresponding composite (samples V1, V2, V3).

The lightness parameter of discoloured composites at high temperatures (L^*_{max}) diminishes with x_{BPA} only if a small amount of the solvent is combined with a bigger amount of x_{BPA} ($x_{OD} < 32.5$, $x_{BPA} \geq 2.5$ (samples V6 and V 11), but remains practically independent for all other samples (Figure 4b).

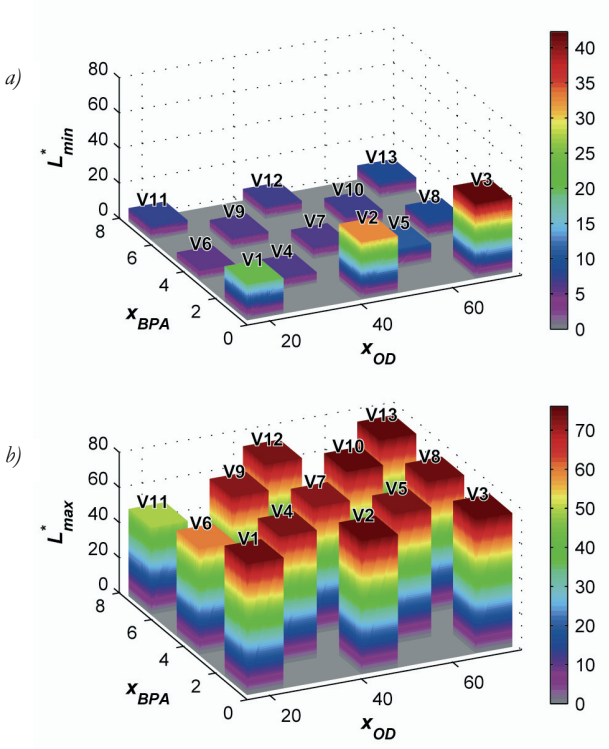

Figure 4:
The minimum lightness at coloured $T < T_1$ states (a) and the maximum lightness at discoloured $T > T_2$ states (b) of thirteen TC composites V1-V13. Every bar represents a single value obtained for corresponding sample (see also Figure 1)

The total colour (dE_{00}) and the lightness contrast values (dL^*) calculated for all samples are presented in Figure 5.The colour contrast dE_{00} and the lightness contrast dL^* conform to a similar dependence on the molar ratios of the developer (x_{BPA}) and the solvent (x_{OD}). At low values of x_{BPA} both of them decrease with increasing x_{OD}, and at low values of x_{OD} they diminish with x_{BPA}. But when $x_{BPA} \geq 2.5$ and $x_{OD} \geq 32{,}5$, practically no dependence on the molar ratio of either component was observed.

As the measurement or calculation of dE_{00} and dL^* brought very similar results, only $L^*(T)$ functions will be considered in our further investigations.

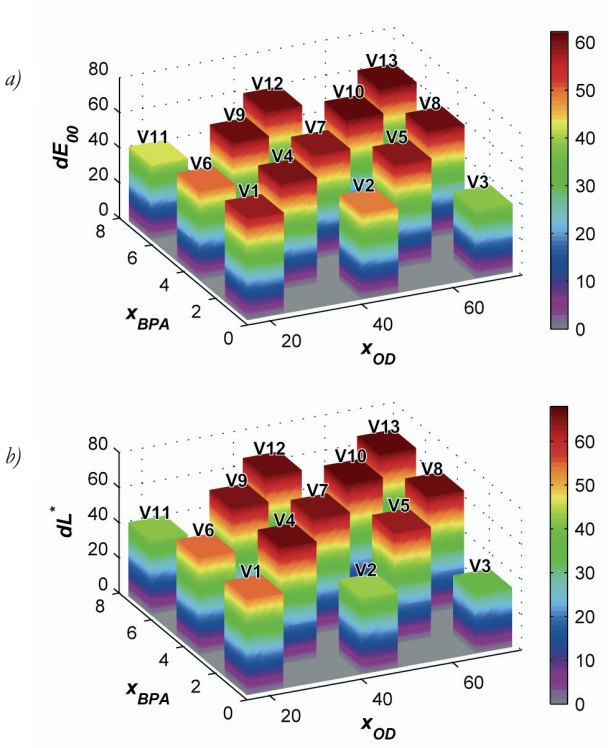

Figure 5:
The total colour (a) and the lightness contrast (b) of thirteen TC composites

3.3 Temperature sensitivity interval at heating

High total colour contrast is not the only important parameter in practical applications. Another very important parameter is the width of the temperature sensitivity interval, for it describes more precisely the activetion temperature. Our TC systems with the smallest amount of the developer (x_{BPA} < 2.5, samples V1, V2, V3) exhibited a wide temperature sensitivity interval T_2 - T_1 (Figure 6a). For other composites studied, the width of the temperature sensitivity interval increased with x_{OD}. This could be attributed to greater mobility of the developer molecules at higher concentrations of the solvent. Much more informative and useful in terms of practical application of TC materials is the parameter defined as the rate of lightness contrast $(dL^*)/(T_2 - T_1)$ shown in Figure 6b. The highest values of the rate of lightness contrast were observed for TC samples V4, V5, V7, V8, V10 and V13.

We could suppose that composites within this area of the concentration map (see also Figure 1) will exhibit the greatest colour change in the narrowest temperature interval.

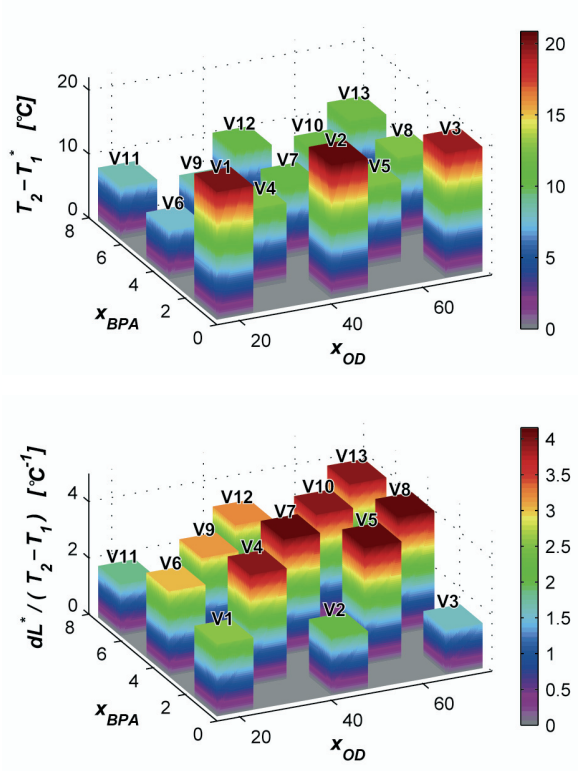

Figure 6:
Temperature sensitive interval (a) and rate of lightness contrast (b) of thirteen TC composites

3.4 Width of the lightness hysteresis loop

All our TC composites exhibited relatively narrow hysteresis loops, up to 2 °C (Figure 7). The width of the hysteresis loop increases with x_{BPA} at x_{OD} < 32.5 (V1, V6, V11) and with x_{OD} at x_{BPA} < 2.5 (V1, V2, V3). The samples on the top-right to bottom-left diagonal of our concentration map (V4, V7, V10 and V13) differ only very slightly as regards the hysteresis width.

The optimum parameters of the TC composites studied could be achieved for samples represented by the top-right to bottom-left diagonal of our concentration map (except for V1). The OD/BPA concentration ratios of these samples (V4, V7, V10 and V13) were in the interval of 10-13. The results of our experiment have shown that TC composites with very similar temperature-dependent colorimetric properties could be prepared by applying different BPA/CVL ratios, but to keep the parameters unchanged the OD/BPA ratio should not be changed very much.

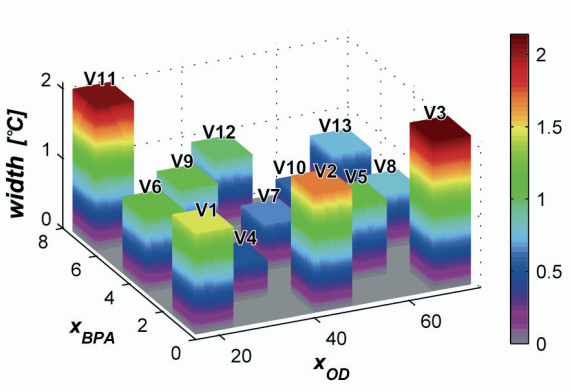

Figure 7:
Width of the lightness hysteresis loop of thirteen TC composites

4. Conclusions

In this study thirteen TC composites were prepared with varying developer/dye and solvent/dye ratios, the former within the interval of 1-7, the latter within the interval of 20-70. The prepared composites were investigated in terms of their total colour contrast and lightness contrast, their temperature sensitivity interval and the width of the hysteresis loop in the temperature interval of 35-60 °C. Samples with low concentrations of the developer ($x_{BPA} < 2.5$) or the solvent ($x_{OD} < 32.5$) exhibited the lowest total colour contrast, a wide temperature sensitivity interval, lower rate of lightness contrast and broader hysteresis loops. All other samples in our concentration scheme were found to produce almost the same total colour contrast. This indicates that there is a relatively large area of the developer/solvent ratios, where all the dye is in its coloured form at low temperatures and in its colourless form after heating to a sufficiently high temperature. The temperature-sensitivity interval is slightly influenced by the amount of the solvent in these samples. The rate of lightness contrast ($°C^{-1}$) is similar for the samples lying on- and under the top-right to bottom-left diagonal of our concentration map. Increasing the amount of the developer seems to lower the rate of the lightness contrast.

The width of the hysteresis loop depends approximately to the same extent on the developer and the solvent concentration ratio. Increasing one or the other ratio causes widening of the hysteresis loop.

These results show that the optimum composition of a TC system is represented by the molar ratios of components that correspond to the concentration ratios lying on the top-right to bottom-left diagonal of our concentration map. When the developer/dye ratio is increased, the colorimetric properties remain unchanged if the solvent/developer ratio is kept approximately unchanged. These results indicate that we are able to prepare TC composites with the same behaviour within a relatively large range of dye/solvent concentrations.

To fully grasp and elucidate the thermally-induced colour changes of TC composites in dependence on the mutual ratios of their components (dye, developer and solvent), several chemical and physical analyses need to be performed. Furthermore, another question arises: the question whether similar results could be expected in the case of leuco dye-based TC composites using different dyes, developers and solvents.

Acknowledgments

This work was supported by the Ministry of Education, Youth and Sports of the Czech Republic, Research Project No. MSM 0021627501, and the Slovenian Research Agency (Programme No. P1-0030). The Czech-Slovenian contact project MEB 091102/ BI-CZ/11-12-010 is also acknowledged.

References

Burkinshaw, S., Griffiths, J. and Towns, A., 1998. Reversibly thermochromic systems based on pH-sensitive spirolactone-derived functional dyes. *Journal of Materials Chemistry*, 8(12), pp. 2677-2683

Gunde M. K., Friškovec, M., Hauptman, N., Kulčar, R., Kaplanová, M., Panák, O. and Vesel, A., 2011. Functional properties of the leuco dye-based thermochromic printing inks, ed. In: *Proceedings of TAGA*, 2011, TAGA. in print

Johansson, L., 2006. *Creation of Printed Dynamic Images*, Linköping University.

Kerry, J. and Butler, P., 2008. *Smart Packaging Technologies for Fast Moving Consumer Goods*. John Wiley & Sons.

Kulčar, R., Friškovec, M., Gunde, M. K. and Knešaurek, N., 2011. Dynamic colorimetric properties of mixed thermochromic printing inks. *Coloration Technology*, 127(6), pp. 411-417.

Kulčar, R., Friškovec, M., Hauptman, N., Vesel, A. and Gunde, M. K., 2010. Colorimetric properties ekof reversible thermochromic printing inks. *Dyes and Pigments*, 86(3), pp. 271-277.

Kulčar, R., Friškovec, M., Knešaurek, N., Sušin, B. and Gunde, M. K., 2009. Colour changes of UV-curable thermochromic inks. In: Enlund, N. and Lovreček, M. (eds.), *Advances in Printing and Media Technology*. Darmstadt, Germany: IARIGAI, pp. 429-434.

Luthern, J. and Peredes, A., 2000. Determination of the stoichiometry of a thermochromic color complex via Job's method. *Journal of Materials Science Letters*, 19(3), pp. 185-188.

Luthern, J. and Peredes, A., 2003. Determination of the stoichiometry of a thermochromic color complex via the method of continuous variation. *Journal of Materials Science Letters*, 22(12), pp. 881-884.

MacLaren, D. and White, M., 2003a. Competition between dye-developer and solvent-developer interactions in a reversible thermochromic system RID B-6479-2009. *Journal of Materials Chemistry*, 13(7), pp. 1701-1704.

MacLaren, D. and White, M., 2003b. Dye-developer interactions in the crystal violet lactone-lauryl gallate binary system: implications for thermochromism, RID B-6479-2009. *Journal of Materials Chemistry*, 13(7), pp. 1695-1700.

MacLaren, D., and White, M., 2005. Design rules for reversible thermochromic mixtures. RID B-6479-2009. *Journal of Materials Science*, 40(3), pp. 669-676.

Panák, O., Jašurek, B., Vališ, J., Kaplanová, M. and Gunde, M. K., 2011. Printability of thermochromic offset inks and their interactions with dampening solution. In: Enlund, N. and Lovreček, M. (eds.), *Advances in Printing and Media Technology*. Darmstadt, Germany: IARIGAI, in print

Panák, O., Kaplanová, M., Gunde, M.K. and Friškovec, M., 2010. Rheological properties of thermochromic offset inks. In: Simoncic, B. (ed.) *5th International Symposium on Novelties in Graphics*, 27–29 May 2010, Faculty of Natural Sciences and Engineering, Department of Textiles, pp. 529-533.

Phillips, G. K., 2000. Combining thermochromics and conventional inks to deter document fraud. In: Van Renesse, R.L. and Vliegenthart, W.A. (eds.), *SPIE*, April 7, 2000, pp. 99-104.

Ricketts, J. H. and Head, G. A., 1999. A five-parameter logistic equation for investigating asymmetry of curvature in baroreflex studies. *American Journal of Physiology - Regulatory, Integrative and Comparative Physiology*, 277(2), pp. R441-R454.

Seeboth, A., Klukowska, A., Ruhman, R. and Lötsch, D., 2007. Thermochromic polymer materials. *Chinese Journal of Polymer Science,* 25(2), pp. 123-135.

Seeboth, A. and Lötsch, D., 2008. *Thermochromic phenomena in polymers*. Smithers Rapra.

Seeboth, A., Lötsch, D., Potechius, E. and Vetter, R., 2006. Thermochromic effects of leuco dyes studied in polypropylene. *Chinese Journal of Polymer Science*, 24(4), pp. 363-368.

Sharma, G., Wu, W. and Daa, E., 2005. The CIEDE2000 color-difference formula: Implementation notes, supplementary test data, and mathematical observations. RID A-1154-2007. *Color Research and Application*, 30(1), pp. 21-30.

Small, L. D. and Highberger, G., 1999. *Thermochromic ink formulations, nail lacquer and methods of use.* 424/61 edn. US: A61K 7/04.

White, M. and Leblanc, M., 1999. Thermochromism in commercial products RID B-6479-2009. *Journal of chemical education*, 76(9), pp. 1201-1205.

Zhu, C. and Wu, A., 2005. Studies on the synthesis and thermochromic properties of crystal violet lactone and its reversible thermochromic complexes. *Thermochimica Acta*, 425(1-2), pp. 7-12.

Topicalities

Edited by Raša Urbas

Contents

News & more

After drupa '12 - where is the future?

With completely changed landscape and in spite of generally lower figures, drupa continues on a very high level and still remains the focal point of the entire world printing and media community. The traditional trade show is on the crossroads, just as is the related industry sector. Next drupa, planned for June 2016 again in Düsseldorf, will be certainly a different event, with significantly changed profile. New high technology systems will bring completely new business models.

The dominating themes of drupa 2012 were automation, packaging printing, digital printing, hybrid technologies, web-to-print applications and environmentally responsible printing. Although multimedia and cross-media issues took much attention, there were impressive innovations in all printing processes. Inkjet printing demonstrated its key role that is prevailing over other digital solutions. With some further development, the inkjet quality will become comparable to offset. However, conventional printing technologies showed vigor and developing potential, especially in the industrial and packaging printing. Higher speeds, larger formats, more efficiency and expanded range of substrates is a response to the challenges of digital printing. It is clear that for at least some time both technologies will remain existing together, sometimes as complementary solutions.

Of course, sustainability was again a top issue, with many manufacturers demonstrating environmentally responsible solutions. These are not limited to chemistry-free processes or reduction of carbon emission, but go as far as biological degradation of waste, using microorganisms to clear photopolymer residues in the water.

One of very visible characteristics of this year's drupa was strong penetration of new economies, thus marking the strong geographical shift from Europe, Japan and North America. Brasil, China, Korea and Taiwan were very well represented at the show, definitely taking over more and more market share.

Along with the drupa innovation park and drupa cube, many specialized programs gave an added value to the trade show itself, offering daily events on diverse topics, like Packaging day, Creative weekend, Magazine day, Book day, Newspaper day, Future of print etc.

drupa 2012 was a good outlook into the future, that offered an insight in new technology and market opportunities. Next show in 2016 will demonstrate what the future will really be like.

iarigai at drupa 2012
Open doors event

The most important international print and media trade show drupa 2012, hosted an event in which iarigai has presented the mission and the goals of the Association and recent actions in networking and promoting the research.

Open doors event attracted a wide audience, from members, researchers, representatives of the trade press and students.

After Mladen Lovreček, Secretary general introduced the speakers, Mr. Manuel Mataré, the drupa project manager welcomed the participants on behalf of the Düsseldorf Trade Fair. He specially addressed the young generation, in whose hands the future of printing and media will soon be.

Dr. Anne Blayo, president of iarigai, portrayed the new mission and future goals of the Association in networking people, ideas and knowledge, especially pointing out the importance of joint interdisciplinary research project.

One of the highlights of the event was the promotion of the new peer-reviewed quarterly - Journal of Print and Media Technology Research, presented by Nils Enlund, Editor-in-Chief. He stressed the importance of scientific publishing as a link between the research and printing and media industries. As the publisher, iarigai is certain that the journal will be widely accepted, not only as a new publishing channel, but also as an important link between the academic community and the related industries.

Open doors event was an opportunity to present some of the organizations, which - although in different environment - have similar goals in developing the international cooperation. FESPA was thus presented by Mr. Nigel Stefens, CEO, while Professor Wolfgang Faigle, president, introduced the International Circle of Educational Organizations.

iarigai is a worldwide international alliance for networking and international cooperation in the scientific research for the printing and media industry.

Environmental conference on drupa

Over 80 industry professionals attended the Lean & Green International Environmental Conference organised at drupa. Attendees and speakers were drawn from printers, suppliers, industry associations, universities, NGOs and governments to make it a fully cross-industry event with some dynamic debates.

The conference addressed the duality of economic and environmental benefits (Lean & Green) as an industry strategy. This initiative underlines that effective responses on these issues requires creative cooperation across the entire industry process chain. The event was jointly organized by the World Print & Communication Forum (WPCF) and the PrintCity Alliance.

Spotless flexographic solution

Recently announced Spotless Flexographic Solution is an independent software that enables flexo printers to reduce printing costs by decreasing the need of specific colors. It is developed as a solution for replacing spot colors with accurate recipes for four color process printing.

It is a program solution that comes together with hardware or the Eye-One spectrophotometer. For conversion of spot colors in process technique it uses expanded color gamut, provided by Kodak flexo printing plates Flexcel NX.

Certified paper for more color

Evercopy Colour Laser is composed of 100% recycled fiber content waste paper and thus meets the requirements of the Blue Angel environmental standard. It is produced according to the special methods, ensuring excellent printing properties. From the environmental point of view the paper contains no chemical ingredients - no de-inking, optical brighteners or chlorine bleaching are used in production. It is resistant to aging according to the DIN 6738 standard and it provides copy quality according to the EN 12281 standard. Evercopy Colour Laser is also FSC certified and produced according to ISO 9001 and ISO 14001 standards.

The new paper features high whiteness and excellent recycling properties. Homogeneous paper surface provides a smooth shiny color prints.

New technology for digital offset printing

One of the most attractive new products displayed at drupa 2012 was a new and revolutionary printing system, which is announcing new trends in the future development of printing.

Nanographic Printing™ technology combines the performance of offset with the versatility of digital printing and is applicable for mainstream commercial, packaging and publishing markets. It is expected to ignite a second revolution in print.

Specially designed presses print in up to eight colors, operate at high speeds of up to 13 000 pages per hour for sheetfed and up to 200 meters per hour for web, at 600 dpi or 1 200 dpi resolution. Sheet formats span B3, B2 and B1 while web formats range from 560 to 1 020 mm.

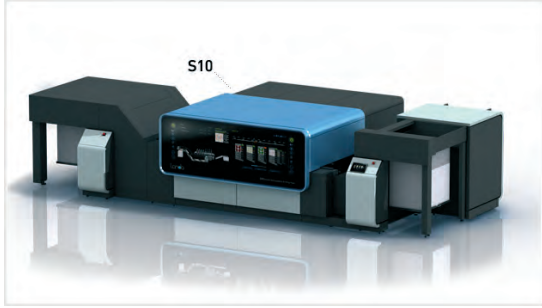

The new technology is intended not to replace offset printing, but to complement it. For the foreseeable future, offset printing will continue to be the preferred method for producing run lengths of tens of thousands or hundreds of thousands, but the market is demanding shorter and shorter run lengths.

The printing process begins with the ejection of billions of microscopic droplets of water-based of the newly developed ink onto a heated blanket conveyor belt. Each droplet of aqueous this NanoInk lands at a precise location on the belt, creating the colour image. As the water evaporates, the ink becomes an ultra-thin dry polymeric film, less than half the thickness of offset images.

The resulting image is then transferred to any kind of ordinary paper, coated or uncoated, or onto any plastic packaging film - without requiring pre-treatment. The NanoInk film image instantaneously bonds to the surface, forming a tough, abrasion-resistant laminated layer without leaving any residual ink on the blanket.

Solid ink technology for inkjet printing

The new waterless ink system removes the need for special treated paper, extra print heads and bonding agents. Waterless inks are easy to handle and replace. The new color printing system has two printing units (twin engine) which enable printing of 500 feet or 2 180 full-color pages per minute or 2 050 color pages A4 format paper in one minute. The four color system enables printing on different papers (plain uncoated, untreated, offset, recycled, newsprint, calendared, ground wood, mechanical fiber, bond or laser) in 50 g/m^2 to 160 g/m^2.

It is primarily designed for printing personalized marketing materials, promotional printing and publishing of smaller editions. Special features of the machine are surveillance cameras that monitor the quality of printed

material. The combination of workflow and the powerful engine creates a truly automated document factory and positions businesses to capture more profitable jobs and produce them more efficiently and economically.

There are two available system versions with one or two printing units. The first could be anytime upgraded to the second one, and the latter due to duplicated design enables double-sided printing in one pass. According to the manufacturer, this is the fastest inkjet production printing system on waterless bases in the world.

The system, under the name CiPress™ 500 was recently introduced by Xerox.

Ultra high throughput digital textile printer

The new digital textile printer is designed for printing of fashion and furnishing fabrics with great productivity, reliability and cost per print, providing an excellent solution for low cost digital textile printing at short and long runs. The Xennia Osiris printer uses up to 8 colors (process or spot colors), and can accommodate up to 12 by request, with a print width of up to 1.85 m and a print quality superior to that of rotary screen printing. Production speeds of up to 30 m/min at full coverage are possible. High ink coverage allows decoration of very heavy fabrics with intense colors.

The digital textile printer is supplied as a self-contained system comprising blanket motion system, highly robust fixed array industrial continuous inkjet printhead carriage, rapid change fluid controllers, substrate wind and unwind stations, in-line digital drying unit, control electronics, operating PC and software. It uses an adhesive blanket system for substrate control, including an entry roller with optional heating for temporary adhesion of the substrate.

The powerful integrated XenJet print software allows users to prepare print jobs and print images quickly and simply using an intuitive interface. New images can be loaded rapidly allowing fast introduction of new designs, and images can be varied on the fly to allow mass customization. Selectable print modes allow different combinations of colors, ink coverage, throughput and quality to be achieved. Fast ink changeover in a matter of minutes enables easy spot color changes.

The Xennia Osiris is recommended for use with high performance ink range, including reactive, disperse and acid dye inks. Using original inks, the printer delivers excellent print quality on a wide range of textile substrates. These inks offer high levels of color performance and wash, crock and light fastness.

The system was introduced in Barcelona at the International Exhibition of Textile Machinery (ITMA).

A multi-purpose film

DPF 4300 is micron opaque matte white calendered film with removable adhesives.

This multi-purpose clean removable film is appropriate for easy on and easy off applications. It offers flexibility as well as high opacity for covering previous graphics.

It assures good resistance to scuffing, tearing and abrasion which improves the graphic protection. DPF 4300 is rated for outdoor durability up to 4 years (unprinted) while printed durability is dependent on the ink system used.

Special metalized papers

A series of special materialized paper comes with different impressions in relief and is suitable for finishing with hot foil.

Distinguished by its exceptional strength it is suitable for manufacture of covers, boxes, book, brochure, packaging and other applications. High gloss finish gives it the added value. The paper is available in 150 or 300 g/m^2.

Unique method of testing digital workflows

The European Color Initiative (ECI), has developed together with FOGRA and Ugra the Technical Page 2 for the Altona Test Suite 2.0. It offers unique method to test components and systems in digital prepress and prints workflows for their capability to process PDF/X-4. The Altona Technical 2 addresses transparency, OpenType fonts, optional content (aka layers), JPEG2000 compression, smooth shades, overprint, 16-bit images and more.

European Color Initiative

The Altona TestSuite 2.0 consists of several components and all the remaining segments will be made available by the end of year 2012.

Writing with light

Special functional pigments have been developed with new properties. When used to inscribe barcodes on animal ear tags, electronic components, and water bottles, they are robust, forgery-proof, and a very practical answer to highly specific user requirements.

In laser marking which provides a permanent and forgery-proof method of inscribing plastics two different types of pigment are available. Both produce high-speed, high-contrast, and high-definition markings. To date, the main use for Micabs is for the laser marking of animal ear tags. The pigment enables high-speed marking and is resistant to UV radiation and manure. The pigments are a clever combination of chemicals and various polymers. They consist of tiny spheres in a polymer matrix; when this is irradiated with a laser, it triggers a direct reaction that produces the desired coloration. The new pigments have been developed by Merck.

Plastics decoration guide

A comprehensive work has been published on surface finishing by means of hot stamping and related technologies. This universal reference with the title ″Kurz Plastics Decoration Guide″ is intended to support practitioners throughout the planning and implementation phases of decoration projects. The main aim of this publication is to offer a reliable guide in the decoration process.

The guide embodies the decades of collective know-how and experience that has been gained in Kurz in a wide variety of decoration processes.

Besides in-depth information about the characteristics of the various decoration processes, the guide also includes a comprehensive chapter on stamping dies and stamping machines. The contents are rounded off by a number of practical aids, for example formulae to calculate the stamping pressure or the required foil quantity. The Plastics Decoration Guide is available in both German and English version.

Large format printing systems

A series of large format industrial printers opens new opportunities to move jobs to digital and create business advantages that allow larger production more in less time.

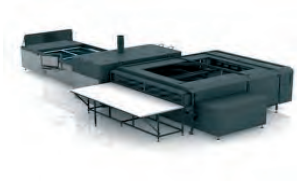

Model FB7600 enables printing on a wide variety of media - flexible and rigid materials, up to 25 mm thick. It offers a variety of productivity enhancements, including in-line saturation control for back-lit applications, hot folders and job queue, to help PSPs expedite their workflow. The device can print up to 95 full boards an hour and has a new point-of-purchase (POP) print mode that produces 55 full boards an hour with indoor quality.

New Scitex Inks adhere better on plastics and improve flexibility on corrugated media, allowing customers to reduce the time required for finishing and expand their businesses with new applications. The inks also have reduced odor offering reassurance that the prints produced are suitable for use in indoor environments. The edge-to-edge printing feature saves time and reduces material waste during the finishing process. Existing owners of the earlier version FB7500 Industrial who want improved versatility and efficiency can easily upgrade their existing technologies with the industrial press upgrade kit.

Another device, the XP5500 Industrial Printer was designed for high-volume PSPs that require a reliable, 24/7 printing solution. The device prints up to 325 m^2/hr (3 500 ft^2/hr) in billboard mode Designed for high-volume PSPs seeking a UV-curable alternative to solvent ink printing, the model XP2500 Industrial Printer offers a low cost per square foot at print speeds up to 265 m^2/hr (2 850 ft^2/hr). Customers can choose one of the new print modes for high ink coverage, enabling PSPs to produce billboards or close-view applications without switching inks. The specially formulated ink provides media versatility and operational efficiency for a variety of outdoor and indoor applications.

The new HP Scitex Industrial Press was introduced at SGIA Expo in New Orleans, USA.

Software for wide-format production

A new modular software solution for wide format printing was introduced at the FESPA 2012 trade show in Barcelona. It is comprising Editor, RIP, SmartProfiler and PrintStations. The solution was presented as the GMG Production Suite.

New solution offers completely new design of color management for wide-format printing. It can be applied to various output devices which offer flexible management and editing functions. It is applicable with both, PC and Mac platforms. Modular color management provides a more reliable production performance for large format printing.

A special feature of the this color management is a savings module, by which the use of colors is optimized, which in turn provides a more cost-effective printing. The capacity of the modules can easily be upgraded at any time.

New solutions for test printing

With proof printing as an important step in the production chain, a package of three new solutions for validation prints have been introduced recently. New products are composed of inkjet Epson printing system and raster process managing EFi eXpress for Proofing´s feature set.

Three new integrated printing systems named "Design". Thanks to this solution any specific requirements regarding quality, price and performance of customers can be achieved. The system includes pre-designed settings configurations definitions of compatible media. Direct setting of spectrophotometer for direct calibration of the printer is an additional option. Beside that EFI eXpress presents a part of a software package modular solution.

The WT7900 Design Edition model features the possibility of using white ink coverage for proofing flexographic and gravure print jobs on packaging foils. Printer can print on roll or cut sheets up to 609 mm (24 inches).

Design Edition 4900 is intended for prints with larger color space. The product supports complete borderless printing on different roll media sizes (from 203 to 432 mm).

The model 3880 Design Edition is designed for small pre-press studios. Printing width of this printer is also 432 mm.

UV inkjet system for label printing

The system represents a highly efficient solution compared to conventional printing of labels, which includes direct laser finishing. Short-run printing and variation capabilities allow production proofing and test marketing.

It enables 5-color dual-sided printing (CMYK+W) and printing on preprinted or pre-die-cut rolls. Average production speed in 5-color mode is around up to 70 fpm and up to 120 fpm in high-speed mode.

The use of special high quality UV printing inks guarantees lowest cost, while the system eliminates plates, dies, changeovers, enabling make-ready labor and highest quality of label prints (with resolutions of up to 1080 dpi) on variety of different substrates including papers and foils.

The solution uses drop-on-demand (DOD) print heads with grayscale capabilities. According to the manufacturer it provides exceptional durability with no over varnish needed.

The SEI finishing unit is equipped with double high efficient laser, which enables direct cutting, while up to nine cutting knives allow direct longitudinal cutting and rolling the materials in multiple rolls including paper and foils.

The system, under the name EFI Jetrion® 4900 is manufactured by EFI, while the finishing unit is a product of SEI Laser Converting.

New digital inkjet press

drupa 2012 was the stage for launching the new inkjet press, which was developed by the German manufacturer KBA together with one of the biggest print business RR Donnelly.

This technologically advanced machine uses frontline piezo inkjet technology that boasts four variable droplet sizes and an optimized screening algorithm. The two arrays of 56 inkjet heads each form an arch over large central impresssion cylinders for four-colour printing on both sides of the web, but can still be moved aside for cleaning and maintenance purposes. This arrangement provides for optimum web guidance and facilitates an outstanding print quality and register accuracy. The intelligent web lead without turner bars enables a contact-free web run.

KBA

This new piezoelectric-based digital inkjet machines will be, according to the manufacturers, intended for the use in commercial, newspaper, packaging and security sectors.

Inktrays

Inktrays is a new product specially designed and offering different solutions.

These customized PET Inktrays are intended for all flexopresses and trays are produced according to customer's specific needs. Their use is simple because there is no need for previous ink folding, stamping, there is no leakage, cleaning or other preparations.

The biggest advantage is in reduced costs for inktrays, saved time for preparation, which leads to reduction of down time and allows bigger production and therefore increases the profit. The product is available for most of the standard flexo presses. Inktrays is a product of the Swedish company Wasberger/Grafotronic.

Printing rolls

TecScreen are new high resolution printing rolls which by special coating and lamination enable printing of labels and similar applications, Braille and hazard symbols in high quality.

Rolls can be processed conventionally with films, in a continuous printer, or common digital UV imagesetters. TecScreen screen printing plates are available in different dimensions.

New generation of flexo plates

Digital printing plates are medium hard digital plates which can be used for a broad range of applications, especially for printing packaging with solvent based inks. They are available in two different thicknesses 114 and 170 µm. Base material is polyester film which enables relatively high plate roughness (72 or 61), depending on the plate thickness. Plates are suitable for absorbent and non-absorbent substrates ranging from textured to even surfaces.

Due to structural properties of plates wide tonal range (more open intermediate depths, finer highlight dots and less dot gain) for clean printing of fine image elements (150 lpi), fine line work, text and smooth solids can be easily achieved.

The plates are showing high resistance to solvent based inks and are suitable for water based inks and conditionally for UV inks.

They can easily be processed with standard processing equipment due to color change during main exposure. It can be used with all laser systems suitable for imaging flexo printing plates.

High quality standard flexo printing plates are manufactured according to DIN ISO 9001 and DIN ISO 14001 standards and requirements.

FlintGroup

New Nyloflex® FAM Digital printing plates are developed and manufactured by Flint Group.

Precision nonstop winding system

New winding system provides smooth nonstop winding and unwinding enabling endless printing independent of the material. The material rolls are loaded by an integrated lift and load system, by which the floor contact and contamination are practically eliminated. Besides an optional web guide providing perfect edge alignment of the reel, an integrated isolation dancer module is used to decouple the winding process from the press and therefore avoid impact usually caused by changes in web tension. A shiftable lay-on roller plus a fully adjustable taper tension control provides perfect winding quality.

The intelligent UR Precision winding system and automated roll change technology are developed by Kocher + Beck, a German company for special printing equipment.

PUR binding for short-run production

DigiBook 300 is a PUR (Polyurethane Reactive) perfect binder for short run production. PUR is the strongest, most flexible binding adhesive available and offers several significant advantages over other binding solutions.

When inks, coatings or digital print toners are present in the spine area these can compromise the strength of typical hot-melt perfect binding. PUR is resistant to this and will form a super-strong bond with all weights and finishes of paper stocks. In addition PUR works well with synthetic and recycled-content stock.

The DigiBook 300 is an innovative bookbinding machine designed and built for the very latest market requirements. It is easy to use, even by non-specialized personnel, with job specifications entered via a touch screen panel with icon graphics. This allows the programming of all precision operations in just a few seconds, including start-up and shutdown of the machine.

It is suited to both traditional and digital printers needing short runs of PUR perfect bound books to the most professional of standards. These innovative machines are equipped with a patented closed gluing system where the spine and side gluing is applied by a slot applicator for the utmost binding quality and accuracy.

There are a thousand alphanumeric memories available which allow repeat jobs to be saved for later recall, thus providing totally automatic setup in a few seconds.

The DigiBook 300 binding machine uses a new and innovative application system which is covered by no less than seven international patents. The application is direct and hermetically sealed, without any odor or toxic fume emissions and does not require extraction fans, thus allowing the use of polyurethane glue in 2 kg cartridges in a simple and waste free manner. DigiBook 300 is a product of the Morgana Systems, UK.

Bookshelf

3D Printing: High-impact Emerging Technology

What You Need to Know: Definitions, Adoptions, Impact, Benefits, Maturity, Vendors

3D printing is a form of additive manufacturing technology where a three dimensional object is created by laying down successive layers of material. 3D printers are generally faster, more affordable and easier to use than other additive manufacturing technologies. 3D printers offer product developers the ability to print parts and assemblies made of several materials with different mechanical and physical properties in a single build process. Advanced 3D printing technologies yield models that closely emulate the look, feel and functionality of product prototypes.

A 3D printer works by taking a 3D computer file and using and making a series of cross-sectional slices. Each slice is then printed one on top of the other to create the 3D object.

Since 2003 there has been large growth in the sale of 3D printers. Additionally, the cost of 3D printers has declined. The technology also finds use in the jewelry, footwear, industrial design, architecture, engineering and construction (AEC), automotive, aerospace, dental and medical industries.

This book is the ultimate resource for 3D Printing. Here the most up-to-date information can be found, with the analysis and to all issues.

Chapters have extensive references and links which are covering everything related to 3D Printing: 3D printing, Pad printing, Lenticular printing, History of printing, Woodblock printing, Movable type, Printing press, Etching, Mezzotint, Aquatint, Lithography, Chromolithography, Rotary printing press, Offset printing, Hot metal typesetting, Screen printing, Dye-sublimation printer, Phototypesetting, Dot matrix printer, Laser printer, Thermal printer, Inkjet printer, Stereolithography, Digital printing, Additive manufacturing, Three-dimensional space, Prototype, 3D scanner, Rapid prototyping, Selective laser sintering, Fused deposition modeling, Economies of scale, Global spread of the printing press, Digital Light Processing, Stratasys, Sintering, Direct metal laser sintering, 3D microfabrication, Two-photon absorption, Nonlinear optics, Dots per inch, MeshLab, 3D modeling, RepRap Project, Direct digital manufacturing, Digital fabricator, Self-replicating machine, Solid freeform fabrication, Planographic printing, Relief print, D-Shape, Decorative laminate, Dimension (company), Laser engraving, Mimeo.com Inc., Ozalid process, Photogravure, Photozincography, Reprography, Split-fount Inking, Stochastic screening, Surface printing, Thermal transfer.

This book explains in-depth the real drivers and workings of 3D Printing. It reduces the risk of technology, time and resources investment decisions by enabling a comparison of understanding of 3D Printing with the objectivity of experienced professionals.

3D Printing: High-impact Emerging Technology
Author: Kevin Roebuck
Publisher: Tebbo (2011)
ISBN 978-1743042700
316 pages
Paperback

Handbook of Printing Processes

Deborah L. Stevenson

Graphic Arts Center Publishing Co. (2011)
ISBN: 978-0883621646
272 pages
Hardcover

This publication provides a introduction to all steps of print production for every major printing process. Related topics covered include binding and finishing, paper and ink. Emerging technologies such as waterless printing and stochastic printing are also discussed. The contents include: conventional art and copy preparation; electronic prepress production; colour reproduction; film assembly; image carriers; presswork; nonimpact printing; binding and finishing; paper; and ink.

The Chemistry and Technology of Printing Inks

Norman Underwood

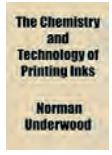

General Books LLC (2012)
ISBN 978-0217519274
38 pages
Not illustrated
Paperback

This historic book may have numerous typos, missing text, images, or index. Readers can download a free scanned copy of the original book (without typos) from the publisher.

A first-class grade of carbon black should always be used for blacks and lakes precipitated on very softgrained aluminum hydrate should be used for colors. An ink that separates out color or pigment to the very slightest extent should be avoided as the slightest piling on the plate makes a very bad looking job. The latitude allowed on flat-bed or rotary cylinder presses using electrotypes cannot be allowed in an ink for offset work. For tints in offset work and in fact for any colored work except black, a base consisting of equal parts of magnesium carbonate ground in a thin varnish to a stiff paste and a mixture of zinc white and aluminum hydrate also ground in varnish will be found not only a good reducer but also to give the necessary body and working qualities to the ink.

Information Graphic
How Complex Ideas Can Be Communicated Via Graphics

"If you can't explain it simply, you don't understand it well enough" (Albert Einstein)

Our everyday lives are filled with a massive flow of information that we must interpret in order to understand the world we live in. Considering this complex variety of data floating around us, sometimes the best - or even only - way to communicate is visually.

This unique book presents a fascinating historical perspective on the subject, highlighting the work of the masters of the profession who have created a number of breakthroughs that have changed the way we communicate. *Information Graphics* has been conceived and designed not just for designers or graphics professionals, but for anyone interested in the history and practice of communicating visually.

The in-depth introductory section, illustrated with over 60 images (each accompanied by an explanatory caption), features essays by *Sandra Rendgen, Paolo Ciuccarelli, Richard Saul Wurman and Simon Rogers*; looking back all the way to primitive cave paintings as a means of communication, this introductory section gives an excellent overview of the subject.

The second part of the book is entirely dedicated to contemporary works by the current most renowned professionals, presenting 200 graphics projects, with over 400 examples - each with a fact sheet and an explanation of methods and objectives - divided into chapters by the subjects Location, Time, Category, and Hierarchy.

Features:
- ◇ 200 projects and over 400 examples of contemporary information graphics from all over the world - ranging from journalism to art, government, education, business and more
- ◇ Historical essays about the development of information graphics since its beginnings
- ◇ Exclusive poster by *Nigel Homes*, who during his 20 years as graphics director for *TIME* revolutionized the way the magazine used information graphics

Information Graphics
Authors: Sandra Rendgen et al.
Edited by Julius Wiedemann
Publisher: Taschen (2012)
ISBN 978-3836528795
480 pages
246 mm x 372 mm
Hardcover

Surface Phenomena and Latexes in Water-borne Coatings and Printing

The current state of waterborne polymers, paints, coatings, inks and printing technology is presented in the 16 papers addressed both to people who formulate and process them and people who use them.

Author: Mahendra K. Sharma
Publisher: Springer, 2010;
reprint of hardcover (1995)
ISBN: 978-1441932471
240 pages
Paperback

Events

International Paper Physics Conference and 8th International Paper and Coating Chemistry Symposium

Stockholm, Sweden
10 to 14 June 2012

Innventia and the Royal Institute of Technology KTH will organize a joint event - the International Paper Physics Conference and the 8th International Paper and Coating Chemistry Symposium which will be arranged in Stockholm. By that paper scientists will have the opportunity of the ultimate meeting forum.

The aim of the International Paper Physics Conference is to discuss the physical properties of paper and board-type materials, covering also other structures of paper type from wood fibers, including the latest developments in biocomposites and nanostructured materials. The chosen topics (Paper, coating and barrier properties, Experimental methods and Computational methods and simulations) of the program will cover the latest experimental and theoretical findings as well as advanced physical simulations. Beside the general topics there will be a number of specially invited sessions aiming at bringing scientists together for in-depth discussion on actual topics in paper physics.

The purpose of the 8th International Paper and Coating Chemistry Symposium is to cover the latest developments in the fields of paper chemistry, coating chemistry and nanotechnology for the paper industry. Discussing the performance of chemical additives in papermaking and coating operations is the main scope of this year's symposium.

The two conferences will be arranged together as a way for the paper and coating chemistry and the paper physics communities to interact and to offer the paper industry an insight into the latest research developments in these fields.

Nanotech Conference & Expo

Santa Clara, California, USA
18 to 21 June 2012

TechConnect is a global technology outreach & development organization which organizes each year the TechConnect World conference. It is supposed to be one of the largest multi-disciplinary, multi-sector conference and marketplace of vetted innovations, innovators and technology business developers and funders. The TechConnect World houses four world-class technical events focused on advancements in Nanotech, Microtech, Biotech, Cleantech and the technology overlap between these converging domains. As technologies commercially mature from the purely research stage, they are advanced into the TechConnect Summit and partnering programs in which IP and Early-stage companies are reviewed and selected by the board of corporate and investment partners.

IEEE IAS Pulp & Paper Industry Technical Conference

Portland, Oregon, USA
17 to 21 June 2012

IEEE (the Institute of Electrical and Electronics Engineers) conference will offer an informative and educational three day technical program followed by tutorial sessions. Already announced keynote speaker will share ideas on emerging innovations and sustainability in the Forest Products Industry.

At the conference 28 new technical papers on industry applications in pulp and paper mills will be presented, augmentted by 16 exhibitors showing the latest technologies designed to improve efficiency, reliability and safety. The event will also offer some multi-track tutorials including a Paper Machine Drives Sort Course sponsored by TAPPI and an update on changes to the NFPA70E-2012 Standard for Electrical Safety in the Workplace.

IC Conference

Budapest, Hungary
19 to 22 June 2012

IC - the International Circle of Educational Institutes for Graphic Arts Technology and Management is an informal network which with all its members provides scientific, engineering and economic education covering the fields of graphic arts. This year the network will once again organize an annual IC conference which will be 44th in a role.

The conference will be hosted by RejtQ Sándor Faculty of Light Industry and Environmental Engineering of the Óbuda University, on the 40th anniversary of the Faculty. The scope of the conference will encompass areas such as scientific or educational topics from the fields of Graphic Arts Technology, Management and Communication, in a wider sense.

Young Reader Asia-Pacific Summit

10 to 11 July 2012
Bangkok, Thailand

This first WAN-IFRA "Young Reader Asia-Pacific Summit" in Thailand on 10-11 July 2012, will look into successful, award-winning young reader initiatives of newspapers in Asia and abroad. It will provide insights into attracting young readers to newspaper content, no matter what platform. Participants will also have the chance to attend in-depth pre- and post-conference workshops where they will explore how to build success through engaging the young readers.

64th World Newspaper Congress - 19th World Editors Forum

Kiev, Ukraine
2 to 5 September 2012

The World Association of Newspapers and News Publishers (WAN-IFRA) organizes the annual global summit meetings of the world's press under the attractive topic ˝Shaping the Future of the Newspaper˝. The summit will combine two events - World Newspaper Congress and World Editors Forum which´s programs of 2012 will share the strategies and exchange the ideas of newspaper business on all platforms. The events will examine the birth of new strategies for growth in circulation and digital advertising, advances in paywalls, new revenues, new product creation, enriched content experiences, novel marketing services, exciting print innovation and much more.

More than 1 000 chief editors, publishers, managing directors, CEOs and other senior newspaper executives are expected to take part at the Editors Forum, Congress and Info Services Expo 2012 in Kiev.

Nanotech 2012 brings together specialists from a wide range of fields of science, technology and business. Conference program will include different topics from fabrication and characterization, advanced materials, electronics and microsystems, medicine and biotechnology to energy and environment.

Organizers are expecting more than 350 featured exhibitors and more than 4 000 attendees from over 70 countries. The event will be held at the Santa Clara Convention Center, Santa Clara, California.

LOPE-C 2012

Munich, Germany
19 to 21 June 2012

LOPE-C - Large-area Organic and Printed Electronics Convention is the official annual conference and exhibition of the OE-A (Organic and Printed Electronics Association). As the world´s leading conference and exhibition for the large, rapidly growing market for organic and printed electronics, LOPE-C is the perfect place to generate new business.

It depicts the entire value chain in key sectors such as the chemicals, printing and microelectronics industries, and it brings together all suppliers, equipment manufacturers and service-providers as well as end users in various application fields in the process.

This year´s conference will present one congress with six different components:

- ◊ plenary sessions
  which will be delivered by internationall experts
- ◊ business conference and investor forum
  which will focus on commercialization
- ◊ technical conference
  focused on new technologies and applications
- ◊ scientific conference
  with sessions provided by established and young esearchers and scientists
- ◊ poster and interactive session
  on the related topics
- ◊ short courses
  featuring established industry and academic experts.

LOPE-C 2012 will cover the latest commercial and technological achievements in organic, inorganic and printed devices, systems and materials. In addition to the high-level business and technical conference with noted speakers from academia and industry, plus keynote sessions and pre-conference seminars, LOPE-C 2012 will feature an industry exhibition providing a comprehensive overview to showcase the rapidly emerging products, services and global manufacturing capacities in the field of organic and printed electronics.

The event will be an excellent opportunity that will bring together industry representatives, scientists and engineers and it will give the participants an overview of the latest applications and technologies. LOPE-C 2012 will be held in the Munich International Congress Center (ICC).

High Performance Graphics

Paris, France,
25 to 27 June 2012

High Performance Graphics is the international forum for performance-oriented graphics systems research including innovative algorithms, efficient implementations, and hardware architecture.

Forum was founded in 2009 to synthesize and expand two important conferences in computer graphics - Graphics Hardware and Interactive Ray Tracking. The first mentioned is as annual conference focused on graphic hardware, architecture, and systems and the latter an innovative symposium focusing on the emerging field of interactive ray tracking and global illumination techniques. By combining and expanding these two communities the best of both fields is joined in a conference covering a broad range of interactive 3D graphic systems and algorithm research. The conference will bring together researchers, engineers and architects which will have the opportunity to discuss the complex interactions of massively parallel hardware, novel programming models and applications as well as efficient graphic algorithms. The conference is co-located with the Eurographics Symposium on Ren-dering in Paris, France.

Serigrafia SIGN FutureTEXTIL

São Paolo, Brazil, 18 to 21 July 2012

Serigrafia is Brazil's largest trade show for screen, textile and digital printing, image transfer, communications graphics. It represents a benchmark for technology in products and services for these sectors. Joint under one name - Serigrafia SIGN FutureTEXTIL 2012 - three trade shows comprise Latin America's largest event for machines, equipment, products and services for screen, textile and digital printing, communications graphics, signs and promotional material.

This event attracts around 600 exhibiting brands and more than 45 000 visitors. The trade will occupy a total of 35 000 sqm of Expo Center Norte Exhibition Center in São Paulo. It represents the biggest platform for sector trends in screen printing and communication graphics.

Labelexpo Americas

Chicago, USA
11 to 13 September 2012

Labelexpo Americas, is the largest converting show in the Americas for the label, product decoration, web printing and the related converting industry.

The event introduces new materials, cutting edge printing processes, high added value solutions, innovation product decorations and much more. Label printers will have the opportunity to see new solutions in machinery, cutting edge technology, press innovations, laser die cutting, RIFD, high technology label materials, films, sleeves and wrap, etc. Live demonstrations of the working machinery and materials will offer new knowledge about the global label trends and technologies. The show will therefore be an excellent opportunity to study solutions for various current issues, to look for future technologies and to identify new trends in label printing.

SIGGRAPH 2012

Los Angeles, California, USA
5 to 9 August 2012

SIGGRAPH is the international conference and exhibition on computer graphics and interactive techniques.

Main aim of this 39th conference is to bring numerous of computer graphics and interactive technology professionals from all over the world to one place for the industry's most respected technical and creative programs focusing on research, science, art, animation, music, gaming, interactivity, education, and the web. The program will be focused on the emerging technologies, while technical papers will be published in a special publication.

SIGGRAPH 2012 also includes a three-day exhibition of products and services from the computer graphics and interactive market which will take place from 7 to 9 August 2012.

Cross Media 2012

London, United Kingdom
3 and 4 September 2012

Cross Media 2012 is a brand new, highly relevant and focused event that brings together offline and online channels in a business context.

Digital technology has changed the face of all media, including print. The main aim of it is to bring together print and digital channels in a business context. Cross media - Concept or communications wishes to deliver across multiple platforms or media. These platforms include print, web, direct mail, email, data management, mobile, apps, SMS, PURLS, QR codes, Social Media and Video.

It's the perfect opportunity to present cross-platform technologies, products and services to a broad audience that is looking for applications and solutions in this rapidly developing field.

The event will feature over 100 exhibitors and five seminars on the related themes.

ICFPE 2012

Tokyo, Japan
5 to 8 September 2012

The fields of flexible and printed electronics are still at early stage and have multidisciplinary features. International Conference on Flexible and Printed Electronics (ICFPE) aims to gather and evaluate all the aspects of science, technology, and business in the fields of printed and flexible electronics (FPE).

The goal of this conference is to offer a common meeting ground for all FPE-related research organizations and individuals who affiliate with different professional societies and/or organizations, and subsequently to accelerate the growth of these fields. It also focuses on reviewing the emerging applications that will directly benefit from mechanical flexibility and printed processes such as transistors, photonic devices, solar cells, batteries, displays, RFID, sensors and many others.

This third in a role ICFPE conference is expected to be much larger than previous edition, due to expansion in the current research.

International Conference on Digital Printing Technologies

Quebec, Canada
9 to 13 September 2012

Society for Imaging Science and Technology (IS&T) introduces one of the leading forums for discussion of advances and new directions in non-impact and digital printing technologies.

This comprehensive, industry-wide conference includes all aspects of the hardware, materials, software, images, and applications associated with digital printing systems, including drop-on-demand ink jet, wide format ink jet, desk-top and continuous ink jet, toner-based electrophotographic printers, production digital printing systems and thermal printing systems, as well as the engineering capability, optimization and science involved in these fields.

39th annual International research conference of iarigai

Graphic communication and beyond

9 to 12 September 2012
Ljubljana, Slovenia

Continuing almost 50 years of tradition in networking the researchers worldwide, iarigai announces its next event - the 39th International Research Conference, which will this year take place in Ljubljana, Slovenia from 9 to 12 September 2012. The conference will be hosted by the University of Ljubljana - Faculty of Natural Sciences and Engineering.

The conference, entitled Graphic communication and beyond, will appeal to numerous scientists from all over the world. Participants from almost 20 different countries will join together to present their recent research results and discuss the future development of media.

More than 40 high-class contributions, divided in 13 different sessions, will provide an interesting overview of the latest development in the graphic field. Invited and keynote lectures, featuring top international experts in the field, will give an added value to the event, along with the expected panel discussion on the research for the media future. The preliminary program is already announced on the conference web site.

The conference will be - among others - mainly dedicated to the topics of flexo printing, printed electronics, digital print media, packaging, color reproduction, online and mobile media, and many more interesting topics. Papers selected for a presentation will be printed in the form of extended abstracts for conference participants, while complete edited versions of papers presented will be published in Vol. XXXIX of the series "Advances in Printing and Media Technology", to be published in November 2012. During the conference issue No. 3 of the Journal of Print and Media Technology Research will be promoted, this one completely dedicated to the printed electronics.

As one of the most beautiful European cities Ljubljana presents an excellent venue choice. Even though it is a middle-sized European city, it maintains the friendliness of a small town and simultaneously possesses the characteristics of a metropolis. Here, at the meeting point of the cultures of east and west the old comes together in harmony with the new. Renowned for being a major regional center of culture, business, media and science, Ljubljana also takes pride in its image as a green city. It is a very unique city dotted with pleasant picturesque places where you can expect all kinds of nice little surprises. Ljubljana is a city of culture.



It is home to numerous theatres, museums and galleries and boasts one of the oldest philharmonic orchestras in the world. Ljubljana has round 270 000 inhabitants and it is considered a city that suits both its residents and many visitors. Given its geographical position and short distances between places in Slovenia Ljubljana presents a perfect base for exploring the country´s diverse features and beauty. Within a single day you can visit the Slovenian coast and high mountainous regions and experience the Mediterranean, Alpine and continental climate.

Call for papers

Authors are invited to prepare and submit complete, previously unpublished and original works, which are not under review in any other journals and/or conferences.

The journal will consider for publishing papers on fundamental and applied aspects of at least, but not limited to, the following topics:

- Printing technology and related processes

  Conventional and special printing; Packaging, Printed functionality (incl. polymer electronics, sensors, and biomaterials); Printed decorations; Printing materials; Process control

- Premedia technology and processes

  Color reproduction and color management; Image and reproduction quality; Image carriers (physical and virtual); Workflow and management

- Emerging media and future trends

  Media industry developments; Developing media communications value systems; Cross-media publishing

- Social impact

  Media in a sustainable society; Consumer perception and media use

Submissions for the journal are accepted at any time. If meeting the general criteria and ethic standards of the scientific publication, they will be rapidly forwarded to peer-review by experts of high scientific competence, carefully evaluated, selected and edited. Once accepted and edited, the papers will be printed and published as soon as possible.

There is no entry and/or publishing fee for authors.

Authors are asked to strictly follow the guidelines for preparation of a paper (see abbreviated version on inside back cover). Complete guidelines can be downloaded from

http://www.iarigai.org/publications/

Papers not complying with the guidelines will be returned to authors for revision.

Submissions and queries should be directed to

journal@iarigai.org or office@iarigai.org

Subscriptions 2012

Journal of Print and Media Technology Research is distributed by subscription only, solely or in package with the annual edition of the Advances in Printing and Media Technology. Following subscription models are available:

Journal of Print and Media Technology Research*
ISSN 2223-8905

A	**Regular** annual subscription (4 issues p. a.)	300 EUR
B	**Members** of iarigai - one copy (4 issues) free of charge **Additional** copies for members - discount 20%	240 EUR

Advances in Printing and Media Technology - Vol. 39**
(hard bound book with selected and edited full conference papers)
ISSN 2225-6707, ISBN 978-3-9812704-4-0

C	**Regular** rate per copy	155 EUR
D	**Members** of iarigai - one copy free of charge **Additional** copy for members - discount 20%	124 EUR

Two-in-one package (JPMTR and Advances - Vol. 39)**
(valid only if ordered together)

E	**Annual** subscription to the journal + **current volume** of the Advances in Print & Media Technology Research (full regular price 455 EUR)	359 EUR
F	**Additional** package for members (extra discount 26 EUR)	333 EUR

Select one of the offered subscription models (A - F) and place your order online at:

http://www.iarigai.org/publications

(open: Order/Subscribe here)

or send an e-mail order to: office@iarigai.org

* Single copies of JPMTR can be purchased only if available on upon a separate request
** Vol. 39 of the Advances In printing and Media Technology will be published in November 2012

JPMTR 1(2012)2, 77-134
June 2012

No. 2-2012

ISSN 2223-8905
CODEN: JPMTBI

Journal of Print and Media Technology Research

A peer-reviewed quarterly

PUBLISHED BY

The International Association of Research Organizations for the Information, Media and Graphic Arts Industries

Washingtonplatz 1, D-64287 Darmstadt, Germany
http://www.iarigai.org E-mail: journal@iarigai.org

A mission statement

To meet the need for a high quality scientific publishing platform in its field, the International Association of Research Organizations for the Information, Media and Graphic Arts Industries, iarigai, publishes this quarterly peer-reviewed research journal.

The journal will foster multidisciplinary research and scholarly discussion on scientific and technical issues in the field of graphic arts and media communication, thereby advancing scientific research, knowledge creation, and industry development. Its aim is to be the leading international scientific journal in the field, offering publishing opportunities and serving as a forum for knowledge exchange between all those interested in contributing to or learning from research in this field.

By regularly publishing peer-reviewed, high quality research articles, position papers, surveys, and case studies as well as, in a special section, review articles, topical communications, opinions, and reflections, the journal promotes original research, international collaboration, and the exchange of ideas and know-how. It also provides a multidisciplinary discussion on research issues within the field and on the effects of new scientific and technical developments on society, industry, and the individual. Thus, it serves the entire research community, as well as the global graphic arts and media industry.

The journal covers fundamental and applied aspects of at least, but not limited to, the following topics:

Printing technology and related processes

Conventional and special printing
Packaging
Printed functionality (including polymer electronics, sensors, and biomaterials)
Printed decorations
Printing materials
Process control

Premedia technology and processes

Color reproduction and color management
Image and reproduction quality
Image carriers (physical and virtual)
Workflow and management
Content management

Emerging media and future trends

Media industry developments
Developing media communications value systems
Online and mobile media development
Cross-media publishing

Social impact

Media in a sustainable society
Consumer perception and media use

The Journal of Print and Media Technology Research is published both in print and electronically.

Further details and guidelines for authors can be found on the inside back cover, as well as downloaded from http:// www.iarigai.org/publications/journal

Subscriptions

http:// www.iarigai.org/publications/journal/order or send a request to office@iarigai.org

✉ Contact e-mail: journal@iarigai.org

2-2012

Journal of Print and Media Technology Research

A peer-reviewed quarterly

The journal is publishing contributions in the following fields of research:

- Printing technology and related processes
- Premedia technology and processes
- Emerging media and future trends
- Social impacts

For details see the Mission statement inside

Submissions and inquiries
journal@iarigai.org and office@iarigai.org

More information at
www.iarigai.org/publications/journal

Publisher

The International Association of Research Organizations for the Information, Media and Graphic Arts Industries
Washingtonplatz 1
D-64278 Darmstadt
Germany

Prited in Croatia by Narodne Novine d.d.